

**Generation and Stability of Microemulsion to Improve Heavy Oil Recovery by
Waterflooding with Chemical Additives at Cold Conditions**

by
Jungin Lee

A thesis submitted in partial fulfillment of the requirements for the degree of
Master of Science
in
Petroleum Engineering

Department of Civil and Environmental Engineering
University of Alberta

© Jungin Lee, 2018

Abstract

Thermal methods which are commonly applied to recover heavy oil have many limitations such as heat loss to thin or deep reservoirs due to temperature difference found in different parts of reservoirs, difficulty in recovering oil in low permeability deposits, high energy and water waste, and so forth. To solve these issues, nonthermal heavy oil recovery method, which is chemical flooding by in-situ emulsification, was investigated in this extensive study. Commercially available chemicals along with chemicals synthesized in the lab were first screened for their capacity to generate stable Winsor type 4 heavy oil-in-water emulsions using glass tube tests and microscopic visualization experiments. After the initial screening, stabilization tests and concentration tests were conducted for the purpose of cost optimization. Selected chemicals were then further synthesized to create Nano-fortified Pickering emulsions to create even stronger emulsions stability that can survive harsh reservoir conditions. Created complex Pickering solutions were then injected into glass bead samples, sandpacks, Berea sandstone cores, slim tube sandpacks at various rates in order to test and ensure their strength to generate in-situ heavy oil-in-water emulsions in porous media of various types. A novel, environmentally friendly, cost-effective chemical flooding method using biodiesel condensate (Biodiesel-in-water emulsion) was also investigated for its ability to recover heavy oil by in-situ heavy oil-in-water emulsion generation. Lastly, hard brines were introduced in the study to better simulate the real reservoir brine conditions and understand the impact that divalent ions can have on emulsion stability. Research results demonstrated that Pickering solutions, biodiesel-in-water emulsions, hardness resistant chemicals can help recover oil by heavy oil-in-water emulsification in porous media. Full Winsor type 4 emulsion production and significant increase in recovery could be observed with the addition of low concentration polymer (0.35%) as an emulsion stabilization agent to chemicals injected for sandpack flooding experiments at hard brine of low and high

salinity conditions. These results confirmed polymer's potential as a robust co-emulsification agent that can significantly help improve heavy oil recovery.

This thesis is dedicated to my beloved heroine – my mother

Acknowledgements

First and foremost, I would like to express my sincere gratitude to my supervisor Dr. Tayfun Babadagli for his continuous support throughout this research over the past 2 years. I would like to thank him for teaching me the importance of respect (professional, personal, philosophical, etc.), time-management, work ethic, confidence (in oneself, in life and in one's academic work), and meticulousness. I feel absolutely honored to have had this special opportunity to work under the close supervision of a deservedly well-known and established petroleum engineering expert/scholar. I would also like to thank him for having trusted me, encouraged me and giving me the opportunity to be creative, flexible, and dynamic in my research while also ceaselessly guiding me with his insights, suggestions, advice, and answers so that I did not get lost. I reflect on and value every laughter and tear from the past 2 years working in his lab. That was true education.

I would also like to express sincere gratitude to my lab supervisors (EOGRRC's technicians) Georgeta Mihaela Istratescu, Lixing Lin, and Todd Kinnee for their professional and patient help with my experiments. I am thankful to Mihaela for her kind and wise advice, both professional and personal, and the time she dedicated to educate me during this research. I will never forget all of her sincere and valuable advice. I would like to thank Lixing for patiently and compassionately supporting me during my experiments. I want to thank Todd for his truthful and knowledgeable advice. I am also thankful to Pamela Keegan for editing my thesis and papers with much patience and dedication. Her expertise in technical writing and communication really facilitated my writing process and this shall never go unacknowledged.

I would also like to express my gratitude to my lovely friends - Rachael F, Jesus David M, Stephen D, Ehab E, Yulia W, Jad A, Raphael S who have humbled me and will humble me through and through with their kindness, sincerity, generosity, humor, and wisdom.

I sincerely acknowledge the sponsorship from Prof. Tayfun Babadagli's NSERC Industrial Research Chair in Unconventional Oil Recovery (industrial partners are Petroleum Development Oman, Total E&P Recherche Développement, SiGNa Oilfield Canada, CNRL, SUNCOR, Touchstone Exploration, Sherritt Oil, PEMEX, Husky Energy, Saudi Aramco, Devon, BASF, and APEX Eng.) and an NSERC Discovery Grant (No: RES0011227).

Last but not the least, and most importantly, my special thank goes to my strong-willed, hilarious, generous, relentlessly inquisitive, sweet, always a poet-at-heart superwoman mother who is the absolute and unconditional love of my life.

Table of Contents

Chapter 1: Introduction	1
1.1 Introduction	2
1.2 Statement of the Problem	3
1.3 Aims and Objectives	5
1.4 Structure of the Thesis	6
Chapter 2: Characterization of Microemulsions as a Screening Tool of Chemicals and Nano Materials	
Screening for In-situ Recovery of Heavy Oil	9
2.1 Preface	10
2.2 Introduction	10
2.3 Materials	12
2.4 Methodology	14
2.4.1 Glass Tube Test	14
2.4.2 Concentration Test	15
2.4.3 Stabilization Test	16
2.5 Results	16
2.5.1 Glass Tube Test Results and Discussions	16
2.5.2 Concentration Test Results and Discussions	22
2.5.3 Stabilization test	26
2.6 Conclusions	38
Chapter 3: Improvement of Microemulsion Generation and Stability Using New Generation Chemicals and Nano Materials During Waterflooding as a Cost-Efficient Heavy-Oil Recovery Method	40
3.1 Preface	41
3.2 Introduction	42
3.3 Materials	43
3.4 Methodology	44
3.4.1 Design of the Pickering emulsion	44
3.4.2 Zeta potential	46
3.4.3 Glass tube concentration test	46
3.4.4 Sandpack flooding	47
3.4.5 2-D Glass bead visualization	47
3.4.6 Berea sandstone core flooding	48
3.4.7 Slim tube sandpack flooding	50
3.5 Results	51
3.5.1 Zeta potential measurements	51
3.5.2 Stabilized Emulsions of an anionic surfactant Alforterra S23-7S-90 and silica nanoparticles hydrophobized with DTAB	52
3.5.3 Glass tube concentration test (Emulsion stability)	54
3.5.4 Sandpack flooding oil recovery	55
3.5.5 2-D Glass bead visualization (in-situ emulsion generation)	61
3.5.6 Berea sandstone core flooding	62

3.5.7 Slim tube sandpack flooding experiments	63
3.6 Conclusions.....	65
Chapter 4: Microemulsion Flooding of Heavy Oil using Biodiesel under Cold Conditions.....	66
4.1 Preface	67
4.2 Introduction	68
4.3 Materials.....	69
4.4 Methodology.....	70
4.4.1 Steam treatment of the BD-W emulsion samples.....	70
4.4.2 Spreading test.....	71
4.4.3 Glass tube test	72
4.4.4 Microscopic visualization	72
4.4.5 Sandpack flooding	72
4.5 Results.....	73
4.5.1 Steam-treated biodiesel-in-water emulsion sample.....	73
4.5.2 Spreading test.....	75
4.5.3 Glass tube tests.....	77
4.5.4 Microscopic visualization	77
4.5.5 Sandpack flooding	84
4.6 Conclusions.....	87
Chapter 5: Impact of hard divalent cations on heavy oil-in-water emulsification.....	88
5.1 Preface	89
5.2 Introduction	90
5.3 Materials.....	90
5.4 Methodology.....	93
5.4.1 Glass tube test	93
5.4.2 Sandpack flooding test	94
5.5 Results.....	96
5.5.1 Glass tube tests.....	96
5.5.2 Sandpack flooding	98
5.6 Conclusions.....	104
Chapter 6: Conclusion and Future Work.....	106
6.1 Conclusions and Contributions	107
6.2 Limitations and Future Work	108
References	109
Chapter 1.....	109
Chapter 2.....	110
Chapter 3.....	113
Chapter 4.....	115
Chapter 5.....	116

List of Figures

Figure 1—Left: promising system, Right: less promising system.	14
Figure 2—Manual particle selection using ImageJ (APS 0.8 wt. %).	23
Figure 3—APS 3 particle distribution plot.	24
Figure 4—HORA particle distribution plot.	24
Figure 5—PSB 20 particle distribution plot.	25
Figure 6—APS 3, 0.6 wt. % coalescence process.	26
Figure 7—APS 3 0.6 wt.% + Zirconium Oxide 0.4 wt.% coalescence process.	30
Figure 8—Dodecyl trimethyl ammonium bromide (DTAB).	45
Figure 9—Core flooding set up.	47
Figure 10—Schematic diagram of glass bead visualization setup.	48
Figure 11—Top view of the glass bead model.	48
Figure 12—Schematic diagram of Berea sandstone core set up.	49
Figure 13—Slim tube experiment setup.	50
Figure 14—Emulsion with DTAB results.	53
Figure 15—Microscopic visualization results.	54
Figure 16—Particle distribution of the Winsor type 4 emulsion samples (a): Immediately after (b): 3 hours later.	55
Figure 17—Produced samples from low salinity water flooding at 1ml/min.	55
Figure 18—Produced samples from colloidal dispersion flooding after low salinity water flooding at 1ml/min.	56
Figure 19—Produced samples from colloidal dispersion flooding at 1ml/min.	56
Figure 20—Produced samples colloidal dispersion flooding at 0.2ml/min.	56
Figure 21—Sandpack flooding oil recovery at various rates.	57
Figure 22a,b—Heavy oil chemical flooding type curve generated from sandpack flooding results using optimal flow rate.	58
Figure 23—Zoomed in view of the glassbead model.	62
Figure 24—Berea sandstone core flooding results.	63
Figure 25—Visualization of emulsions.	64
Figure 26—Results from 0.3 ml/min.	65
Figure 27—Results from 0.03 ml/min.	65
Figure 28—SBDWE treatment set up.	70
Figure 29—Biodiesel condensates (Babadagli and Ozum 2012).	71
Figure 30—Sandpack flooding set up.	73
Figure 31—SBDWE samples with varied injected biodiesel concentrations.	74
Figure 32—Spreading test.	76
Figure 33—Glasstube test results.	77
Figure 34—Original biodiesel and its interaction with oil.	78
Figure 35—Micrographic analysis of SBDWE (Steam treated BioDiesel in Water Emulsion) and SWBDE (Steam treated Water in BioDiesel Emulsion).	78
Figure 36—SBDWE1 and heavy oil.	80
Figure 37—SBDWE1 with heavy oil after addition of silica.	80
Figure 38—SBDWE1 (24 hr after being maintained in the oven at 50°C).	80
Figure 39—Silica added SBDWE1 case (24 hr after being maintained in the oven at 50°C).	80
Figure 40—SBDWE6 without addition of silica.	81
Figure 41—SBDWE6 with silica (initial).	82
Figure 42—SBDWE6 with silica: expansion of oil phase (final).	82
Figure 43—SBDW3 #2 before adding silica (3 week old).	83
Figure 44—SBDW3 #2 case after adding silica (3 week old).	83
Figure 45—STDW6 sample.	84
Figure 46—collected samples at every 0.1 PV	85
Figure 47—Recovery results from sandpack flooding experiments.	85
Figure 48—Dramatic improvement in oil recovery with addition of Xanthan gum.	86
Figure 49—produced emulsion types with PVI.	99
Figure 50—produced emulsion types with cumulative oil recovery.	103
Figure 51—Sandpack flooding results (Cum. recovery vs PVI).	103

List of Tables

Table 1—Chemical properties of oil.	12
Table 2—Chemicals Screened and Evaluated in this Study.	13
Table 3—Detailed standards to screen chemicals based on their ability to create stable oil-in-water emulsions.	17
Table 4—AAS, IOS, LTS surfactants.	18
Table 5—APS, PSB, NP, Arquad, HORA.	19
Table 6— Ionic liquid, Na ₂ CO ₃ , NaHCO ₃ , carbonate powders.	21
Table 7—DES 1, DES 2, DES 3.	22
Table 8—Gray value histograms of micrographs at various concentrations (APS 3, HORA) – Salinity: 3.8%.	23
Table 9—Micrographs taken at various concentrations (APS 3, HORA) - Salinity: 3.8%.	23
Table 10—Micrographs taken at various concentrations (PSB 20) - Salinity: 6.35%.	25
Table 11—Gray value histograms of micrographs at various concentrations (PSB 20) - Salinity: 6.35%.	26
Table 12—Properties of stabilizing agents.	27
Table 13—Glass tube test of alfoterra and added stabilizing agents.	28
Table 14—Micrographs of stabilized emulsions taken at regular time intervals (APS 3).	29
Table 15—Glass tube test of HORA and added stabilizing agents.	33
Table 16— Micrographs of stabilized emulsions taken at regular time intervals (HORA).	34
Table 17—Glass tube test of Tween20 and added stabilizing agents.	36
Table 18—Micrographs of stabilized emulsions taken at regular time intervals (PSB 20).	37
Table 19—Sara results.	44
Table 20—Solution A.	46
Table 21—Zeta potential results.	51
Table 22—DTAB emulsion evaluation	53
Table 23—Microscopic visualization of oil droplets in the emulsion phase.	60
Table 24—Biodiesel property.	69
Table 25—SBDWE generation under various conditions.	74
Table 26—Change in SBDWE stability over time.	76
Table 27—Aspiro surfactants.	91
Table 28—Enordet surfactants.	92
Table 29—Sandpack flooding.	95
Table 30—Glass tube results and core flooding results from IOS0332 with colloidal solution without addition of polymer.	95
Table 31—Low salinity tests with Enordet series and SDS and SDBS.	96
Table 32—Alcohol-based Enordet surfactants.	97
Table 33—Aspiro surfactant series 1.	97
Table 34—Aspiro surfactant series 2.	98
Table 35—Glass tube experiment results and micrographic visualization.	100

Chapter 1: Introduction

1.1 Introduction

Heavy oil is a widely-distributed, important resource which can be found in countries such as Canada, Venezuela, USA, and China. For heavy oil reservoirs, viscosity and density reduction are the most commonly used recovery mechanisms (Mohsenzadeh et al. 2015). Thermal EOR methods are most commonly applied for heavy oil recovery and these application methods include SAGD (Steam-Assisted Gravity Damage), CSS (Cyclic Steam Stimulation), and steam flooding and in-situ combustions. However, the aforementioned methods are known to consume a huge amount of fresh water and fuels and cause CO₂ emission. Steam injection methods can also lead to heat loss to the overburden, underburden, and aquifer due to temperature difference (Farouq 1976; Wu et al. 2012; Gu et al. 2015). In addition, thermal methods are also inappropriate for thin formations, reservoirs with huge depths and low formation permeability (Farouq 1976).

As an alternative to the thermal methods, non-thermal oil recovery methods are recommended. Common non-thermal methods for the optimal oil recovery include alkaline flooding, surfactant flooding, polymer flooding, and alkaline-surfactant-polymer flooding. Recently, unconventional oil recovery methods, such as nanoparticle application, in heavy oil recovery have also gained wide attention. Nanoparticles can enhance oil recovery by forming Pickering emulsions or altering wettability of the porous media (Binshang et al. 2005; Kazemzadeh et al. 2014; Arab et al. 2018; Ogolo et al. 2012). With appropriate chemicals selection and their suitable application, heavy oil recovery can be significantly improved by emulsification as the main mechanism (Chopra et al. 2010; Sheng 2001).

The objective of this study is cost-effective enhanced heavy recovery by in-situ emulsification. Various emulsification/emulsion stability tests are conducted such as glass tube tests, microscopic visualization test, particle size distribution analyses, glass bead flooding tests, sandpack flooding tests, core flooding tests, and slim tube flooding tests (1m in length) to obtain stable Winsor type 4 oil-in-water emulsion production. In order to achieve this goal, first, commonly available conventional, commercial chemicals such as anionic and cationic surfactants, carbonate powders, anionic polymers, ionic liquids along with unconventional chemicals such as nanofluids and lab-synthesized DES (Deep Eutectic Solvents) are tested for

their capacity to generate emulsions by glass tube tests and microscopic visualization. Concentration tests and stabilization tests are conducted for cost optimization and particle size distribution analyses are carried out for more fundamental visualization of emulsion stability. After the screening process, selected chemicals that have displayed optimal capacity to generate emulsions are hybridized to produce complex colloidal dispersions, which can survive harsh reservoir conditions and lead to efficient heavy oil recovery through tight emulsification. Created solutions are then used to conduct sandpack flooding, glassbead flooding, Berea sandstone, core flooding and long slim tube flooding to test their ability to enhance heavy oil recovery by in-situ emulsification. Produced emulsion samples are collected at various periods to observe the emulsion properties such as emulsion types and emulsion phase behaviour.

In an effort to decrease the recovery costs even further, a cost-effective novel method to enhance heavy oil recovery by emulsification, i.e. biodiesel-in-water steam flooding. is investigated. Biodiesel-in-water emulsions required for these tests are synthesized in the lab through steam treatment of low concentration biodiesel. This thesis discusses the detailed steam treatment methods to generate biodiesel-in-water emulsions that can be used for biodiesel-in-water flooding. BDW with polymer was shown to improve the recovery results by ~ 39% recovery at just 0.5 PV with heavy oil of 3900 cP, which is an astonishing recovery. Then, finally, the impact of hard divalent cations on the emulsion stability is discussed. Diverse chemicals are tested for their ability to form emulsion by glass tube tests and sandpack flooding experiments.

1.2 Statement of the Problem

There are heavy oil fields that do not offer favourable conditions for the application of thermal methods due to factors such as thin formations (less than 3 ft.), excessive depths (greater than 3,000 ft.), and low formation permeability. As an alternative to these thermal methods not appropriate for the reservoirs with the aforementioned conditions, non-thermal exploitation of these reservoirs by chemical flooding is explored. However, chemical flooding can be accompanied by following challenges:

Challenge 1: Compatibility between chemicals and heavy oil. Matching up chemical characteristics with the oil properties, salinities, and hard divalent cation content of the reservoir brines requires rigorous screening and evaluation. Phase behaviour visualization is often applied

as a method to study compatibility (Yang et al. 2010; Barnes et al. 2010). However, the high viscous nature of heavy oil can have a significant impact on visualization and therefore traditional phase behaviour screening tests with light oil must be adjusted.

Challenge 2: Emulsion generation and handling emulsion stability loss in the porous media. Even after having selected or screened optimal chemicals from rigorous screening tests through glass tube tests and microscopic visualization, it is not guaranteed that the selected chemicals will be able to achieve in-situ emulsion generation in a real reservoir for reasons such as chemical adsorption on the surface of porous media, loss of equilibrium ratio between oil, and water in the porous media. To deal with these challenges, experiments using porous mediums must be conducted to test the robustness of the chemicals (Zhang and Somasundaran 2006).

Challenge 3: Controlling the costs of chemical flooding procedure. Chemical flooding can be a costly oil recovery application if it is not optimized and the chemicals are not synthesized properly (Raffa et al. 2016). Concentration optimization of commercial oil recovery chemicals should be researched along with synthesizing novel, cheaper chemicals that can improve heavy oil recovery.

Challenge 4: Negative impact of hard divalent ions in oil recovery. Reservoir brines from real reservoir fields are composed of many types of divalent ions. Glover et al. (1979) stated that divalent cations can influence the microemulsion phase behaviour. Therefore, it is important to understand the impact that cations can have on emulsion generation, and appropriate chemical combinations must be generated.

These challenges bring our attention to the following questions:

1. What are the chemicals or the combinations of chemicals that are robust enough to survive harsh reservoir conditions and enhance heavy oil recover by in-situ emulsification?
2. What are the ways to decrease the concentration of efficient but potentially-costly chemicals to ensure cost-effective chemical injection operation?

3. How does the compatibility between the chemicals and oil change depending on brine composition?
4. What are some other innovative ways to improve oil recovery using chemicals?
5. Can environmentally-friendly biodiesel be applied in heavy oil recovery as a non-thermal heavy oil recovery method as a surfactant additive? If so, what would be the most cost-effective method to successfully apply this method?
6. What kind of impact can hard divalent ions have on heavy oil recovery by in-situ emulsification and how can these challenges be effectively handled?

1.3 Aims and Objectives

In this research, economically viable chemical flooding methods using various traditional chemicals (surfactants, polymers, alkaline powders) and new generation chemicals (nanofluids, biodiesel-in-water emulsion, complex colloidal solution), which can recover heavy oil through in-situ emulsification, are studied and tested through various experimental methods. More specific aims include:

1. Conduct glass tube experiments to screen conventional and new-generation chemicals for enhanced heavy oil recovery applications based on their emulsification capacity. Tested chemicals include surfactants (anionic, cationic, non-ionic), polymer, alkaline powders, ionic liquids, steam treated biodiesel in water emulsion, and nanofluids. After the screening, concentration tests with the selected chemicals displaying robust emulsion stability are conducted at various brine salinity conditions for the purpose of cost optimization.
2. Sandpack ($\Phi = \sim 35\%$), core flooding ($\Phi = \sim 19\%$) setups are established to test the capacity of selected chemicals from the glass tube screening tests to improve oil recovery through in-situ emulsification.
3. Conduct visualization experiments to confirm in-situ emulsion generation at a microscopic level and macroscopic level using Hele-shaw glass chambers and 2D glassbead visual sandpack models ($\Phi = \sim 35\%$). Differing behaviours of chemicals at the interface between heavy oil and brine are recorded and studied.

4. Application of steam treated biodiesel-in-water emulsion in enhanced heavy oil recovery is considered. The fundamental goal is formulating stable biodiesel-in-water emulsion with steam to obtain homogenized emulsion samples that can be used for enhanced heavy oil recovery as a surfactant additive. The soluble and IFT reducing characteristic of biodiesel-in-water emulsion is further exploited with low concentration polymer for effective sandpack flooding to enhance heavy oil recovery.
5. Brine environments with various TDS (Total Dissolved Solids) amounts are created to simulate real reservoir conditions for chemical testing and to understand the impact of TDS on compatibility between chemicals, heavy oil and brine.

1.4 Structure of the Thesis

This paper-based thesis contains 6 chapters. Chapter 2 and Chapter 3 contain two papers that were previously presented at conferences and submitted for peer review. Chapter 4 is a conference paper which will be presented in December 2018. Chapter 5 is a short chapter of experiments that presents solutions to some of the challenges arising from studies in previous chapters.

Chapter 1

This chapter presents an introduction to this thesis. The importance of chemical flooding in heavy oil recovery is discussed followed by limitations found in current and previous chemical flooding methods. Research questions arising from these limitations are presented and aims and objectives to challenge these limitations follow.

Chapter 2

Laboratory scale screening of various chemicals is conducted to test their capacity to generate stable heavy oil-in-water emulsion. First, various commercially available chemicals are screened by glass tube tests along with microscopic visualizations to observe the emulsification effect. Salinity tests are also conducted to determine the optimal salinity conditions for the most efficient chemicals selected. After screening the high performing chemicals at their optimal salinity conditions, concentration tests are

conducted to determine the optimal concentration of selected chemicals for better cost management. Cost-effective emulsion stabilization is the main objective of chapter.

Chapter 3

Continuing the study introduced in Chapter 2, performance of selected chemicals from the previous chemical screening experiment is discussed after they have been further to generate a stable complex colloidal solution. Rate dependency core flooding, sandpack flooding, and slim tube sandpack flooding experiments are conducted repeatedly to further confirm the in-situ emulsion generation capacity of the chemicals in a setting similar to a real reservoir. Zeta-potential is also measured to confirm the stability of the synthesized complex colloidal solution.

Chapter 4

This chapter introduces a novel flooding method using biodiesel and polymer for their potential to be applied in heavy oil recovery. The chapter elaborates on the detailed procedure of steam treated biodiesel-in-water emulsion (SBDWE) flooding, starting with the steam treatment process of biodiesel-in-water emulsion and its eventual injection into a sandpack to confirm its capacity to enhance heavy oil recovery. Chemicals such as polymer and silica are introduced in this study for further SBDWE stabilization.

Chapter 5

This chapter discusses the impact that hard divalent cations can have on emulsion stability. Hard divalent cations are introduced in this study in order to simulate brines of a real reservoir setting. Commercially available chemicals which are hardness resistant are tested at various salinity conditions. Importance of selecting an appropriate chemical for different brine conditions with addition of polymer as a stabilizing agent of emulsions is discussed. Glasstube tests along with sandpack flooding experiments are conducted to observe the behavior of chemicals and oil in their interaction with hard brines.

Chapter 6

This chapter summarizes the conclusions and contributions of this thesis. The limitations and recommendations are also presented in this chapter for the improvement in future work.

Chapter 2: Characterization of Microemulsions as a Screening Tool of Chemicals and Nano Materials Screening for In-situ Recovery of Heavy Oil

Chapter 2 is a modified thesis-appropriate version of SPE 186344. The SPE conference paper was presented at SPE/IATMI Asia Pacific Oil & Gas Conference and Exhibition held in Jakarta, Indonesia, 17-19 October 2017. The journal version of this conference paper has been published in Journal of Petroleum Science and Engineering.

2.1 Preface

This paper reports laboratory scale screening of different chemicals based on microemulsion generation and the feasibility to be recommended for non-thermal heavy oil recovery applications. The objective of this study is to discover optimal chemicals that can form Winsor type 4 oil in water emulsions with heavy oil.

The study was performed through visualization of microemulsions generated using vials and microscopic images. The impact of brine salinity on the emulsification was studied thoroughly in order to identify the synergy between the selected chemicals and the heavy oil. An alcohol propoxy sulfate surfactant from the Alfoterra series, Alfoterra S23-7S-90, a non-commercial surfactant blend HORA-W10, performed best for emulsion formation at low salinity conditions (2.5 wt.%, 3.8 wt.%), whereas Polysorbate-type nonionic surfactant Tween 20 performed best for high salinity conditions (6.35 wt.%, 7.6 wt.%). The observed performance was obtained for oil with a viscosity of 4.812 mPas and 11.74 °API. Moreover, the results helped creating an initial performance correlation, with dependence on two variables: crude oil composition and synthetic brines. Attempts were also made to stabilize oil-in-water emulsions formed with Alfoterra S23-7S-90, HORA-W10, Tween 20 using nanofluids (metal oxides), sodium carbonate, and an anionic polyacrylamide-based polymer (PolyFlood MAX-165). Emulsions were visualized under the Axiostar plus transmitted-light microscope and their stability was studied in order to screen the most optimal chemical (or chemical combinations) available for low cost heavy oil recovery.

Key words: Emulsion stability, heavy-oil recovery, pickering emulsions, nano-fluids, surfactants.

2.2 Introduction

Economically recovering heavy oil is found to be challenging due to recent decline in oil prices. Thermal methods such as CSS (cyclic steam stimulation), steam flooding, SAGD (steam-assisted gravity drainage), are predominantly used in the heavy oil industry for enhanced recovery. These methods can improve the ability of heavy oil flow in reservoirs by changing the physical properties of oil such as viscosity and density (Mohsenzadeh et al. 2015). However, for thin or deep heavy oil reservoirs, steam injection methods are not economically feasible due to the heat losses to the overburden, underburden, and aquifer (Wu et al. 2012). Other drawbacks of thermal

methods include high consumption of energy and fresh water as well as CO₂ emission. These thermal methods drawbacks led to increase in popularity of non-thermal methods such as chemical injection. Chemical methods include alkaline flooding (emulsification), surfactant flooding (IFT reduction), polymer flooding (improvement in sweep efficiency), and ASP (alkaline-surfactant-polymer) flooding. Surfactant EOR (enhanced oil recovery) technique is used to help lower IFT, which leads to enhanced oil displacement efficiency. The use and application of a suitable surfactant could promote the generation of low enough IFT's and therefore facilitate the emulsion formation, thus, to improve the displacement efficiency. Moreover, the formation of emulsions can also help reducing water mobility and improving volumetric sweep efficiency (Chopra et al. 2010; Sheng 2001).

Alkaline flooding can also enhance oil-in-water emulsification between oil and brine using surfactants naturally existent in heavy oil. However, the flooding may become ineffective if the chemical is adsorbed on the rock surface or has reactions. Therefore, it is important to create emulsions that are sufficiently stable enough to eventually achieve enhanced oil recovery. This technique might not lead to high recovery factors but it may turn out to be economically efficient due to low cost of application as long as oil-compatible (and inexpensive) chemicals such as silicon dioxide, sodium carbonate are selected. Therefore, the application of low IFT chemical flooding for heavy oil requires careful laboratory screening work. When selecting a chemical for chemical EOR, attention should be paid to the structure of the chemicals that are suitable for certain reservoir characteristics such as salinity, hardness of water (divalent ion concentration), temperature, and oil type (viscosity, SARA, TAN). Chemical synthesis (mixture of different chemical types such as surfactants, nanofluids, alkalis, polymers) is another option to ensure emulsion generation and, more importantly, stability.

Obtaining low IFT through visual laboratory-based oil and water phase behavior tests is often the main tool for screening suitable chemicals for emulsification at optimal application conditions (Barnes et al. 2008). This paper describes the implemented workflow for glass tube experiments, combined with the results of the visualization of the screened chemicals. Chemical structure correlations generated from the glass tube experiments with the purpose of defining optimal chemical combinations with several stabilizing agents for enhanced emulsion stability.

2.3 Materials

OIL

Heavy dead crude oil from an oil field in Western Saskatchewan was used throughout the experiments. Density and viscosity of the oil were measured to be 0.981kg/m³ and 4,812 cP at room temperature (~25°C). The API gravity of the oil is 11.74°. The heavy oil has a mean TAN (Total Acid Number) of 3.2 mg KOH/g.

Asphaltenes and resins play a significant role in the viscosity of heavy oil (Wu et al. 2012). Asphaltenes and resins have different molecular weights but share the same chemical composition. They both are amphiphilic, which refers to the preference to move to the water and oil interface, when in contact with water. Relatively low molecular weight resin reaches the oil and water interface faster than asphaltene and, therefore, disturbs the asphaltene solubility resulting in flocculation of asphaltene around the water droplets. The asphaltene aggregates are known to be responsible for natural emulsion stability (Daniel-David et al. 2008; Sjöblom 2001). The asphaltene and resin content of the oil used is given in Table 1.

Table 1—Chemical properties of oil.

Specification	Unit	Value	Test method
Saturates	Wt.%	29.36	SARA
Aromatics	Wt.%	25.65	SARA
Resins	Wt.%	29.51	SARA
Asphaltenes	Wt.%	14.78	SARA

BRINES AND CHEMICALS

Synthetic brine was used in the aqueous phase. 2.5%, 5.1%, and 7.6% brine samples (NaCl) were prepared to represent different salinity conditions and were dyed with a water-based tracer IFWB-C7 fluorescent dye for enhanced visualization. Fluorescent-dyed brine samples were used for glass tube tests. 3.8% and 6.35% brine samples without the fluorescent dye were used for stability experiments where stabilizing agents were added in order to enhance emulsion stability. The pH of the brine solutions of different salinities was measured to be 6.7. The list of chemicals for the glass tube tests are presented in **Table 2**.

Table 2—Chemicals Screened and Evaluated in this Study.

Chemicals	Type	Abbreviation	Active matter (%)
AAS J13131	Alcohol Alkoxylate Sulfate (or alkyl ether sulfate)	AAS 1	29.1
AAS J11111	Alcohol Alkoxylate Sulfate (or alkyl ether sulfate)	AAS 2	27.67
AAS J771	Alcohol Alkoxylate Sulfate (or alkyl ether sulfate)	AAS 3	29.7
Alfoterra 145-8S-90	Alcohol Propoxy Sulfate	APS 1	89.2
Alfoterra 145-4S-90	Alcohol Propoxy Sulfate	APS 2	82.2
Alfoterra S23-7S-90	Alcohol Propoxy Sulfate	APS 3	85.1
IOS 0332	Internal Olefin Sulfonate	IOS 1	27.99
IOS 0242	Internal Olefin Sulfonate	IOS 2	18.99
IOS 0352	Internal Olefin Sulfonate	IOS 3	69.4
LTS-18	Alkyltoluene Sulfonate	LTS	14.27
Arquad 2C-75	N/A	Arquad	N/A
[BMIm] ⁺ [BF ₄] ⁻	Ionic liquid	IOL	N/A
Tween 20	Polysorbate 20	PSB 20	N/A
Tween 80	Polysorbate 80	PSB 80	N/A
WITCONOL NP-40	Nonylphenol (4) ethoxylate	NP	N/A
DES 1 (Reline)	2 hydroxyethyl trimethyl ammonium chloride, urea	DES 1	N/A
DES 2 (Ethaline)	Hydroxyethyl trimethyl ammonium chloride, 1,2,3 Propane triol	DES 2	N/A
DES 3	Sodium carbonate, 1,2,3 Propane triol	DES 3	N/A
HORA-W10	Non-commercial surfactant blend	HORA	N/A
SDS	Sodium Dodecyl Sulfate	SDS	N/A
Na ₂ CO ₃	Sodium Carbonate	Na ₂ CO ₃	N/A
C ₁₈ H ₂₉ NaO ₃ S	Sodium Dodecylbenzenesulfonate	C ₁₈ H ₂₉ NaO ₃ S	N/A
NaC ₁₂ H ₂₅ SO ₄	Sodium Dodecyl Sulfate	NaC ₁₂ H ₂₅ SO ₄	N/A

2.4 Methodology

2.4.1 Glass Tube Test

Glass tubes and their caps were prepared and held in a rack for stability. Brine solutions/oil mixtures with oil-brine ratio of 1:1 (2 g each) were made up in different tubes and the concentration of the surfactant solution was kept at 1.5 wt.% for the initial glass tube test. 1.5 wt.% concentration was chosen based on the preliminary screening of chemicals. Preliminary screening displayed that for most chemicals listed in this research, the concentration of chemicals lower than 1.5 wt. % could not lead to any type of observable emulsification. Emulsions were observed and analyzed at distinct times (after 1, 6, 24 hours, and 7 days). At various time intervals, emulsion quality was tested by naked-eye observation and light manual agitation and the results were recorded. Barnes et al. (2008) addressed in their study that promising behavior is the smooth movement of uniform oil-in-water emulsions while less promising behavior is the formation of viscous gels or oil globules. Promising systems are kept for several weeks for further observation (**Figure 1**). For unstable emulsion systems, a rapid phase separation between the oil and brine is observed. For stable emulsions, the emulsion samples in the tubes are uniformly black and a Winsor type 4 emulsions are formed. It is common to calculate the ESI (emulsion stability index) using an Eq. 1 (Wang et al. 2017) to determine the stability of the emulsions in an emulsion stability study. However, due to the high viscosity of heavy oil used and possible attraction forces caused by chemicals causing emulsion or oil to spread on the inner surface of the tube, the equation could not be applied in this study. It is important to be cautious of the inner oil coating of the glass tube surface that can interfere with naked-eye visualization. Such inner surface coating can negatively influence the accurate measurements of volume of the emulsion layer and the total volume of samples.



Figure 1—Left: promising system, Right: less promising system.

$$ESI = \left(1 - \frac{Vol.Emulsion}{Vol.Total}\right) \times 100\% \quad (1)$$

Glass Tube Test Emulsification

The most common method to create an emulsion in the modern chemical enhanced oil recovery industry is to use surfactants. Whether a surfactant will create an oil-in-water emulsion or a water-in-oil emulsion can be determined by using Bancroft's rule (2013). Bancroft's rule states that in order to create a water-in-oil emulsion, the continuous phase of the emulsion should be where the surfactant is most soluble. For example, as sodium dodecyl sulfate is hydrophilic, it has the ability to form an oil-in-water emulsion as the continuous phase of oil-in-water emulsion is water (Bancroft 2013; Stamkulov 2008). The continuous phase of oil-in-water emulsions is water. Oil-in-water emulsions are less viscous than the crude oil, which allows the emulsion to be displaced more easily than the crude oil itself.

Emulsification and oil entrainment are considered to be a recovery mechanism that can lead the oil to be produced as a low viscosity oil-in-water emulsion (Liu 2007; Johnson 1976). Alkalis can also be used to create emulsions when mixed with heavy oil for enhanced oil recovery. Alkalis can neutralize the organic acids that exist in the heavy oils creating in-situ surfactants (Liu 2006). To create emulsions, the IFT between the chemical/brine mixture and oil must be low otherwise the liquid phases cannot be "mixed" spontaneously. If the IFT is not sufficiently low, in order to create new interfaces such as that represented by the Laplace equation, the Gibbs free energy of formation must be overcome by adding extra energy (shear force). The lower the IFT, the lower the extra force, which is required for the two liquids to mix. Therefore, In order to create a stable emulsion and obtain effective mixing without adding additional extra force, obtaining low IFT is essential (Mohsenzadeh 2015). In this work, chemicals of various classes are tested for their ability to form an oil-in-water emulsion by using light manual agitation. Therefore, it is essential to obtain low IFT between oil and water by finding chemicals that can demonstrate good synergy with the provided brine and heavy oil.

2.4.2 Concentration Test

Concentration tests were conducted with optimal surfactants selected from the previous glass tube test. The concentrations of the surfactants were varied to observe the impact of the

concentration of surfactants on droplet sizes and their distribution. The test helped determine the optimal concentration (cost-effectiveness) for each surfactant, which could then be used for further testing of emulsion stability by adding several stabilizing agents.

Surfactants (APS 3, HORA, PSB 20) of various concentrations (1 wt.%, 0.8 wt.%, 0.6 wt.%, 0.4 wt.%, 0.2 wt.%) were injected with brine samples of two different salinities (3.8 wt.%, 6.35 wt.%). They were subsequently mixed with heavy oil to create emulsion samples and injected into the visualization glass chamber to be viewed under the transmitted-light microscope. The impact of surfactant concentrations on the particle size distribution was studied. Large oil droplets indicate the coalescence of oil droplets due to the loss of emulsion stability. An optimal emulsifier should not lead to a change in particle size distribution with time. ImageJ software was used to process the gray value histogram and generate particle size data necessary to plot particle distribution graphs (Barboriak 2005; Girish 2004).

2.4.3 Stabilization Test

Surfactants of a specific concentration were injected into the prepared synthetic brine samples (sodium chloride) of a certain salinity with which the surfactants performed optimally in the previous glass tube test. After the injection of a surfactant, heavy oil was added and the samples were manually agitated. Formed emulsions were then immediately injected into the visualization glass chambers and studied under the Axiostar plus transmitted-light microscope. Surfactant concentration (0.6 wt.%) was selected based on the particle distribution plot (Figs. 3 to 5). Emulsion formed with surfactants with and without addition of stabilizing agents were observed under the microscope at regular time intervals (immediately after, 5 minutes later, 10 minutes later, 15 minutes later, 1 hour later, 7 hours later).

2.5 Results

2.5.1 Glass Tube Test Results and Discussions

The screening and performance criteria used for chemical evaluations are presented in **Table 3**. The criteria in the table were selected based on the properties required for effective visualization and analysis of Winsor type 4 heavy oil in water emulsification.

Table 3—Detailed standards to screen chemicals based on their ability to create stable oil-in-water emulsions.

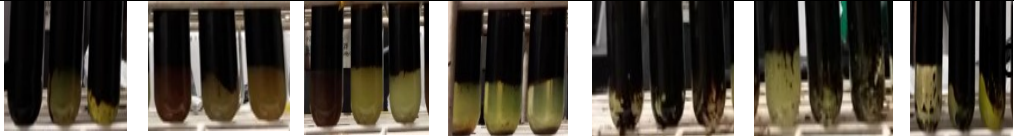
	✓✓	✓	x
Formation of emulsion	Full oil-in-water emulsion (Winsor type 4)	Some oil-in-water emulsion (Winsor type 3)	No emulsion
Stability	Stability that lasts for more than 1 minute before the full separation	Less than 1 minute	No emulsion
Inner surface oil coating	Severe inner surface oil coating	Some inner surface oil coating	No inner surface coating
Oil flow	Easy movement of oil (better than brine/oil mix)	Some movement of oil	Viscous gel
Precipitation	Precipitation		No precipitation

AAS, IOS, LTS Surfactants

Table 4 displays the results of emulsion formation with AAS, IOS, and LTS surfactants at various salinity conditions. Surfactants were first added to the brine samples of 2.5%, 5.1%, and 7.6% salinities, then oil was added and lightly agitated. Immediately after the agitation, it was observed that AAS 1 surfactant could not create an emulsion with a brine sample of 2.5% salinity. This mixture also seemed to coat the inner surface of the glass tube interfering with the glass tube visualization. Similar results were obtained with both 5.1% and 7.6% brine samples. The results remained consistent after 1 hour, 6 hours, 24 hours, and 7 days with no formation of emulsions. Therefore, these samples were discarded after 7 days. AAS 3 could lead to some emulsion formation (Winsor type 3), particularly with a brine of 2.5% salinity but the stability was lost within a minute. Similar results were observed in an emulsion formed with a brine sample of 5.1 wt.% salinity. However, AAS 3 could not form emulsion with a brine sample of 7.6% salinity. Some unstable emulsion was formed with AAS 2 with a brine sample of 2.5% salinity. Viscous gel and precipitation were observed for mixtures formed with 5.1% and 7.6% brine samples. Seven days later, all the mixtures became viscous gels and were discarded. IOS surfactants (IOS 1, IOS 2, IOS 3) and LTS could not form any emulsion; severe inner surface

coating of the glass tubes due to the viscosity heavy oil and attraction forces between the glass tube and the surfactant made it difficult to observe the fluid behavior within the glass tubes.

Table 4—AAS, IOS, LTS surfactants.

	AAS 1	AAS 3	AAS 2	IOS 1	IOS 2	IOS 3	LTS
Formation of emulsion (after agitation)	2.5%:✓	2.5%:✓✓	2.5%:✓✓	2.5%:x	2.5%:x	2.5%:x	2.5%:x
	5.1%:x	5.1%:✓	5.1%:x	5.1%:x	5.1%:x	5.1%:x	5.1%:x
	7.6%:x	7.6%:✓	7.6%:x	7.6%:x	7.6%:x	7.6%:x	7.6%:x
Stability	2.5%:✓	2.5%:✓	2.5%:x	2.5%:x	2.5%:x	2.5%:x	2.5%:x
	5.1%:x	5.1%:✓	5.1%:x	5.1%:x	5.1%:x	5.1%:x	5.1%:x
	7.6%:x	7.6%:✓	7.6%:x	7.6%:x	7.6%:x	7.6%:x	7.6%:x
Inner surface oil coating (interference of visualization)	2.5%:✓✓	2.5%:x	2.5%:x	2.5%:✓	2.5%:✓✓	2.5%:x	2.5%:✓
	5.1%:✓	5.1%:x	5.1%:x	5.1%:✓	5.1%:✓✓	5.1%:✓	✓
	7.6%:✓	7.6%:x	7.6%:✓✓	7.6%:✓	7.6%:✓✓	7.6%:✓✓	5.1%:✓ ✓ 7.6%:✓ ✓
Oil flow (movement)	2.5%:✓	2.5%:✓✓	2.5%:✓✓	2.5%:x	2.5%:x	2.5%:✓	2.5%:x
	(hard to visualize)	5.1%:✓✓	5.1%:✓	5.1%:x	5.1%:x	5.1%:x	5.1%:x
	5.1%:✓ 7.6%:✓	7.6%:✓✓	7.6%:✓	7.6%:x	7.6%:x	7.6%:x	7.6%:x
Precipitation	2.5%: x	2.5%:x	2.5%: x	2.5%:✓✓	2.5%:x	2.5%:✓✓	2.5%:✓
	5.1%:✓	5.1%:x	5.1%:✓	5.1%:✓✓	5.1%:x	5.1%:✓✓	✓
	7.6%:✓✓	7.6%:x	7.6%:✓	7.6%:✓✓	7.6%:x	7.6%:✓✓	5.1%:✓ ✓ 7.6%:✓ ✓
Visual							

APS, PSB, NP, Arquad, HORA

APS 1 could create a Winsor type 3 emulsion with a brine sample of 2.5% but an immediate loss of emulsion stability followed. APS 2 could create an unstable, Winsor type 4 emulsion with a

brine of low salinity, and Winsor type 3 emulsions with brines of higher salinities. It should be noted that, due to the rapid emulsion stability loss after the agitation of the emulsion formed with APS 2, full emulsion formation with the 2.5% brine sample could not be captured as seen in Table 5. Emulsions that were formed with APS 1 and APS 2 lost their stability rapidly. APS 3 could form a stable emulsion and was particularly stable when mixed with a brine of lower salinity. PSB 20, 80 were shown to form stable emulsions with brines of higher salinities (5.1%, 7.6%). NP and Arquad could not form any emulsion and NP, in particular, led to severe inner surface oil coating, which interfered with the glass tube visualization. It can be assumed that high viscosity of the fluids inside the glass tube or the attraction forces existing between the glass and fluid mixture are responsible for such severe inner surface coating of the glass tubes. For PSB 20, 80, at low salinity, particularly with a brine sample of 2.5% salinity, emulsion did not formed. However due to the momentary mixing of the oil and water phase (which led to the smooth oil flow) (Table 5), it appears as if Winsor type 4 emulsions were formed with a brine sample of low salinity. HORA could form emulsions after agitation but the emulsions could not stay stable for longer than 1 min before reaching the full phase separation. Its stability loss with brine samples of 2.5%, 5.1%, and 7.6% salinities had comparable results.

Table 5—APS, PSB, NP, Arquad, HORA.

	APS 1	APS 2	APS 3	PSB 20	PSB 80	NP	Arquad	HORA
Format ion of emulsi on (after agitatio n)	2.5%:✓ 5.1%:x 7.6%:x	2.5%:✓ ✓ 5.1%:✓ 7.6%:✓	2.5%: ✓✓ 5.1%: ✓✓ 7.6%: ✓✓	2.5%:x 5.1%:✓ 7.6%:✓✓	2.5%:x 5.1%:✓ 7.6%:✓✓	2.5%:x 5.1%:x 7.6%:x	2.5%:x 5.1%:x 7.6%:x	2.5%:✓✓ 5.1%:✓✓ 7.6%:✓✓
Stabilit y	2.5%:x 5.1%:x 7.6%:x	2.5%:x 5.1%:x 7.6%:x	2.5%: ✓✓ 5.1%: ✓ 7.6%: ✓	2.5%:x 5.1%:✓ 7.6%:✓✓	2.5%:x 5.1%:✓ 7.6%:✓✓	2.5%:x 5.1%:x 7.6%:x	2.5%:x 5.1%:x 7.6%:x	2.5%:✓ 5.1%:✓ 7.6%:✓
Inner surface oil coating (interfe	2.5%:✓ 5.1%:✓✓ 7.6%:✓✓	2.5%:x 5.1%:x 7.6%:✓	2.5%: x 5.1%: x 7.6%:	2.5%:x 5.1%:x 7.6%:x	2.5%:x 5.1%:x 7.6%:x	2.5%:✓ ✓ 5.1%:✓ ✓ 7.6%:✓	2.5%:✓ ✓ 5.1%:✓ ✓ 7.6%:✓	2.5%:x 5.1%:x 7.6%:x

rence of visualization)			x				✓	
Oil flow (movement)	2.5%:✓✓ 5.1%:✓ 7.6%:x	2.5%:✓ ✓ 5.1%:✓ 7.6%:✓ ✓	2.5%: ✓✓ 5.1%: ✓✓ 7.6%: ✓✓	2.5%:✓✓ 5.1%:✓✓ 7.6%:✓✓	2.5%:✓✓ 5.1%:✓✓ 7.6%:✓✓	2.5%:x 5.1%:x 7.6%:x	2.5%:✓ 5.1%:✓ 7.6%:✓	2.5%:✓✓ 5.1%:✓✓ 7.6%:✓✓
Precipitation	2.5%: x 5.1%: x 7.6%: x	2.5%: x 5.1%: x 7.6%: x	2.5%: x 5.1%: x 7.6%: x	2.5%:✓✓ 5.1%:✓✓ 7.6%:✓✓	2.5%:✓ 5.1%:✓✓ 7.6%:✓✓	2.5%:✓ ✓ 5.1%:✓ 7.6%:✓	2.5%:x 5.1%:x 7.6%:x	N/A
Visual								

Ionic Liquid, Carbonate Powders

Table 6 displays the results of emulsion formation with ionic liquid and carbonate powders with a 2.5%, 5.1%, and 7.6% brine sample. Ionic liquids (ILs) are known as organic solids that have a melting point that is lower than 100°C. They are normally considered to be a good alternative to conventional surfactants because of their advantageous qualities such as environmentally-friendliness, recyclability, high surface activity, and their ability to form a micelle in a harsh environment (Dahbag 2016; Mele 2013). However, an ionic liquid 1-butyl-3-methylimidazolium tetrafluoroborate, also known as BMIM-PF₆ did not perform well and could not form any emulsion in the glass tube test. This is possibly due to the BMIM-PF₆'s hydrophobic nature considering that hydrophilic chemicals in the study were more effective in oil-in-water emulsion formation than hydrophobic chemicals. Sodium carbonate performed well in emulsion formation due to its function as a natural surface active reagent (Ashrafizadeh 2012). It especially showed a good performance with high salinity brine samples. It should be noted that the emulsion samples formed with sodium carbonate were turbid (light-brown color). NaHCO₃ and C₁₈H₂₉NaO₃S failed to form emulsions at various salinity conditions. Sodium bicarbonate is a weaker base than sodium carbonate. Moreover, sodium bicarbonate when reacting with sodium chloride (synthetic brine) can create hydrochloric acid, which is not favorable in emulsion formation.

Table 6— Ionic liquid, Na₂CO₃, NaHCO₃, carbonate powders.

	[BMIm] ⁺ [BF ₄ ⁻] (1-butyl-3-methylimidazolium tetrafluoroborate)	Na ₂ CO ₃ (sodium carbonate)	NaHCO ₃ (sodium bicarbonate)	C ₁₈ H ₂₉ NaO ₃ S (Sodium Dodecylbenzenesulfonate)	CH ₃ (CH ₂) ₁₁ SO ₄ Na (Sodium Dodecyl Sulfate)
Formation of emulsion (after agitation)	2.5%:x 5.1%:x 7.6%:x	2.5%:x 5.1%:✓ 7.6%:✓✓	2.5%:x 5.1%:x 7.6%:x	2.5%:x 5.1%:x 7.6%:x	2.5%:x 5.1%:x 7.6%:x
Stability	2.5%:x 5.1%:x 7.6%:x	2.5%:x 5.1%:✓ 7.6%:✓✓	2.5%:x 5.1%:x 7.6%:x	2.5%:x 5.1%:x 7.6%:x	2.5%:x 5.1%:x 7.6%:x
Inner surface oil coating (interference of visualization)	2.5%:x 5.1%:x 7.6%:x	2.5%:✓ 5.1%:✓ 7.6%:✓✓	2.5%:✓ 5.1%:✓ 7.6%:✓	2.5%:✓ 5.1%:✓ 7.6%:✓	2.5%:✓ 5.1%:✓ 7.6%:✓
Oil flow (movement)	2.5%:✓ 5.1%:✓ 7.6%:✓	2.5%:✓✓ 5.1%:✓✓ 7.6%:✓✓	2.5%:x 5.1%:x 7.6%:x	2.5%:x 5.1%:x 7.6%:x	2.5%:✓ 5.1%:✓ 7.6%:✓
Precipitation	2.5%:✓✓ 5.1%:✓✓ 7.6%:✓✓	2.5%:✓✓ 5.1%:✓✓ 7.6%:✓✓	2.5%:✓✓ 5.1%:✓✓ 7.6%:✓✓	2.5%:✓✓ 5.1%:✓✓ 7.6%:✓✓	2.5%:x 5.1%:x 7.6%:x
Visual					

Deep Eutectic Solvents. Deep Eutectic Solvents (DES) are composed of two or more components that are capable of self-association. DESs are non-toxic, biodegradable, recyclable, non-flammable, environmentally-friendly, and inexpensive (Mohsenzadeh 2015). The effectiveness of DESs in emulsion formation at ambient temperature was investigated (Table 7). DES 1 was synthesized in our laboratory using 2-hydroxyethyl trimethyl ammonium chloride and urea (Pal et al. 2014). DES 2 was synthesized using Hydroxyethyl trimethyl ammonium chloride, 1,2,3 Propane triol. DES 3 was prepared with sodium carbonate, 1,2,3 Propane triol. DES surfactants could not form emulsions with 3.8% and 6.35% brine samples. Non-fluorescent

brine samples were used in this test to avoid any possible chemical reaction between the solvents and the chemical dye.

Table 7—DES 1, DES 2, DES 3.

	DES 1	DES 2	DES 3
Formation of emulsion (after agitation)	3.8%: x	3.8%: x	3.8%: x
	6.35%:x	6.35%:x	6.35%:x
Stability	3.8%: x	3.8%: x	3.8%: x
	6.35%:x	6.35%:x	6.35%:x
Oil flow movement	3.8%: x	3.8%: x	3.8%: x
	6.35%:x	6.35%:x	6.35%:x
Precipitation	3.8%: x	3.8%: x	3.8%: x
	6.35%:x	6.35%:x	6.35%:x
Visual			

2.5.2 Concentration Test Results and Discussions

Optimal Surfactants at Low Salinity Conditions (APS 3, HORA)

From the previous glass tube test (Table 5), APS 3 surfactant, HORA displayed optimal performance in emulsion formation at low salinity conditions. To further observe the impact that the concentration of a surfactant can have on the droplet sizes of emulsion and, therefore, its stability, emulsions of various surfactant concentrations at low salinity condition were observed under the microscope and their gray value histograms were generated using a public domain software ImageJ (**Table 8**). In total, 200 droplets were selected manually to generate the particle size data. Particles were measured using ImageJ as displayed in Figure 2. It should be noted that the emulsion formed with 0.2% concentration of HORA could not be injected into the visualization glass chamber to be visualized under the microscope due to its immediate phase separation (**Table 9**). The emulsion sample formed with 0.2 wt.% HORA was subsequently discarded.

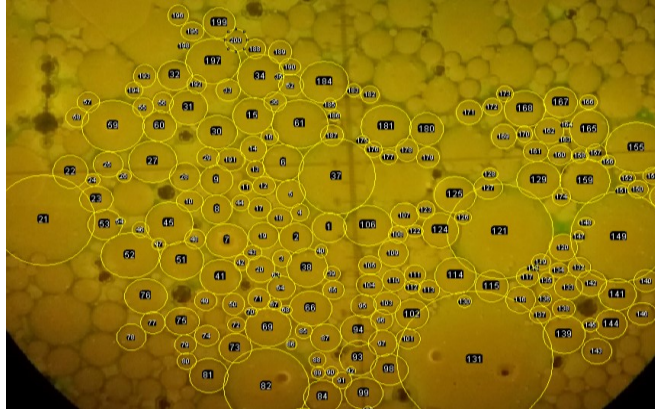


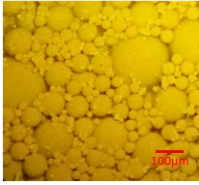
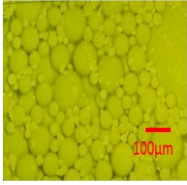
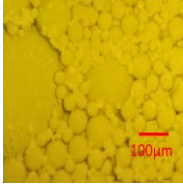
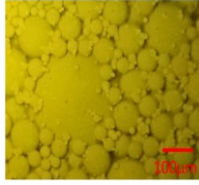
Figure 2—Manual particle selection using ImageJ (APS 0.8 wt. %).

Table 8—Gray value histograms of micrographs at various concentrations (APS 3, HORA) – Salinity: 3.8%.

S \ C	C				
	1%	0.8%	0.6%	0.4%	0.2%
APS 3					
HOR A					N/A

Table 9—Micrographs taken at various concentrations (APS 3, HORA) - Salinity: 3.8%. *S: surfactant C: concentration

S \ C	C				
	1%	0.8%	0.6%	0.4%	0.2%
APS 3					

HORA					N/A
------	---	---	---	--	-----

Figures 3 and 4 displayed that, for both APS 3, HORA, significant enlargement of particle sizes is observed when the concentration of the surfactants is reduced to 0.4 wt.%. This enlargement is due to the rapid coalescence of oil droplets, which indicates fast emulsion stability loss. Since surfactants of a concentration lower than 0.6 wt. % displayed apparent enlargement of particles sizes due to the coalescence of droplets, 0.6 wt.% was selected as the optimal concentration for further emulsion stability tests with APS 3 and HORA in a low salinity environment.

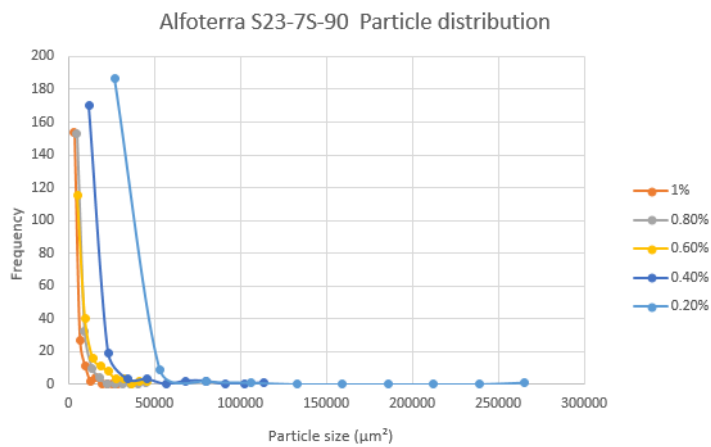


Figure 3—APS 3 particle distribution plot.

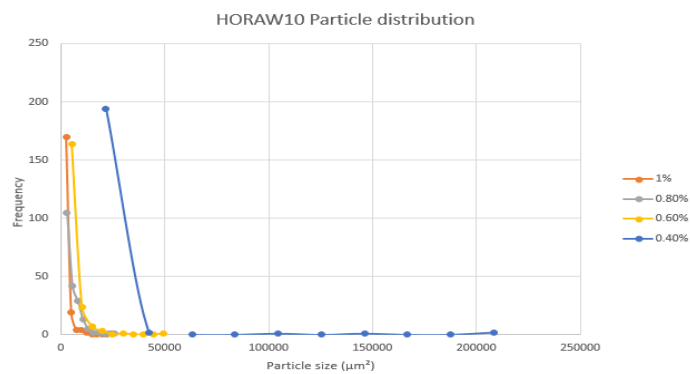


Figure 4—HORA particle distribution plot.

Optimal surfactant at a high salinity condition (PSB 20). From the glass tube experiment (Table 5), PSB 80 and PSB 20 showed optimal performance in emulsion formation at high salinity condition (6.35%) (Fig. 5). PSB 80 and PSB 20 are polysorbate-type surfactants. HLB value of PSB 20 is slightly higher (16.7) than PSB 80 (15). As hydrophilic chemicals have consistently shown better performance in forming an oil-in-water emulsion than hydrophobic chemicals during the glass tube test, PSB 20 was selected for the concentration test. It was observed that with the decrease in concentration of the surfactant, particles of relatively large diameters began to appear (Table 10). This was further studied through gray value histogram analysis (Table 11). This phenomenon occurs due to the rapid emulsion stability loss that comes with faster coalescence of oil droplets due to the decreased concentration of the surfactant. Stability loss seemed more apparent when the concentration of the surfactant was reduced to 0.4 wt. %.

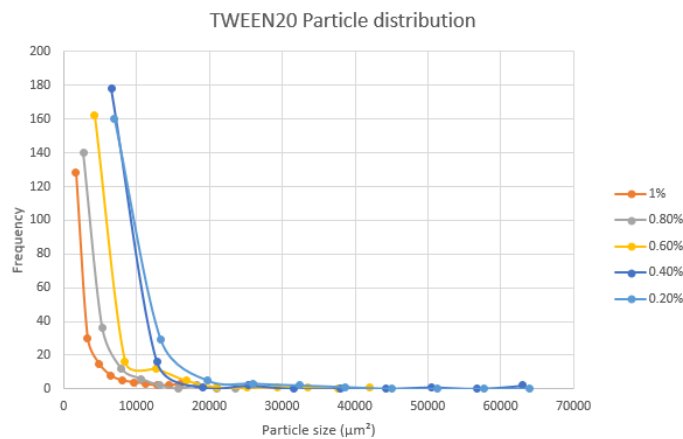
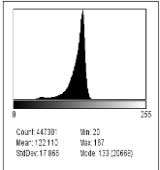
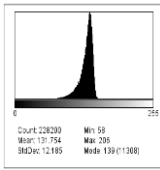
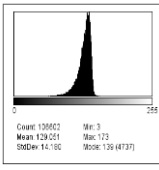
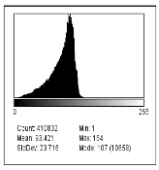
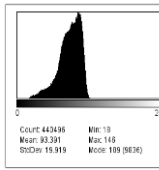


Figure 5—PSB 20 particle distribution plot.

Table 10—Micrographs taken at various concentrations (PSB 20) - Salinity: 6.35%.

		C				
		1%	0.8%	0.6%	0.4%	0.2%
S	PSB					
	20					

Table 11—Gray value histograms of micrographs at various concentrations (PSB 20) - Salinity: 6.35%

	C	1%	0.8%	0.6%	0.4%	0.2%
S						
PSB 20						

2.5.3 Stabilization test

Important factors to consider in modern chemical EOR include investigating the synergy of different processes using various classes of chemicals and thereby reducing the amount of injected chemicals. In order to cost-effectively decrease the interfacial tension, which is typically 30-35 mN/m between oil and water, an appropriate surfactant must be selected. Surfactants have the ability to reduce IFT to 1-5 nM/m depending on the compatibility between the injected chemicals and reservoir fluids (Stamkulov 2008). However, it is important to note that IFT reduction alone cannot guarantee a stable emulsion. There are various factors to consider in order to enhance the stability of an emulsion. Surface films that exist at the oil and water interface can enhance the emulsion stability by increasing the interfacial viscosity. Viscoelastic films can provide a barrier against coalescence. Coalescence is the merging of two or more droplets and leads to a significant loss of structural integrity of emulsion before the phase separation occurs (Alvarado 2011) (**Figure 6**).

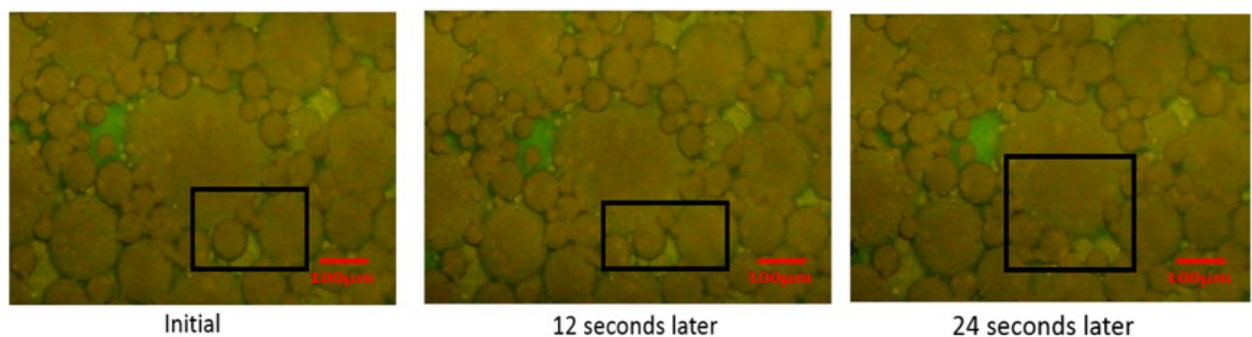


Figure 6—APS 3, 0.6 wt. % coalescence process.

Highly viscous interfaces can slow down the oil-film drainage and, therefore, enhance emulsion stability. The viscoelastic nature of the film can also be influenced by the pH value (Jones 1978).

Minimization of density differences between the oil phase and the water phase can also assist in emulsion stabilization. Reduction of droplet sizes can lead the stability of an emulsion against gravitational separation according to the Stoke’s law (Risch 1988). Several types of stabilizing agents were used in this study to enhance the stability of the emulsions at low and high salinity conditions (**Table 12**).

Table 12—Properties of stabilizing agents.

Stabilizing agents	Electrical			
	Class	Particle Size	Hydrophilicity/solubility	Charge
Aluminium Oxide	Nanofluids	Original: 10 nm Final: N/A	Hydrophilic	Non-ionic
Silicon Oxide	Nanofluids	5-35 nm	Hydrophilic	Non-ionic
Zirconium Oxide	Nanofluids	45-55 nm	Hydrophilic	Non-ionic
PolyFlood MAX-165 (polyacrylamide-based)	Polymer	N/A	Water-soluble	Anionic
Sodium Carbonate	Alkali		Water-soluble	

Emulsions that are stabilized by solid particles are called Pickering emulsion named after S.U. Pickering. When particles are adsorbed at the oil-water interface, a layer of particles is formed around the drops, which sterically inhibits the droplet coalescence therefore, improving the stabilization of emulsion (Binks 2016; Zhang 2010; Chavalier and Bolzinger 2013). The Van der Waals and electrostatic attractions between the charged surfactants and nanoparticles can be utilized to create a structurally stable colloidal layer in the Pickering emulsion system that can help form a stable emulsion (Yoon 2016).

Polymer also has the ability to enhance emulsion stability. Hydrocolloids, which are a heterogeneous group of long chain hydrophilic polymers, can function as an emulsion stabilizer (Saha 2010). These macromolecules can provide a physical barrier against coalescence enhancing the emulsion stability. It is commonly known that lignin, which is the second most abundant natural polymer after cellulose, also has a strong emulsifying ability (Gould et al. 2016).

Polyelectrolytes are charged polymers known to stabilize emulsions through electrostatic interaction. Stamkulov et al. (2008) showed a possibility of stabilizing oil-in-water emulsions by combining hexadecyl amine and a high molecular weight polyelectrolyte. Hexadecyl amine could leave the droplets positively charged, therefore, negatively charged polyacrylic acid adsorb on the positively charged droplets, eventually forming a steric barrier, which can prevent droplet coalescence (Stamkulov 2008). Polymer also has the ability to enhance adsorption of surfactant at the oil and water interface further leading to emulsion stability (Hamedi-Shokrlu and Babadagli 2014).

Decreasing IFT can also lead to higher stability of emulsions. Alkalis such as sodium carbonate can also be used to reduce IFT and create emulsions when mixed with heavy oil for enhanced oil recovery. Alkalis have the capacity to neutralize the organic acids that exist in the heavy oils creating natural surfactants (Lui et al. 2006; Poteau et al. 2005).

Stabilization test results and discussions

Stabilization of emulsions with APS 3 (Brine Salinity: 3.8 %). **Tables 13 and 14** display the results of stability of emulsions formed with APS 3 with or without addition of stabilizing agents. APS 3 is an anionic alcohol propoxy sulfate (Gupta 2016). The stability of emulsions was studied based on their micrographs taken at regular time intervals. Rapid coalescence (**Figure 6**) is a sign of emulsion stability loss. Stable droplet sizes that are kept over time without coalescence or flocculation (**Figure 7**) indicate a stable emulsion.

Table 13—Glass tube test of alfoterra and added stabilizing agents.

	APS 3 (0.6%)	APS 3 (0.6%) + ZrO ₂ (0.4%)	APS 3 (0.6%) + Al ₂ O ₃ (0.4%)	APS 3 (0.6%) + Al ₂ O ₃ (0.2%) + ZrO ₂ (0.2%)	APS 3 (0.6%) + Sodium carbonate (0.4%)	APS 3 (0.6%) + Polymer (0.4%)	APS 3 (0.6%) + Al ₂ O ₃ (0.2%) + Polymer (0.2%)
Formation of emulsion (after	3.8%: ✓✓	3.8%: ✓✓	3.8%: ✓✓	3.8%: ✓✓	3.8%: ✓✓	3.8%: ✓✓	3.8%: ✓✓

agitation)

Stability	3.8%: ✓✓	3.8%: ✓✓	3.8%: x	3.8%: x	3.8%: ✓✓	3.8%: ✓✓	3.8%: ✓✓
Oil flow movement	✓✓	3.8%: ✓✓	3.8%: ✓	3.8%: ✓✓	3.8%: ✓✓	3.8%: ✓✓	3.8%: ✓✓

Glass tube

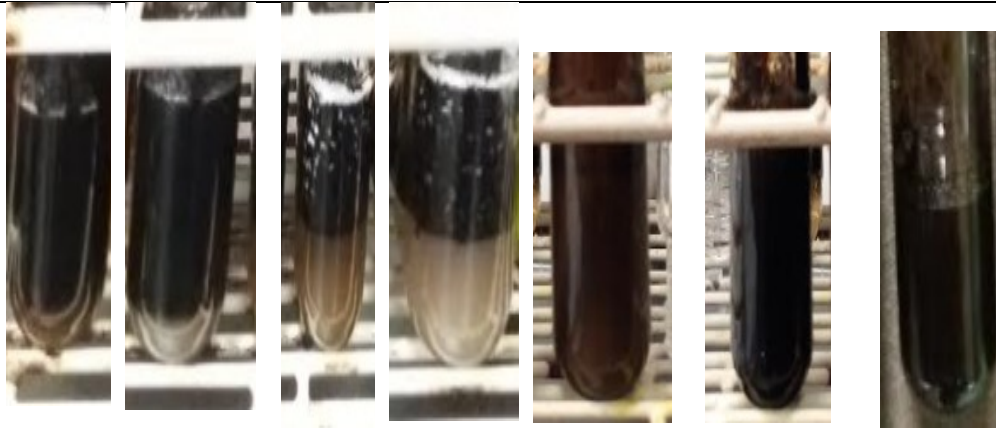
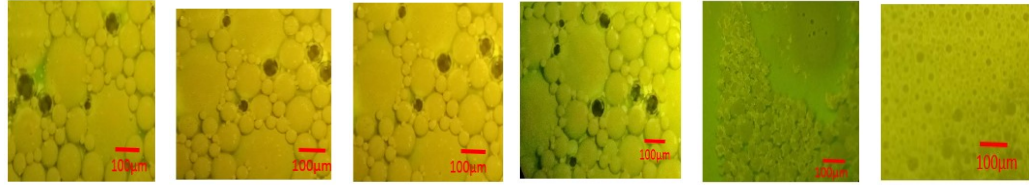


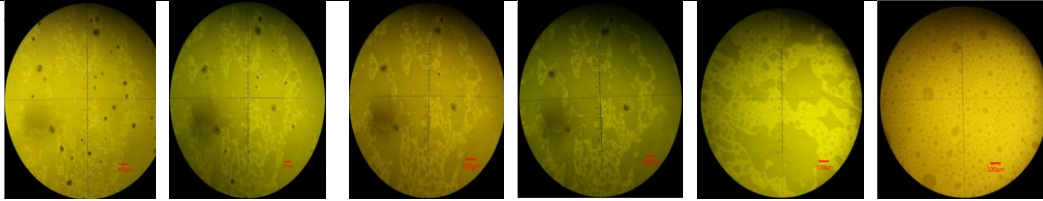
Table 14—Micrographs of stabilized emulsions taken at regular time intervals (APS 3).

Chemicals	Immediately after	5 minutes later	10 minutes later	15 minutes later	1 hour later (different spot in glass chamber) visualization	7 hours later (different spot in the glass chamber) visualization
APS 3 0.6 wt. %						

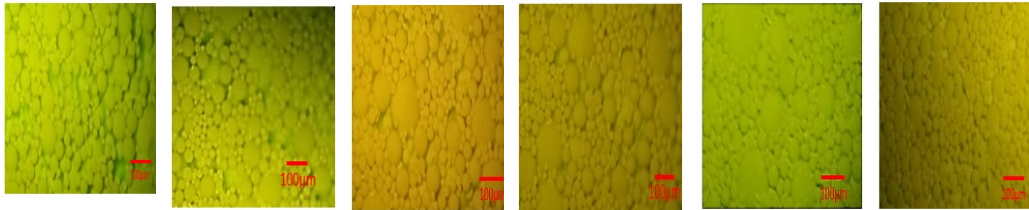
APS 3 0.6
wt.% +
Zirconium
Oxide 0.4
wt.%



APS 3 0.6
wt.% +
Sodium
carbonate
0.4 wt.%



APS 3 0.6
wt.% +
Polymer 0.4
wt.%



APS 3 0.6%
+ Al₂O₃
0.2% +
Polymer
0.2%

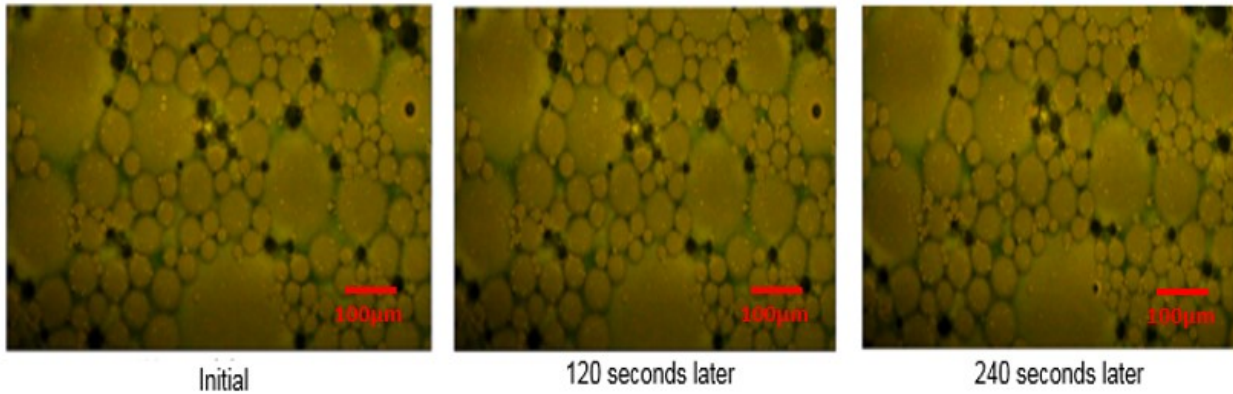
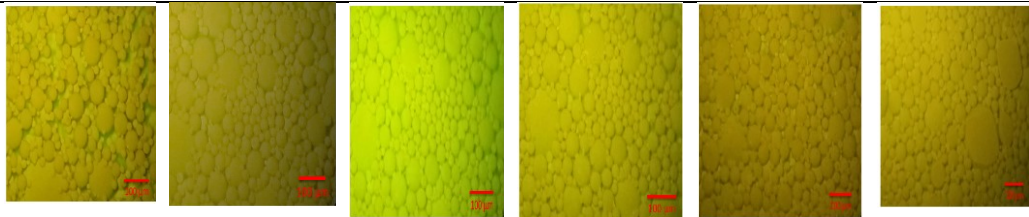


Figure 7—APS 3 0.6 wt.% + Zirconium Oxide 0.4 wt.% coalescence process.

APS 3 (0.6 wt. %) without stabilizing agents. Some flocculation of the oil droplets were observed within the 5 min period along with the rapid appearance of bright precipitates. Oil droplets maintained their size and shape for over 15 min. 1 h later, complete phase separation was observed.

APS 3 (0.6 wt. %) + Zirconium Oxide (0.4 wt. %). Droplet sizes remained consistent and stable for 30 min before the emulsion began to lose its stability. Black spots indicate bubbles formed during the injection of emulsion into the visualization glass chamber.

APS 3 (0.6 wt. %) + Aluminium Oxide (0.4 wt. %). Due to the instability of emulsion and rapid phase separation, the emulsion sample could not be successfully injected into the visualization glass chamber used for microscopic visualization. This emulsion sample was subsequently discarded.

APS 3 (0.6 wt. %) + Aluminium Oxide (0.2 wt. %) + Zirconium Oxide (0.2 wt. %). Due to the instability of emulsion and rapid phase separation, the emulsion sample could not be successfully injected into the visualization glass chamber used for microscopic visualization. This emulsion sample was subsequently discarded.

APS 3 (0.6 wt. %) + Polymer (0.4 wt. %). Oil droplet sizes remained consistent for 7 h. Constant droplet size distribution in the micrograph can indicate high emulsion viscosity as emulsion viscosity is higher when the droplet size distribution is narrow.

APS 3 (0.6 wt. %) + Sodium carbonate (0.4 wt. %). The micrographs in **Table 14** show three distinct phases were observed for this emulsion sample. The three parts consisted of random black spots, white cloudy parts, which expanded over time, and lucid, sheer parts, which reduced over time. It can be speculated that the black spots were flocculation of asphaltene or resin, the white cloudy part could be sodium carbonate and the lucid, sheer parts could be microemulsion. A turbid, stable emulsion sample was observed in the glass tube test.

The reason for the good performance of Zirconium Oxide in comparison with Aluminium Oxide in stabilization of emulsions despite them both having the same hydrophilicity and electrical charge (Table 12) could be that assemblies of nanoparticles of larger sizes are more stable than the assemblies of smaller-sized nanoparticles. Zirconium Oxide has higher particle sizes (45-55 nm) than Aluminium Oxide (10nm). Nanoscopic particles are bound to the interface by an

energy reduction which is comparable to thermal energy hence a constant particle exchange at the interface can make nanoparticles of smaller sizes more susceptible to displacement. And thus, assemblies of larger-sized nanoparticles are more stable (Böker et al. 2007).

APS 3 + Al₂O₃ (0.2 wt.%) + Polymer (0.2 wt.%).

This emulsion system remained as a stable Winsor type 4 emulsion for 1 hour before the separation between the aqueous and oleic phase was observed in the glass tube (Table 13). Stable droplet sizes shown in the micrographs in Table 14 confirm the stability of this emulsion system. However, coalescence is observed in the micrograph taken after 7 hours which indicates the emulsion stability loss. Figure 6 displays the gradual disruption of the interfacial film over 24 sec in the case of the emulsion formed with APS 3 without any stabilizing agents. In the case of a Zirconium Oxide added emulsion with APS 3 (Figure 7), there appeared to be little to no apparent change in the visualization micrographs.

Stabilization of emulsions with HORA (brine salinity: 3.8 %).

Tables 15 and 16 display the stability results of emulsions formed with HORA.

HORA (0.6 wt. %) without stabilizing agents: Some flocculation of the oil droplets were observed under the microscope within the 5 min period along with the appearance of bright precipitates. Oil droplets remained their shape for over 7 h.

HORA (0.6 wt.%) + Zirconium Oxide (0.4 wt. %): In the visualization cell, droplet sizes seemed to decrease over time; the droplet sizes became small and could no longer be visualized at a 100 micrometer scale after 7 h.

HORA (0.6 wt. %) + Aluminium Oxide (0.4 wt. %): Due to the instability of emulsion and rapid phase separation, it could not be successfully injected into the visualization glass chamber used for microscopic visualization. This emulsion sample was subsequently discarded.

HORA (0.6 wt. %) + Aluminium Oxide (0.2 wt. %) + Zirconium Oxide (0.2 wt. %): Due to the instability of emulsion and rapid phase separation, it could not be successfully injected into the visualization glass chamber. This emulsion sample was subsequently discarded.

HORA (0.6 wt. %) + Sodium carbonate (0.4 wt. %): Obvious oil and water phase separation was observed in the visual cell (Table 16). Oil droplets were shapeless and they rapidly increased in size over time. The result from the micrography is in contrast to the glass tube experiment result (Table 15) where HORA could form a stable emulsion with sodium carbonate.

HORA (0.6 wt. %) + Polymer (0.4 wt. %): Large oil droplets comparable to the size of the droplets formed with HORA without any stabilizing agents were observed (Table 16). The size and distribution of the droplets remained constant for 7 h without any visible precipitation, flocculation or coalescence.

HORA (0.6%) + Al₂O₃ (0.2 wt. %) + Polymer (0.2 wt.%). This emulsion system remained stable as a Winsor type 4 for approximately 1 hour before it began losing its stability in the glass tube test (Table 15). Black droplets witnessed in the micrographs in Table 16 represent bubbles formed in the emulsion system during the emulsion injection into the visualization glass chamber. Oil droplet sizes in the emulsion system remained stable and constant for 7 hours without any visible precipitation, flocculation or coalescence.

Table 15—Glass tube test of HORA and added stabilizing agents.

	HORA (0.6%)	HORA (0.6%) + Al ₂ O ₃ (0.4%)	HORA (0.6%) + Al ₂ O ₃ (0.2%) + ZrO ₂ (0.2%)	HORA (0.6%) + Al ₂ O ₃ (0.2%) + ZrO ₂ (0.2%)	HORA (0.6%) + Sodium carbonate (0.4%)	HORA (0.6%) + Polymer (0.4%)	HORA (0.6%) + Al ₂ O ₃ (0.2%) + Polymer (0.2%)
Formation of emulsion (after agitation)	3.8%: ✓✓	3.8%: ✓✓	3.8%: ✓✓	3.8%: ✓✓	3.8%: ✓✓	3.8%: ✓✓	3.8%: ✓✓
Stability	3.8%: ✓✓	3.8%: ✓✓	3.8%: x	3.8%: x	3.8%: ✓✓	3.8%: ✓✓	3.8%: ✓✓

Oil flow movement	3.8%: ✓✓	3.8%: ✓✓	3.8%: ✓✓	3.8%: ✓✓	3.8%: ✓✓	3.8%: ✓✓	3.8%: ✓✓
-------------------	----------	----------	----------	----------	----------	----------	----------

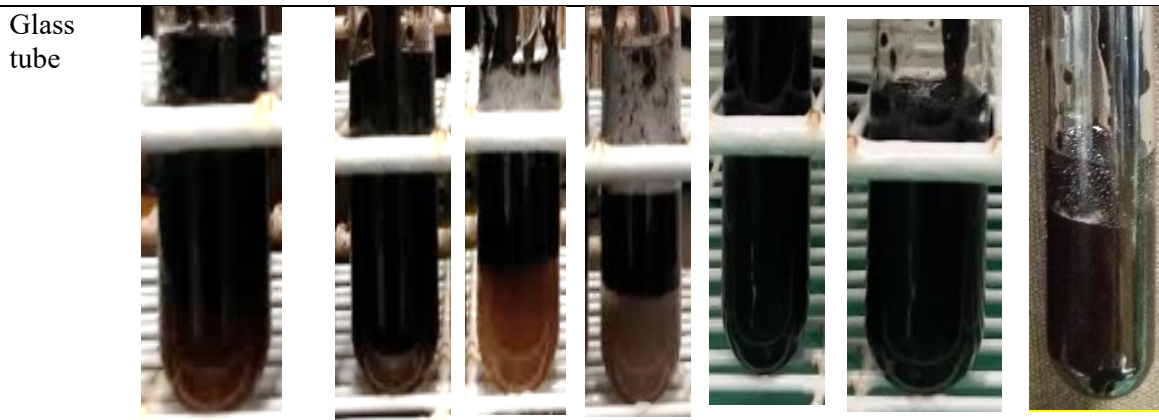
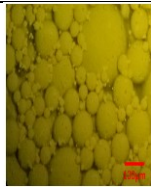
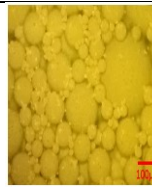
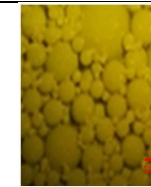
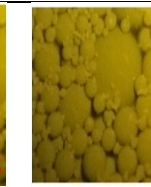
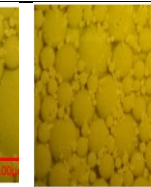
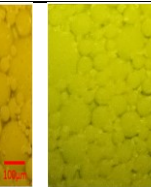
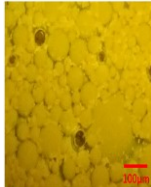
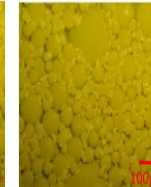
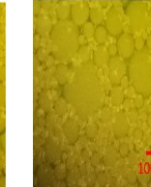
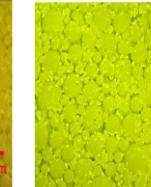
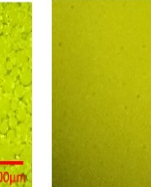
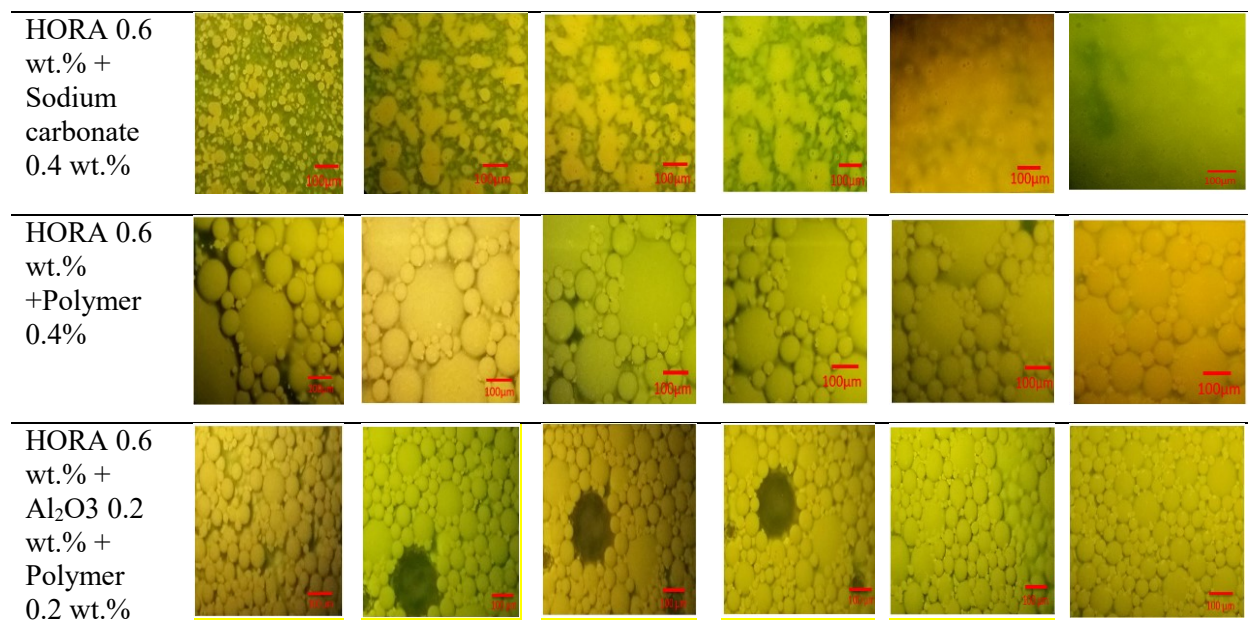


Table 16— Micrographs of stabilized emulsions taken at regular time intervals (HORA).

Chemicals	Immediately after	5 minutes later	10 minutes later	15 minutes later	1 hour later (different spot in glass visualization chamber)	7 hours later (different spot in the glass visualization chamber)
HORA 0.6 wt. %						
HORA 0.6 wt. % + Zirconium Oxide 0.4 wt. %						



Stabilization of emulsions with PSB 20 (brine salinity: 6.35%)

From the previous glass tube experiments (Table 5), it was observed that PSB 20 could perform optimally in emulsion formation at high salinity condition. Therefore, PSB 20 was selected for the emulsion stability test at high salinity condition. Nanofluids, polymer and sodium carbonate (Table 12) were added as stabilizing agents to enhance the emulsion stability. The concentration of the surfactant used for the stability test was 0.6 wt. % based on the results from the previous concentration test (Tables 10-11, Figure 5).

PSB 20 (0.6 wt. %) without Stabilizing Agents: Oil droplet sizes remained constant for 15 min. However, after 1 h, large-sized oil droplets began appearing due to the coalescence of small oil droplets. 7 h later, small oil droplet flocculation and large sized oil droplets were observed.

PSB 20 (0.6 wt. %) + Zirconium Oxide (0.4 wt. %): Oil droplet sizes maintained their size for 1 h. Discernible phase separation can be observed for the microscopic picture taken 7 hours later (Table 18). Distinct green color part indicates the water phase. Rapid loss of emulsion stability can imply the poor adsorption of nanoparticles at the interface of the emulsion.

PSB 20 (0.6 wt. %) + Aluminium Oxide (0.4 wt. %): Oil droplet sizes remained constant for 1 h. Phase separation between oil and water can be seen in the microscopic picture taken 7 h later. Precipitation was observed during the glass tube test.

PSB 20 (0.6 wt. %) + Aluminium Oxide (0.2 wt. %) + Zirconium Oxide (0.2 wt. %): Due to the instability of emulsion and rapid phase separation, the emulsion could not be successfully injected into the visualization glass chamber used for microscopic visualization. This emulsion sample was subsequently discarded.

PSB 20 (0.6 wt. %) + Sodium Carbonate (0.4 wt. %): Three distinct phases were observed in this emulsion sample. Black spots, white cloudy parts, and lucid, sheer parts could be seen. The white, cloudy part expanded over time and the occurrences of the black spots decreased. Black spots can be speculated to be asphaltene or resin precipitation, sodium carbonate could be responsible for the white, cloudy parts and lucid, sheer parts could be microemulsion. Similar results were seen with an emulsion formed with APS 3 and sodium carbonate (Table 14).

PSB 20 (0.6 wt. %) + Polymer (0.4 wt. %): Oil droplets of various sizes were observed and the variance in sizes remained constant for 7 h. There observed to be a visible and steady phase separation between the oil phase and water phase.

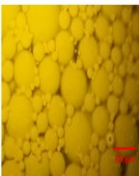
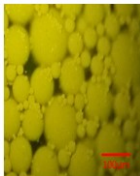
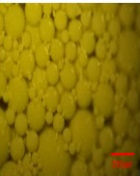
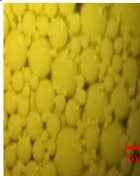
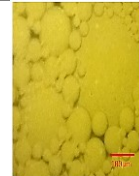
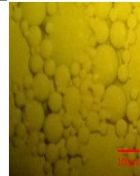
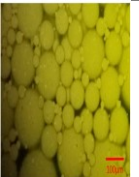
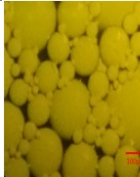
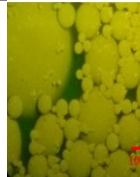
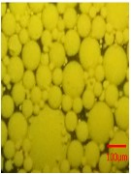
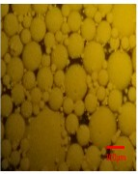
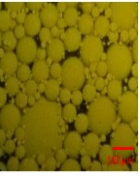
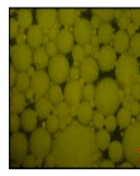
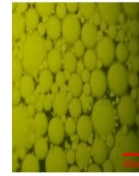
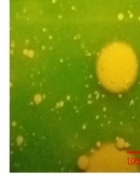
PSB 20 (0.6 wt. %) + Al₂O₃ (0.2 wt. %) + Polymer (0.2 wt. %): (**Table 17**) The stability of this emulsion system remained for approximately 30 minutes before the separation between the two phases was observed creating a Winsor type 3 emulsion. Precipitation and flocculation is observed in the micrograph taken after 1 hour of emulsion formation (**Table 18**).

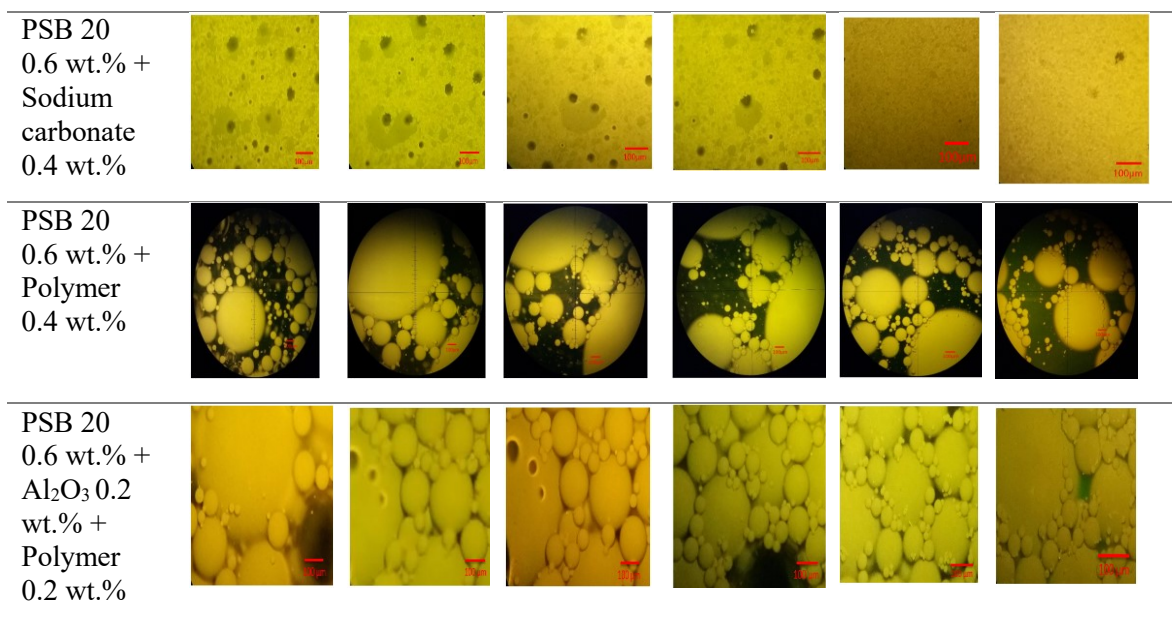
Table 17—Glass tube test of Tween20 and added stabilizing agents.

	PSB 20 (0.6 wt.%)	PSB 20 (0.6%) + ZrO ₂ (0.4%)	PSB 20 (0.6%) + Al ₂ O ₃ (0.4%)	PSB 20 (0.6%) + Al ₂ O ₃ (0.2%) + ZrO ₂ (0.2%)	PSB 20 (0.6%) +Sodium Carbonate (0.4%)	PSB 20 (0.6%) + Polyme r (0.4%)	PSB 20 (0.6%) + Al ₂ O ₃ (0.2%) + Polymer (0.2%)
Formation of emulsion	6.35%: ✓✓	6.35%: ✓✓	6.35%: ✓✓	6.35%: ✓✓	6.35%: ✓✓	6.35 %: ✓✓	6.35 %: ✓✓

(after agitation)							
Stability	6.35%: ✓✓	6.35%: ✓	6.35%: ✓✓	6.35%: x	6.35%: ✓✓	6.35%: ✓✓	6.35%: ✓✓
Oil flow movement	6.35%: ✓✓	6.35%: ✓✓	6.35%: ✓✓	6.35%: ✓✓	6.35 %: ✓✓	6.35%: ✓✓	6.35%: ✓✓
Glass tube							
				precipitation			

Table 18—Micrographs of stabilized emulsions taken at regular time intervals (PSB 20).

	Immediate	5 minutes	10 minutes	15 minutes	1 hour	7 hours later
Chemicals	ly after	later	later	later	(not in exact same spot)	
PSB 20 0.6wt.%						
PSB 20 0.6 wt.% + Zirconium Oxide 0.4 wt.%						
PSB 20 0.6 wt.% + Al ₂ O ₃ 0.4 wt.%						



2.6 Conclusions

Of all the chemicals tested, APS 3, hydrophilic anionic surfactant, showed the highest efficiency in forming a stable emulsion at low salinity-ambient temperature condition. HORA, a blend of surfactants, could form emulsion at low salinity and room temperature conditions by reducing interfacial tension between oil and water. However, the emulsion formed with surfactant without any stabilizing agent could not maintain its stability. Stable emulsion with HORA could be formed with addition of an anionic polyacrylamide-based polymer as a stabilizing agent. As for the high salinity environment, Polysorbate-type surfactant PSB 20 displayed optimal performance at room temperature condition in the initial chemical screening glass tube test. Addition of sodium carbonate, which also performed optimally in the glass tube test, helped enhance the stability of emulsion greatly by increasing pH and inducing natural surfactant generation. Addition of sodium carbonate especially could enhance the stability of emulsions formed with APS 3 and PSB 20. Al₂O₃ did not perform well in stabilizing emulsions that were created with APS 3, HORA. Addition of Al₂O₃+ ZrO₂ led to the rapid phase separation of emulsions formed with previously mentioned surfactants. This implies poor synergy between aluminium oxide and zirconium oxide in their role to improve emulsion stabilization.

Overall, Hydrophilic surfactants were more efficient in creating oil-in-water emulsions than hydrophobic surfactants with the heavy-oil used in this study. And it was observed that a Pickering emulsion system generated with Aluminium Oxide (positively charged at a given pH), an anionic polymer and an anionic surfactant can create a stable emulsion system due to the complex colloidal layer which forms at the oil-water interface which can help stabilize the emulsion. The emulsion system formulated using an aforementioned formula showed higher stability than a system created only with an anionic surfactant.

Chapter 3: Improvement of Microemulsion Generation and Stability Using New Generation Chemicals and Nano Materials During Waterflooding as a Cost-Efficient Heavy-Oil Recovery Method

This chapter contains a modified version of SPE 191171, which was presented at SPE Trinidad and Tobago Section Energy Resources Conference held in Port-of-Spain, Trinidad and Tobago, 25-27 June 2018. The journal version of this paper is currently under review for publication.

3.1 Preface

This study focuses on the ability of complex colloidal solution to stabilize a heavy oil-brine Pickering emulsion by changing the activity at the interface between heavy oil and brine. After testing many different combinations of anionic and cationic surfactants and nano-particles, we formulated the best stability options and created oil-in-water Pickering emulsions stabilized by silica, a cationic surfactant [dodecyltrimethylammonium bromide (DTAB)], and an anionic surfactant [alcohol propoxy sulfate (Alfoterra S23-7S-90)]. Then, various core flooding experiments were conducted in order to demonstrate the practical ability of the created emulsion system and observe its capacity to enhance oil recovery. Rate-dependency flooding tests were also conducted to determine the optimal flow rate required for heavy oil production through emulsification for different permeability media. Ultimately, slim tube sandpack flooding experiment at the optimal rate was conducted to confirm in-situ emulsion generation and to support the potential use of the chemical combination in the heavy oil industry.

3.2 Introduction

Thermal methods predominantly applied for heavy oil recovery have many drawbacks such as high consumption of fresh water, energy, and CO₂ emissions. These disadvantages led the industry to search for lowered cost and more efficient techniques such as non-thermal chemical methods. Common chemical applications include alkaline (A) flooding due to its emulsification mechanism, surfactant (S) flooding, which is based on IFT reduction and emulsification, polymer (P) flooding applied to improve sweep efficiency, and ASP flooding, which combines all aforementioned methods to optimize heavy-oil recovery.

Chemical flooding may become ineffective if the chemical is adsorbed on the rock surface or has reactions with the rock surface leading to emulsion stability loss particularly in the case of alkaline and surfactant flooding. Therefore, it is important to create emulsion that is sufficiently able to maintain stability in the reservoir condition and eventually lead to enhanced heavy-oil recovery. Conventional emulsions stabilized with surfactants or polymers only are known to be thermodynamically unstable. However, emulsions, which have been stabilized by surface-active colloidal particles called Pickering emulsions, are kinetically stable. The irreversible adsorption of the colloid particles at the interface between oil and water gives Pickering emulsions the kinetic stability. This mechanism can provide a barrier to the coalescence of droplets, which indicates stability loss (Zhu et al. 2017; Chavalier and Bolzinger 2013).

This work studies various types of cost-effective oil-in-water Pickering emulsion systems formed with heavy oil of 11.74°API in which oil-water interface is structurally stabilized by a colloidal layer. The emulsion stability of a Pickering emulsion is dependent on the size and packing order and wettability of the nanoparticles at the interface. Studies reported that Pickering emulsions can display stronger stability when they are hybridized with surfactants. Various types of colloidal layers were extensively investigated for their potential in stabilizing the heavy oil-in-water interface as a result of the van der Waals attraction and electrostatic attraction. Negatively charged nanofluids, cationic, and anionic surfactants were used to create a structurally stable colloidal layer. To investigate the practical applicability of the colloidal dispersions in enhanced heavy oil recovery, sandpack flooding and core flooding were conducted. Extracted emulsions

were then visualized under the transmitted light microscope to confirm their stability against flocculation and coalescence.

The result revealed that some colloidal dispersions formed with low-priced silica and surfactants can generate and stabilize oil-in-water emulsions. Oil-water interface formed with the complex colloidal layer can increase the structural stability of the emulsion and help them maintain their stability against coalescence or flocculation. Sandpack flooding and core flooding results also showed that the emulsions produced in-situ in the core can efficiently flow through the sandstone pores as a result of low IFT and emulsification. Those findings are critical in reducing the overall cost of chemical EOR method for heavy oil recovery under cold conditions. This paper introduces a potential chemical combination selected based on its ability to create a complex colloidal oil-water interface that can stabilize oil-in-water emulsion. These chemicals and their optimal combinations were tested for their potential application in cold water flooding for heavy-oil recovery through sandpack flooding, core flooding, and slim sandpack flooding. We expect that a stable nanoscale Pickering emulsion system created with low cost chemicals developed in this work can find practical applicability in the heavy oil industry.

3.3 Materials

Silica nanofluid solution, Ludox CL-X from Sigma-Aldrich, with an average particle size of 22 nm was chosen because of its environmental-friendliness and low cost. Yoon et al. (2017) determined the surface area of Ludox CL-X to be $130 \text{ m}^2\text{g}^{-1}$ using Brunauer-Emmet-Teller method. Cationic surfactants DTAB (dodecyltrimethylammonium bromide) and CTAB (Cetyltrimethylammonium bromide) were obtained commercially. A non-commercial anionic alcohol propoxy sulfate surfactant (Alfoterra S23-7S-90) was used based on its optimal synergy effects it displayed with heavy oil from the previous literature at low salinity conditions (Lee and Babadagli 2017). This surfactant used in this study is non-commercial; therefore, its detailed chemical components and structure are not available to the general public. The chemicals were used without further purification.

Oil and water

Heavy dead crude oil used was obtained from a field in western Saskatchewan, Canada. Density and viscosity of this oil was measured to be 0.981kg/m³ and 4,812 cP, respectively at room temperature (~25°C). The API gravity of the oil is 11.74°. The heavy oil's mean total acid number (TAC) was measured to be 3.2 mg KOH/g. The acid number is measured to determine the amount of soap that can be generated; however, the amount of acid may not be correlated to acid number possibly due to the methods used to measure the acid numbers. Also, it is possible for some components to be unable to generate soap and other application conditions may have a negative influence on the generation of soap (Sheng 2015). SARA analysis of the heavy oil is available in **Table 19**. The pH of the 2.54% brine sample (NaCl) used throughout the experiments is 6.98. 2.54% salinity brine sample was selected based on its optimum compatibility with Alfoterra S23-7S-90 in creating a heavy oil-in-water emulsion as reported in previous studies by Lee and Babadagli (2017).

Table 19—Sara results.

Components	Mass recovered (g)
Saturates	29.36
Aromatics	25.65
Resins	29.51
Asphaltenes	14.78

3.4 Methodology

3.4.1 Design of the Pickering emulsion

Commercially available inorganic nanoparticles such as hydrophilic silica can be hydrophobized in situ with a conventional surfactant such as DTAB as shown in **Figure 8** (Yoon et al. 2016; Binks and Rodriguez 2007). Through the electrostatic interaction, the charged nanoparticles can adsorb oppositely charged surfactant; the surfactant monolayer formation can then increase the hydrophobicity of the particle surfaces, which can lead to surface-active particles. In-situ hydrophobization of originally hydrophilic particles can allow particle attachment at the oil-water interface (Zhu et al. 2017; Goloub and Koopal 2007). Modifying the wettability of

colloidal particles in the liquid media can help prepare particle-stabilized emulsions which enhances the adsorption of them at the liquid-liquid interface (Chen et al. 2017).

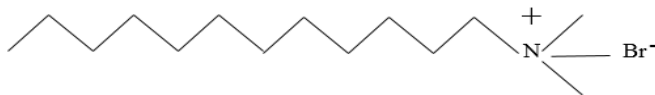


Figure 8—Dodecyl trimethyl ammonium bromide (DTAB).

Cationic surfactant can also help adsorb anionic surfactant onto a negatively charged surface like silica due to the formation of ion pairs (Paria and Khilar 2004). The anionic surfactant selected for this test is Alfoterra as it has gave the optimal results in our previous chemical screening test (Lee and Babadagli 2017). Mixing anionic surfactant and cationic surfactant was also shown to be a novel surfactant methodology that can lead to ultralow interfacial tension (IFT) and high oil solubilization (Li et al. 2016). Mixing oppositely charged particles and surfactant is an important mechanism in the synergistic stabilization of emulsion drops.

One of the biggest problems with using surfactants in a porous media is the possible surfactant adsorption in a porous media, which can be detrimental to chemical flooding used for enhanced oil recovery purposes. Upadhyaya et al. (2007) hypothesized and confirmed that in a colloidal mixture of anionic and cationic surfactants, if the supra-CMC mixture contains a high concentration of anionic surfactant, cationic surfactants can be sequestered in the anionic-rich micelles, which can diminish the adsorption of the cationic surfactant onto negatively charged surfaces. Considering that the concentration of anionic surfactant used in the system was at Supra CMC concentrations, cationic surfactant adsorption can be ruled out as the cause for the gradual oil recovery loss observed in this study. Therefore, silica, DTAB, and Alfoterra S23-7S-90 were used to create a cost-effective complex colloidal solution to give the best optimal recovery results in various experiments, which include glass tube experiment, sandpack flooding experiment, slim tube sandpack flooding experiment, and Berea sandstone core flooding experiment.

3.4.2 Zeta potential

The zeta potential is a key indicator of the stability of colloidal dispersions. It is commonly used to quantify the magnitude of the charge. The zeta potential of silica particle dispersions in aqueous phase (NaCl = 1 mmol) was measured along with zeta potentials of silica dispersion with addition of DTAB, and the zeta potentials of silica with addition of DTAB and Alfoterra S23-7S-90 at pH = 7 using a Malvern Zetasizer Nano ZS instrument employing a dip cell. At least two measurements were conducted for each solution to confirm the validity of the results (Binks and Rodriguez 2007). 1% of heavy oil was added in the sample in order to provide sufficient turbidity required to measure the zeta potential of the sample and investigate possible interaction between oil and the chemicals used in the study. 1 mmol brine concentration was selected due to the limitation of the equipment to measure samples with higher electrolyte concentration such as 2.54 wt% NaCl brine sample used for glass tube experiment and sandpack flooding(s), core flooding, and glass bead visualization in this study.

3.4.3 Glass tube concentration test

1.0 wt% Ludox CL-X (silica) was mixed with brine sample of 2.54 wt% salinity (pH = 6.98). The mixture was created with light manual agitation. DTAB of the varying concentrations from 0 to 0.06 wt%. (Table 20) was then incorporated into the solution to observe DTAB's concentration on its ability to form a stable emulsion and to find the optimal concentration of DTAB in terms of costs. 0.5 wt.% anionic surfactant (Alfoterra S23-7S-90) was added to effectively stabilize the colloidal solution, then oil was added and agitated manually (brine and oil ratio 1:1) for this glass tube concentration test.

Table 20—Solution A.

	Solution A-1	Solution A-2	Solution A-3	Solution A-4
Silica (wt%)	1.00	1.00	1.00	1.00
Cationic DTAB (wt%)	0.00	0.02	0.04	0.06
Anionic Alfoterra (wt%)	0.50	0.50	0.50	0.50

3.4.4 Sandpack flooding

Unconventional heavy oil and bitumen reservoirs in several countries of the world such as Canada and Venezuela are famously known for having huge resources of unconventional heavy oil and bitumen that are characterized by high porosity and high permeability. Therefore, high porosity, high permeability sandpack method was employed to simulate conditions of a typical heavy oil reservoir that are typically good candidates for chemical flooding (Delamaide et al. 2014). The core flooding apparatus was set up with an injection pump (Teledyne ISCO syringe pump), a core holder, and measuring cylinder or vials to collect the sample (Figure 9). The core holder was tightly packed with sands saturated with heavy oil of 11.74 °API. Porosity of the sandpack was measured to be ~35%.

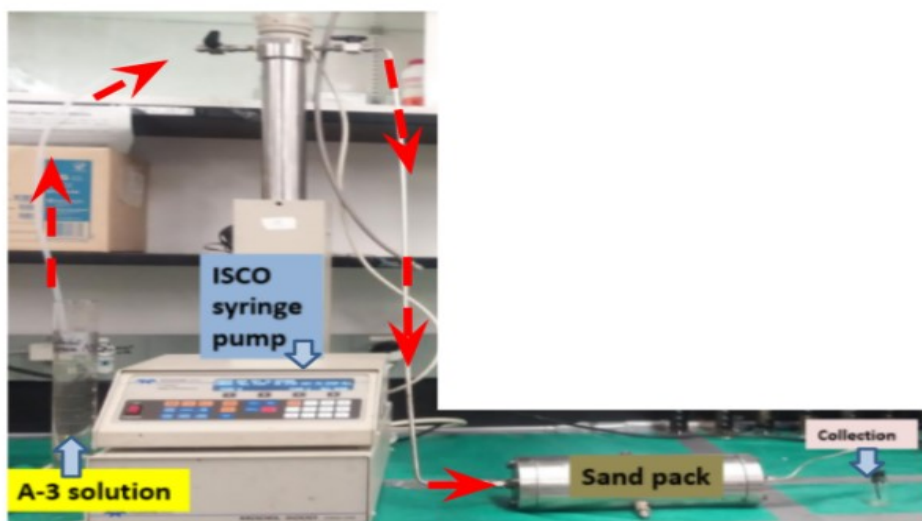


Figure 9—Core flooding set up.

3.4.5 2-D Glass bead visualization

A 2-D visual sandpack model (7 x 14 cm) was made up of a single layer of sintered micro-scale glass beads. The silica glass beads, approximately 3 mm in diameter, were packed between two 9 mm plexi-glass plates. The processes were recorded with a high speed camera to obtain visual data at the pore scale. This experiment was conducted to investigate the dynamics of in-situ emulsion generation at pore scale leading to the formation of residual oil saturation. **Figure 10** shows the schematic diagram of the glass bead visualization setup. This experiment was conducted to visualize and confirm in-situ oil-in-water emulsion generation under conditions closely matching sandpack flooding conditions (Figure 10). Flow rate selected for this glass bead

experiment was 0.2 ml/min, which was found to be the optimal flow rate in previous rate-dependency sandpack flooding experiments (see details in section “Sandpack flooding oil recovery”). The porosity of the glass bead model used in this study was approximately 35%. Arguelles-Vivas (2015) estimated the permeability of glass bead model (3 mm in diameter) in a similar glass bead visualization study to be about 7200 D, which was calculated by using the Kozeny-Carmen equation. Colloidal solution was injected from the injection port of the glass bead model using an ISCO syringe pump (Figure 11). In order to minimize the impact of gravity drainage process and mimic the conditions under which the core flooding test was conducted, the glass bead model was placed horizontally (Figure 10). Glass bead visualization test was conducted to confirm the in-situ emulsion generation in the porous media.

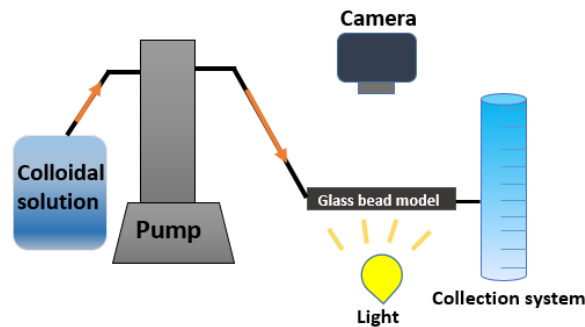


Figure 10—Schematic diagram of glass bead visualization setup.



Figure 11—Top view of the glass bead model.

3.4.6 Berea sandstone core flooding

It must be taken into consideration that the effectiveness of chemical flooding is reduced significantly during core flooding when there is channeling (Ma et al. 2006; Hankins and Harwell 1997). Therefore, in this Berea sandstone core flooding study, an overburden pressure of 100 psi was applied to the core to control possible channeling that can be created during the core

flooding process. The Berea sandstone core experiment set up is displayed in **Figure 12**. The porosity and permeability of the cores used in this study were 19.1% and 273.9 mD accordingly. 93.2 – 93.6 wt. % of chemical compounds found in the Berea sandstone cores were silica with alumina constituting 3.6 to 4.6%. Other compounds include Fe_2O_3 (0.30% – 0.35%), CaO (0.25% – 0.65%), MgO (0.08% – 0.15%), Na_2O (0.75% – 0.85%), and TiO_2 (0.1% max). Sandpack flooding experiment showed that when the flow rate is too low, colloidal solution inside the core potentially loses its stability eventually leading to less oil recovery and unstable emulsion production. Therefore, rate-dependency Berea sandstone core flooding was conducted to remove any possible effect of channeling and to test the capacity of the colloidal solution in a setting with much lower permeability and porosity than that of aforementioned sandpack flooding study. Rate experiments were also conducted to determine the most optimal rate recommended for this particular setting and to emphasize on discovering an optimal flow rate for any chemical flooding scenarios in order to optimize the final production.

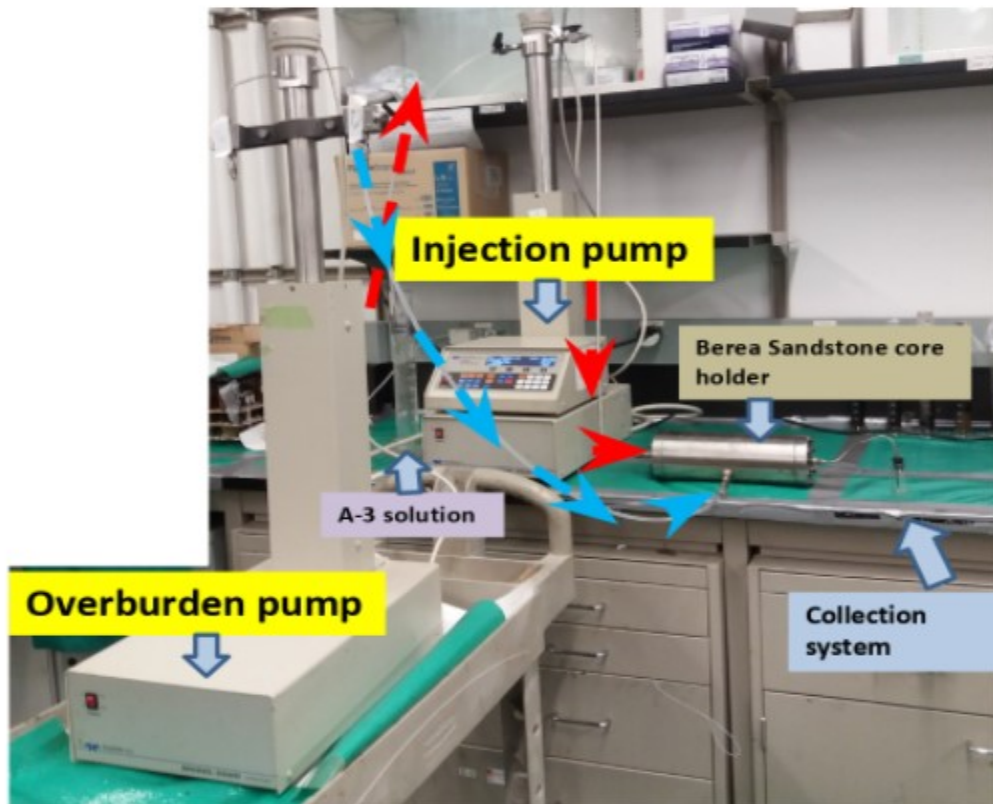


Figure 12—Schematic diagram of Berea sandstone core set up.

3.4.7 Slim tube sandpack flooding

A 1 m length and 1.5 cm diameter slim tube was used for the slim tube sandpack flooding experiment in order to test the in-situ emulsification capacity of the colloidal solution in a condition that can better mimic real reservoir settings than a short sandpack flooding test (Figure 10) and to test the in-situ emulsification potential of the colloidal solution A-3 (Table 20). The colloidal solution was prepared with NaCl (2.54% salinity) before being injected into the system. The reservoir temperature was kept at a room temperature ($\sim 25^{\circ}\text{C}$). The sands of diameters higher than $500\ \mu\text{m}$ were saturated with heavy oil before being placed inside the tube similar to the way the short sandpack experiment was prepared. **Figure 13** displays slim tube experiment setup. Sand screens of the appropriate size were inserted into the both ends of the slim tube to prevent possible sand production. The tube was plugged with rubber stoppers to prevent potential leakage of the solution. Two different flow rates were employed to study the impact of the flow rate on the oil recovery and in-situ emulsion generation. Produced samples were then collected and visualized under the microscope.

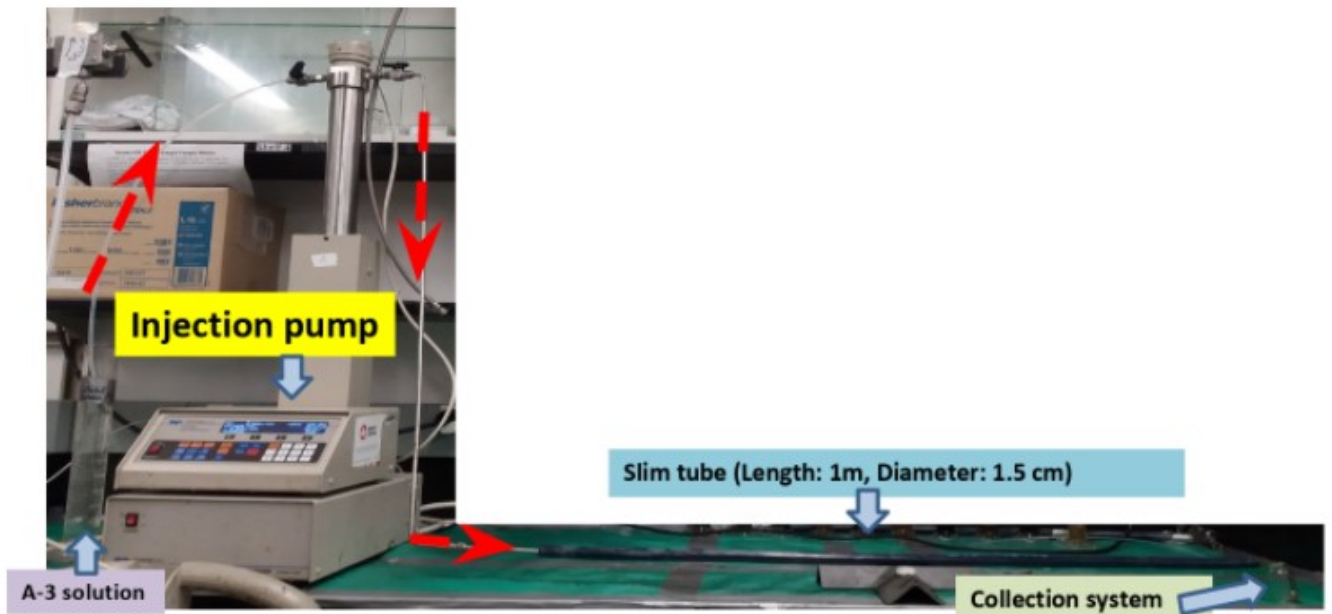


Figure 13—Slim tube experiment setup.

3.5 Results

3.5.1 Zeta potential measurements.

Zeta potential (Table 21) is measured to characterize the diffuse part of the double layer, which controls particle interaction (Yoon et al. 2016). At pH = 6.98, adding cationic surfactant DTAB in the presence of silica (1 wt.%) and oil (1 wt.%) increased the absolute magnitude of zeta potential of the solution by 95 mV rendering the solution incipiently instable at -11 mV. Strong attraction between positively charged DTAB and negatively charged silica nanoparticles can result in aggregation of nanoparticles (Kumar et al. 2012). Colloids with high zeta potential, whether negatively or positively charged, are electrically stabilized whereas colloids with low zeta potentials coagulate or flocculate easily due to the attractive forces that exceed the repulsion. Addition of an anionic surfactant in presence of silica (1 wt.%), DTAB (0.04 wt.%), and oil (1 wt.%) lowered the zeta potential of the complex colloidal dispersion to -92 mV stabilizing the colloidal solution. This indicates the importance of using an anionic surfactant to stabilize the colloidal dispersion at pH = 6.98. Al-Anssari et al. (2017) also reported that adding cationic surfactants in a solution with silica can weaken the stability of solution whereas addition of anionic surfactant can improve its stability. Adsorption of anionic surfactant onto a negatively charged surface like silica is enhanced in the presence of cationic surfactant due to the formation of ion pairs (Paria and Khilar 2004). It must be taken into consideration that if there is a change in pH or ionic strength, zeta potential value can be affected. Generally, zeta potential becomes more positive with the decrease in pH.

Table 21—Zeta potential results.

Brine	Solutions	Zeta potential	STD. Deviation
1mM	Silica (1%) + oil (1%)	-106mV	7.8 mV
	Silica (1%) +DTAB (0.04%) + oil (1%)	-11mV	6.53 mV
	Silica (1%) +DTAB (0.04%) + Alforterra S23-7S-90 (0.5%) + oil (1%)	-92mV	8.95 mV

3.5.2 Stabilized Emulsions of an anionic surfactant Alfoterra S23-7S-90 and silica nanoparticles hydrophobized with DTAB

Figure 15 displays the glass tube results of DTAB stabilized emulsions. A-1 sample is an emulsion stabilized by silica and an anionic surfactant without any addition of the cationic surfactant (DTAB). Stability loss was observed several minutes after the initial manual agitation. After 150 min, the emulsion observed to be separated into two distinct phases. A-2 sample with 0.02 wt % DTAB concentration displayed better stability than the A-1 sample. A thin unidentifiable white layer was formed at the oil and brine interface after 4 h. The white layer, which is caused by creaming, could have been the result from DTAB's aggregation due to its reaction with salt in the brine sample (Goloub and Koopal 1997). Creaming is one of the indicators of the emulsion stability loss. It can be observed at the interface between the oil and aqueous phase and can be prevented by reducing the density difference between the two phases or by more vigorously homogenizing the solution. A-3 sample with 0.04 wt % DTAB concentration showed the most optimal results out of all the samples that were tested forming stable emulsion. A-4 sample with 0.08 wt % DTAB could not be observed through the naked eye glass tube tests due to the severe coating of the inner surface of the glass tube, which is caused by the attraction forces existing between the cationic surfactant and the negatively charged glass surface. Cationic adsorption on silica is a common problem in real reservoir situations possibly caused by high concentration of a cationic surfactant leading the emulsion sample to coat the inner surface due to attraction forces. It took over 24 hours for A-3 emulsion to completely lose stability and creaming at the oil and water interface was observed. The aqueous phase was observed to be light brown in color; lighter than that the aqueous phase of A-2 with less DTAB concentration. The turbid nature of the samples is observed when adding DTAB possibly due to the strong attraction between nanoparticles and micelles leading to the micelle-mediated aggregation of nanoparticles (Kumar et al. 2012). Samples A-1 to A-4 are shown in **Table 22**.

Table 22—DTAB emulsion evaluation

	A-1	A-2	A-3	A-4
Formation of emulsion (IFT reduction)	✓✓	✓✓	✓✓	N/A
Stability	1 hour: ✓ 5 hours: x 24 hours: x	1 hour: ✓✓ 5 hours: ✓ 24 hours: x	1 hour: ✓✓ 5 hours: ✓✓ 24 hours: ✓	1 hour: N/A 5 hours: N/A 24 hours: N/A (Severe coating)
Precipitation	x	x	x	x

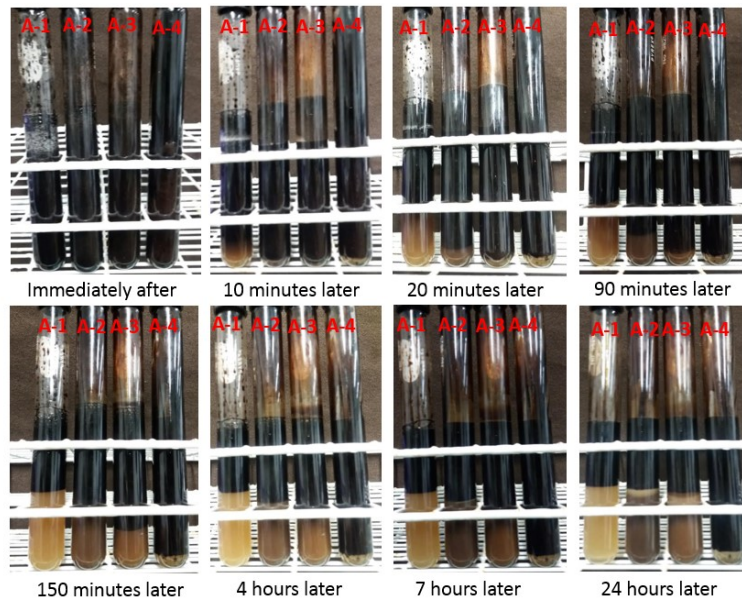


Figure 14—Emulsion with DTAB results.

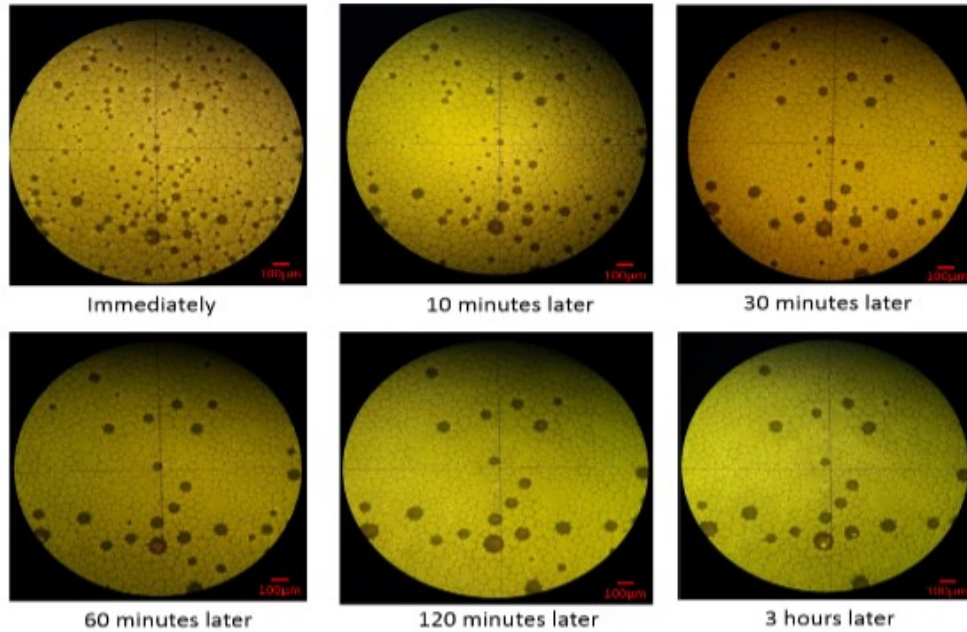


Figure 15—Microscopic visualization results.

3.5.3 Glass tube concentration test (Emulsion stability)

A Winsor type 4 emulsion sample created with the A-3 solution (Figure 15) was visualized under the microscope to observe the emulsion stability. It was observed that the particles remain consistent in size and distribution for 30 min showing little-to-no indication of emulsion stability loss. However, larger sized oil droplets began to emerge 30 min after the injection of the emulsion sample into the glass chamber due to the coalescence of oil droplets (Figure 15). After some loss of emulsion stability at the 30-min mark, the emulsion appeared to remain stable and no visible sign of emulsion stability loss such as coalescence, flocculation, aggregation, phase separation, or sedimentation was observed until after 3h passed, as shown in **Figure 16** (Graham et al. 2008).

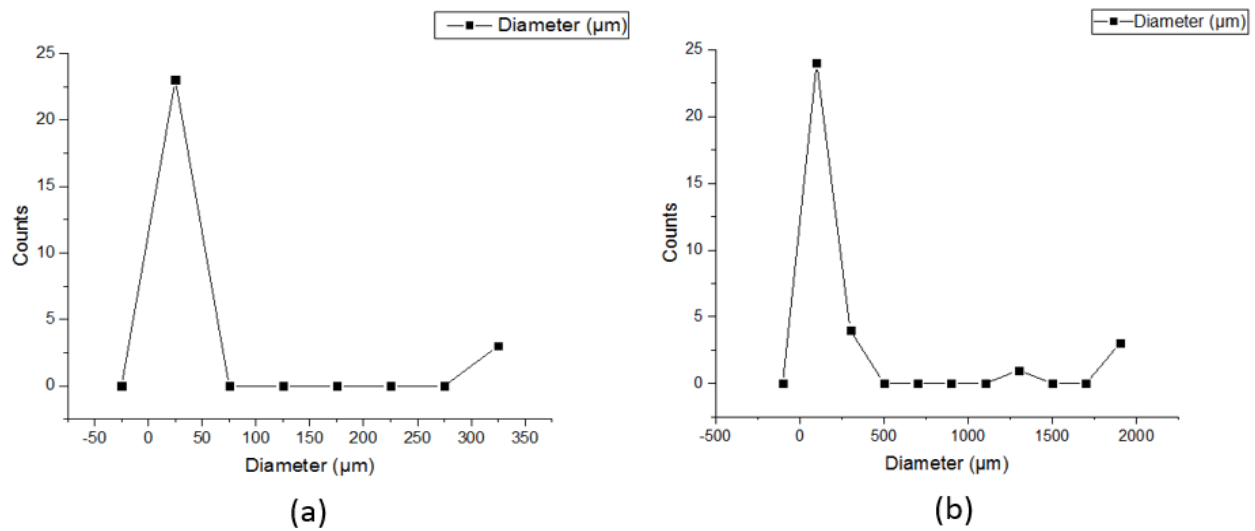


Figure 16—Particle distribution of the Winsor type 4 emulsion samples (a): Immediately after (b): 3 hours later.

3.5.4 Sandpack flooding oil recovery

Low-salinity waterflooding is often appealing because of its low-cost and relatively simple design compared with chemical EOR techniques (Gandomkar and Rahimpour 2015). A sandpack test was conducted to investigate the effect of low-salinity water flooding on heavy oil recovery and compare its performance with sandpack flooding with A-3 solution. After injecting 1 PV low salinity brine (2.54 wt.% NaCl) into the sandpack at 1 ml/min, oil recovery was observed to be 0.1% of OOIP (**Figure 17**).



Figure 17—Produced samples from low salinity water flooding at 1ml/min.

Secondary colloidal dispersion flooding using A-3 after low-salinity water flooding was then conducted at the same injection rate (1ml/min). This led to oil recovery of the original oil in place of 13% (**Figure 18**), which is equivalent to the oil recovery by colloidal dispersion

flooding conducted as the primary oil recovery method (**Figure 19**). However, when the flow rate was reduced to 0.2 ml/min, oil recovery improved significantly by 27% for primary A-3 sandpack flooding (**Figure 20**). Flow rates similar to 0.2 ml/min, such as 0.19 ml/min and 0.3 ml/min, were also selected for further rate-dependency sandpack flooding to observe the emulsion sensitivity to flow rates. Sandpack flooding conducted with aforementioned flow rates all displayed similar oil recovery results of approximately 20%.

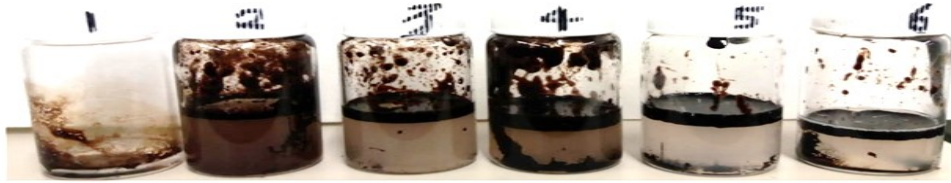


Figure 18—Produced samples from colloidal dispersion flooding after low salinity water flooding at 1ml/min.

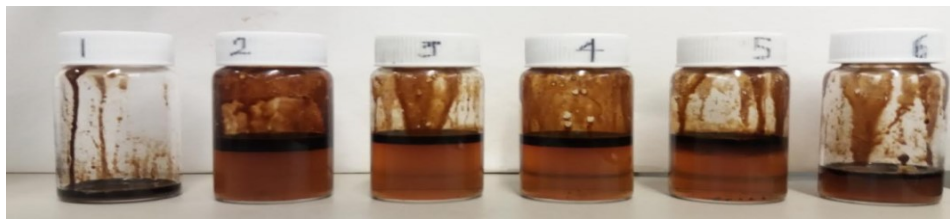


Figure 19—Produced samples from colloidal dispersion flooding at 1ml/min.



Figure 20—Produced samples colloidal dispersion flooding at 0.2ml/min.

Figure 21 further illustrates the oil recovery results from the rate dependency sandpack flooding tests. The results showed that appropriate flow rate is an important parameter in colloidal dispersion flooding. When the duration of the experiment (or soaking time) is very short (1 ml/min) or too long (0.04 ml/min), lower oil recovery was observed. Therefore, it is essential to find an adequate flow rate that can give the colloidal solution enough time to soak but not lose its stability during the soaking time and also can generate enough shearing force, which is initially necessary for emulsification and plays an equivalent role to manual agitation applied in glass tube experiments.

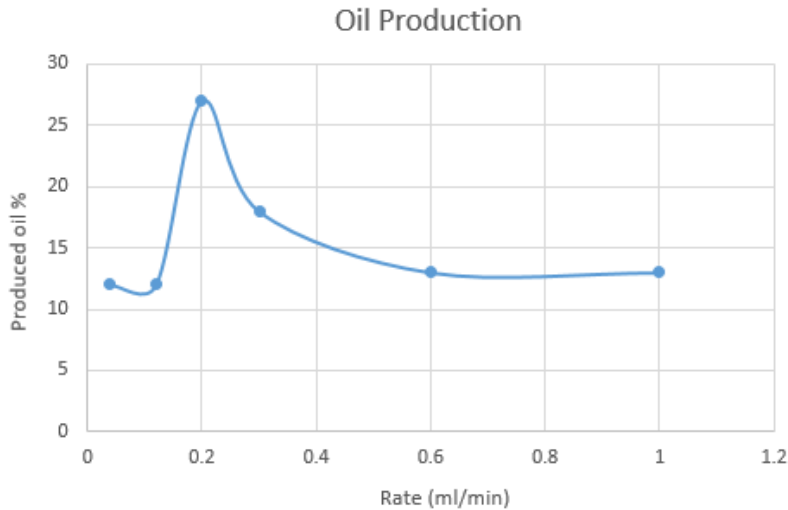


Figure 21—Sandpack flooding oil recovery at various rates.

It is also observed that in the 0.2 ml/min, 0.3 ml/min, and 0.19 ml/min sandpack flooding tests, oil production was observed to decrease after around $1/6^{\text{th}}$ of 1 PV solution injection. Change in produced fluid types at different stages of production is plotted in **Figure 22a**. However, it should be noted that emulsion types indicated in the plot are based on the produced samples after they have been agitated to form Winsor type 4 emulsions and are not an indication of the separated emulsion phase (aqueous phase) of the Winsor type 1 samples before the agitation. Extra agitation was required to observe the nature of the emulsions immediately after the produced sample collection and not after the phases have already been separated. The curves in **Figure 22b** display that at an optimal flow rate (0.2 ml/min), water-in-oil phase is longer leading to higher oil recovery. However, at low recovery flow rates, oil-in-water phase appears to be longer, leading to higher water (brine) production.

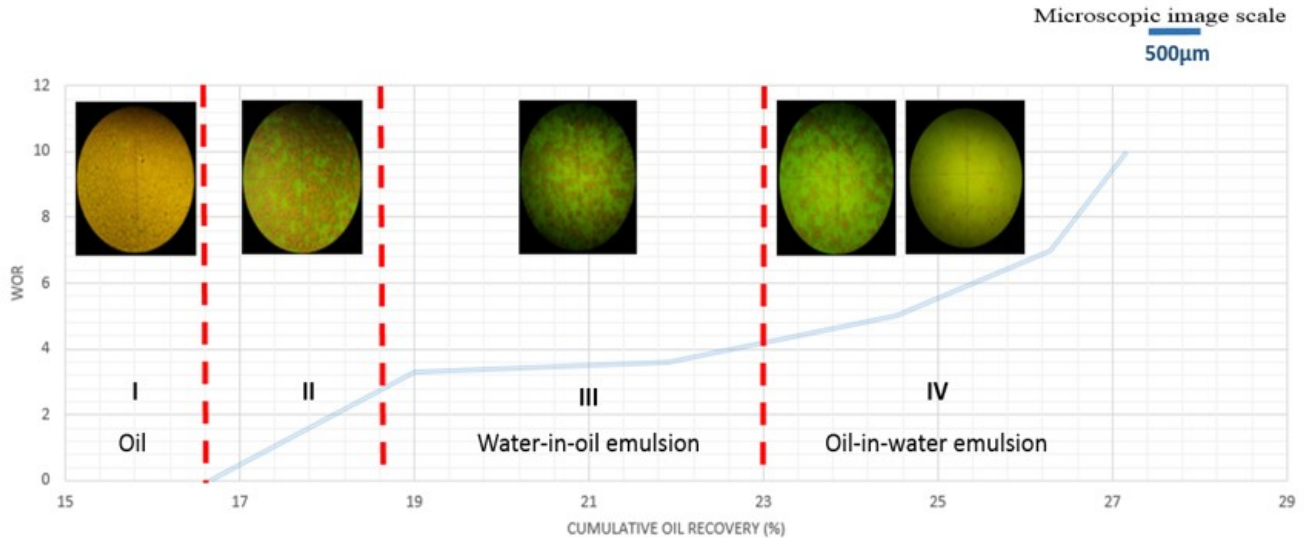


Figure 22a—Heavy oil chemical flooding type curve generated from sandpack flooding results using optimal flow rate.

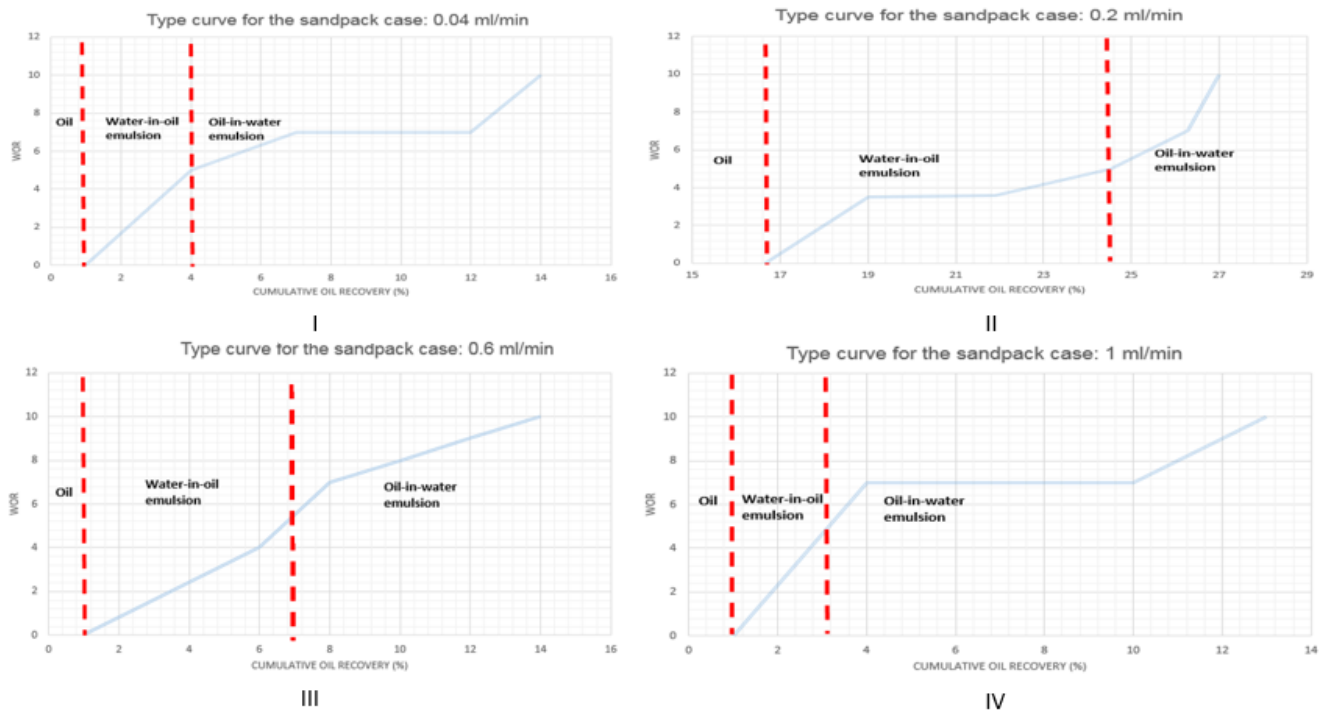


Figure 22b—Heavy oil chemical flooding type curves generated from sandpack flooding results (I: 0.04ml/min, II: 0.2 ml/min, III: 0.6ml/min, IV: 1ml/min).

The possible loss of colloidal stability of A-3 solution in the sandpacks can be due to various factors such as change in brine pH, which is normally incremental during the oil production

process (Binks et al. 2006), change in water content (Arla 2007), loss of equilibrium ratio of brine and oil due to the rapid brine production, and surfactant adsorption to the rock surface. In EOR, surfactant adsorption onto the surfaces of the pore space is a factor that can result in a great chemical loss, which can lead to decreased system performance. Therefore, surfactant adsorption on the surfaces is a factor that should be taken into consideration when designing a complex colloidal solution system. However, surfactant adsorption may not be the biggest contributing factor in A-3 stability loss in this study because supra-CMC mixture can diminish the adsorption of the concentration of a surfactant with a lower concentration than the main surfactant (surfactant with a higher concentration) (Upadhyaya et al. 2007).

Another possible reason for the solution stability loss is the loss of equilibrium ratio of brine and oil due to the rapid production of brine (potentially due to channeling). Emulsions formed with nanofluids can be greatly sensitive to volume ratio of water to oil (Chen et al. 2017). In the glass tube experiments, the colloidal solution was shown to be stable when brine and oil ratio was 1:1. Due to the production of brine, equilibrium ratio of brine and oil can be altered, which leads to the deterioration of the stability of the system. These aforementioned factors could contribute to the gradual loss of production and therefore, solutions to these issues must be discussed. In this study, possible exaggerated production of brine due to channeling is further discussed and studied by conducting Berea sandstone core flooding experiments while also applying overburden to reduce the effect of channeling.

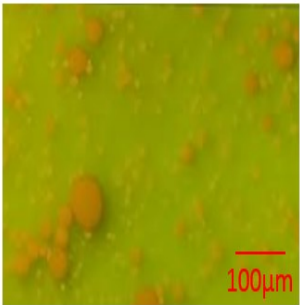
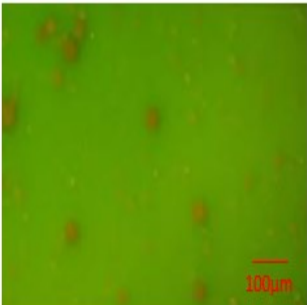
Produced emulsion phases were observed under the microscope immediately after the flooding and again after 30 days passed in order to observe the change in the emulsion phase and determine its stability. Stability of the emulsion will imply the capacity of the colloidal solution to maintain the stability of the emulsion in a real reservoir situation. During 30 days, some separation between the oil and water phases by gravity separation was observed. However, aqueous (emulsion) phase did not become transparent even after 30 days, which implies that the emulsion phase did not completely lose its stability. Liquids of different properties can commonly be separated by gravitational force. The principles governing gravity separation of oil can be described by Stoke's law (Eq. 1). As defined by Stoke's law, oil droplet rise can be affected by change in oil and water density and viscosity or the change in oil droplet size:

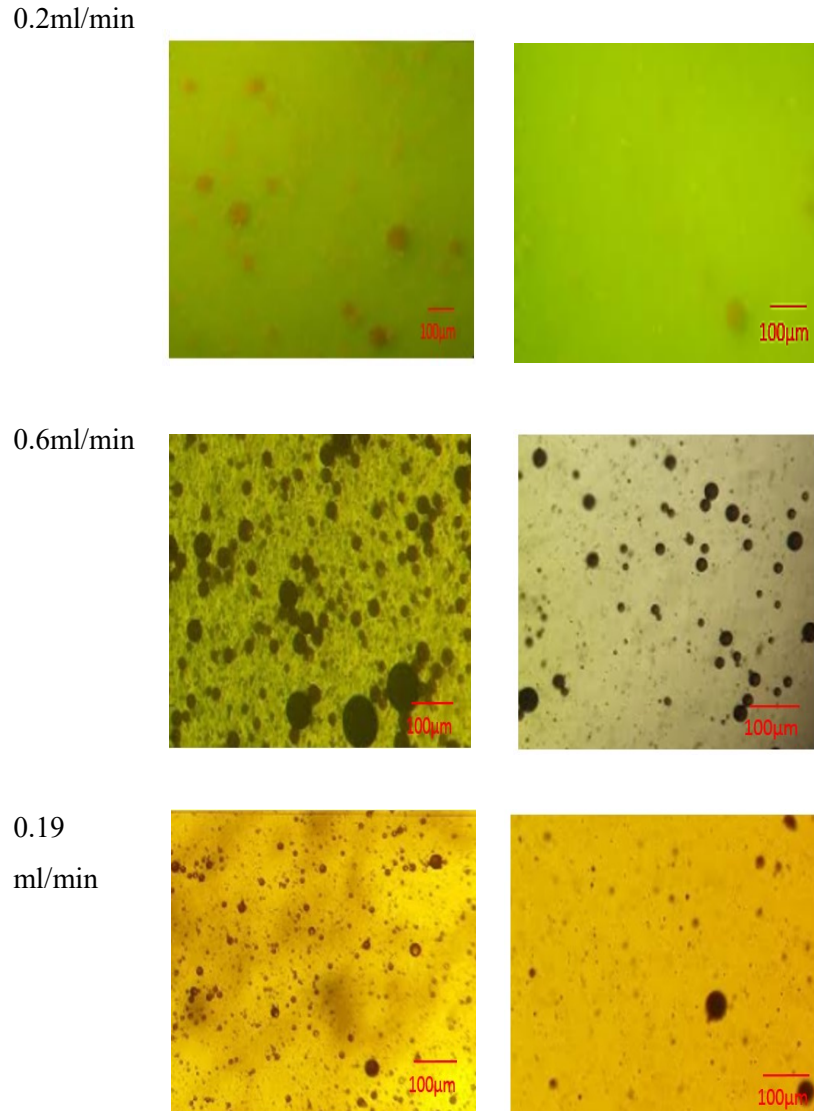
$$V = g \frac{(d_w - d_o)D^2}{18u} \quad (1)$$

where V = Oil droplet rise rate, g = acceleration due to gravity, d_w = water density, d_o = oil density, D = oil droplet diameter, and u = water viscosity.

In this study, change of oil droplet size over time was investigated under the Axiostar plus transmitted-light microscope. It is shown that 30 days later, the number and size of oil droplets decreased significantly due to the separation between oil and water (Table 23). The oil recovery of the original oil in place for the injection of colloidal dispersion was then calculated by measuring produced oil volume. It should be noted that there is a slight difference between the color of oil droplets in the produced emulsion samples of 1 ml/min, 0.2 ml/min sandpack flooding and that of 0.6 ml/min, 0.19 ml/min. The color of oil droplets for the produced samples of 1 ml/min, 0.2 ml/min sandpack flooding may appear to be yellow or light brown, whereas for the 0.6 ml/min and 0.19 ml/min cases, the oil droplets appear to be black in color. This is due to the modification in the micrograph illumination setting, which ultimately enhanced visualization in the case of emulsion samples from the 0.6 ml/min and 0.19 ml/min sandpack flooding. The new method essentially improved the microscopic recognition and visual definition of the oil droplets.

Table 23—Microscopic visualization of oil droplets in the emulsion phase.

Flow rate	Immediately after	30 days later
1ml/min		



3.5.5 2-D Glass bead visualization (in-situ emulsion generation)

Figure 23 shows the dynamic oil-in-water emulsification process observed in the glass bead model. White spots in the model indicate glass beads that are pressed against the wall due to the slight size variation between the glass beads that were used to create the model. 3 mm is the diameter that was consistently used but there were some inevitable erroneous diameters of the beads that led to some uneven lines in the glass bead sample model. Black parts represent glass beads covered with heavy oil.

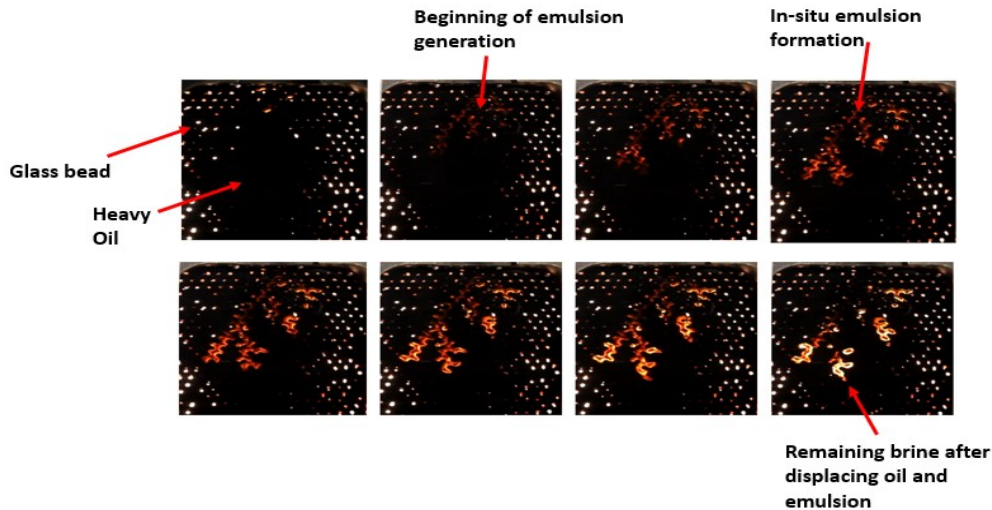


Figure 23—Zoomed in view of the glassbead model.

Glass beads were saturated with heavy oil by injecting heavy oil into the model prior to the solution injection. The solution was injected into the injection port as displayed in Figure 12. Produced oil and emulsion was then collected into a cylinder (Figure 10). Once the solution was injected, emulsion generation started to be observed by obvious color change of the black part (saturated with oil) of the glass bead sample. Some oil saturated black parts become lighter in color (dark brown) until they become even lighter (light brown) and then become transparent yellow-ish color, which indicates the remaining brine after the emulsion and oil displacement (Figure 23). Glass tube experiments previously have displayed that when oil emulsifies with water, the color of the mixture becomes brown (Figure 14). The color change observed in this experiment confirms the capacity of A-3 to generate emulsion and displace it, eventually leading to enhanced oil recovery. Yellow LED light, which was used behind the glass sample to improve the visualization capacity, is responsible for the amber color of the remaining brine; otherwise the remaining brine should be white-transparent.

3.5.6 Berea sandstone core flooding

Berea sandstone core flooding experiments were conducted with the colloidal dispersion solution (A-3) consisting of 1 wt.% silica nanoparticles (22 nm Ludox CL-X), 0.04 wt.% DTAB, and 0.5 wt.% Alforterra S23-7S-90 (Table 20). Colloidal dispersions, when injected at 0.02 ml/min, were experimentally confirmed to give the best recovery results (~14% recovery). Injecting the

colloidal dispersion at 0.01 ml/min yielded the poorest performance (~1.7% recovery). Increasing the amount of injected colloidal dispersion from 1 PV to 2 PV with initial injection at 0.01 ml/min (1 PV) and 0.03 ml/min (1 PV) did not show any significant enhancement in oil recovery (~14% recovery) (Figure 24). This implies the significance of flow rate on the oil recovery especially at the initial stage.

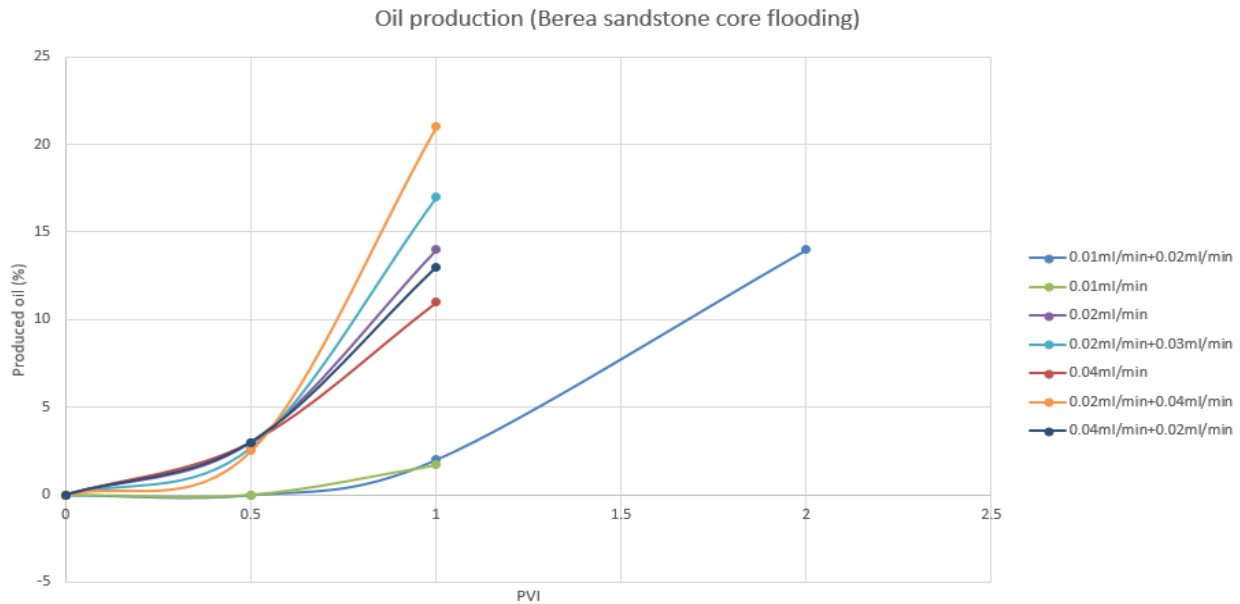


Figure 24—Berea sandstone core flooding results.

Low flow rates such as 0.01 ml/min can be detrimental to oil recovery as it can lead to colloidal dispersion stability loss in the core before being able to achieve in-situ emulsion generation. Dual flow rate experiments (0.02 ml/min and 0.03 ml/min), (0.01 ml/min and 0.03 ml/min) were conducted using different pore volumes as well and it was observed that having different flow rates does not have a significant impact on the oil recovery. Flow rates had to be maintained at a low rate for the sandstone core flooding experiments in order to control the pressure which increased greatly at times due to the tight structure of the sandpack cores (low permeability and porosity).

3.5.7 Slim tube sandpack flooding experiments

Two flow rates of 0.3 ml/min and 0.03 ml/min were selected for the slim tube sandpack flooding tests to observe the possible in-situ emulsion generation with the complex colloidal solution (A-3)

in a slim tube (**Figure 25**). Slim tube experiment results confirmed the capacity of the A-3 solution to generate emulsion at different flow rates (**Figures 26 and 27**), despite the challenges such as length of the tube and the slow flow rate selected for the slim tube flooding. Both flow rates (0.3 ml/min, 0.03 ml/min) gave similar oil recovery results of ~ 30%. Through the microscopic visualization of the emulsion phase of produced samples, emulsion formed at the late-mid production for the 0.3 ml/min case, which is similar in terms of the oil droplet size and distribution to the emulsion generated at the early-mid production stage for the 0.03 ml/min case (**Figure 25**). This is possibly due to the emulsion stability loss with the low flow rate. The relative emulsion stability loss of the 0.03 ml/min case did not seem to carry a significant impact on the final oil recovery results from the slim tube experiment. The resilience of A-3 solution was validated in this slim tube experiment and this can imply possible application of the A-3 solution in a much larger setting such as a real reservoir. However, it must be noted that it is possible for the emulsion phase with slow flow rates (slight loss of emulsion stability) to have a more significant impact on the final recovery during a larger scale operation as the objective is to prevent oil and water phase separation before the production.

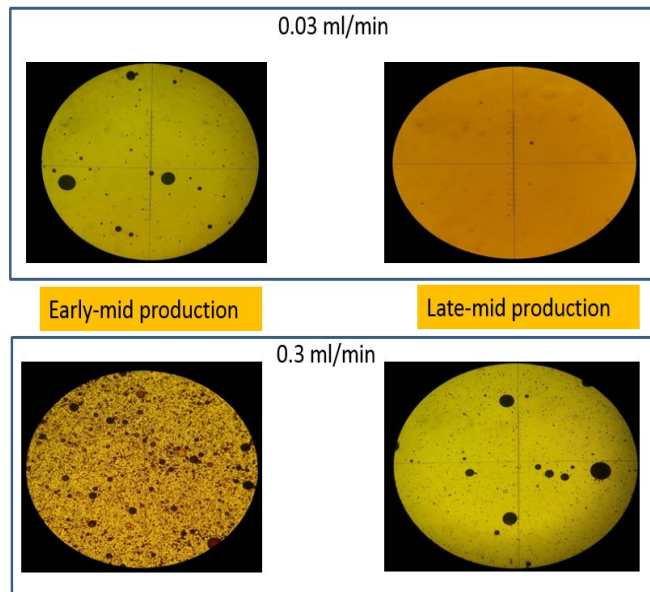


Figure 25—Visualization of emulsions.



Figure 26—Results from 0.3 ml/min.



Figure 27—Results from 0.03 ml/min.

3.6 Conclusions

This study showed that DTAB can significantly improve the stability of a Pickering oil-in-water emulsion system formed with heavy oil of 11.74°, 2.54 wt% brine (NaCl), silica nanoparticles, and an anionic surfactant. Previous studies by Lee and Babadagli (2017) have confirmed that hydrophilic surfactants can create heavy oil-in-water emulsion more effectively than hydrophobic surfactants. Therefore, a hydrophilic anionic surfactant was incorporated in the colloidal system for the experiments. Zeta potential measurements demonstrated the effective attachment of the cationic and anionic surfactants to the silica nanoparticles and proved their ability to form a stable complex colloidal solution at low salinity conditions. Sandpack flooding, core flooding experiments conducted using the colloidal dispersion solution (A-3), confirmed the stability of emulsions and their potential in enhanced heavy oil recovery. Silica (1 wt. %) + DTAB (0.04 wt. %) + anionic surfactant (0.5 wt. %) colloidal solution could improve the oil recovery by approximately 27% in comparison to the brine flooding case (base case) at the optimal flow rate. Glass visualization study further confirmed the ability of the colloidal solution to efficiently generate emulsion in-situ at pore scale at atmospheric pressure and temperature. The significant increase in heavy oil recovery observed from the sandpack flooding and Berea sandstone core flooding through in-situ emulsification confirms the practical applicability of the nanoscale dispersion in the field of heavy oil recovery.

Chapter 4: Microemulsion Flooding of Heavy Oil using Biodiesel under Cold Conditions

Chapter 4 is a modified thesis-appropriate version of SPE 193642, which will be presented at SPE International Heavy Oil Conference & Exhibition to be held in Kuwait City, Kuwait, 10-12 December 2018. The journal version of this paper is currently under review for publication

4.1 Preface

Cost and thermal stability are the major obstacles in using chemical additives for enhanced heavy-oil applications. Visual analysis of biodiesel in water emulsions obtained from the bitumen recovery tests from previous studies demonstrated that high pressure steam can lead to formation of stable emulsion by evaporation of biodiesel and condensation of steam-biodiesel vapor in the reservoir. Hence, biodiesel can be an alternative to commercial surfactants as a low-cost and environmentally-friendly additive for hot and cold production of heavy-oil.

For biodiesel to act as a surfactant and reduce IFT, it must first be condensed. Hence, we first studied the thermal-mechanical processing of biodiesel to generate stable steam treated homogenized biodiesel-in-water emulsion (SBDWE). Addition of chemicals such as silica and polymer (Xanthan gum) to further improve the stability of SBDWE was also considered in this study. Stable SBDWE samples generated at their optimal conditions were then employed for sandpack flooding experiments to observe their capacity to improve heavy oil recovery. In order to create stable SBDWE, biodiesel was first treated with steam at high pressure and high temperature conditions (1.6 MPa, 200°C). Variables such as reactor pressure, concentration of biodiesel in steam, and condensation time were modified independently to determine the optimal conditions for stable SBDWE generation. Surfactant behavior of the SBDWE samples was then tested through various methods (glass tube experiments, spreading tests through transmitted-light microscope, and naked eye visualization)

The results from the experiments suggest that aggregation of the small-sized biodiesel droplets of SBDWE (~1µm) at the interface between heavy oil and SBDWE can form a stable emulsion phase. Creaming of SBDWE is a poor emulsification indication and can be avoided by controlling experimental variables such as injected volume of distillate water, concentration of injected biodiesel, soaking time, and addition of silica nanofluid. Storage of the stable SBDWE is also an important factor as SBDWE properties such as texture, color and stability can change over time. Injected water volume (representing steam) and soaking time are variables that can have a significant impact on the generation of stable SBDWE. Therefore, it is important to maintain a certain volume of water and soaking time during the homogenization treatment. Finally, displacement experiments on sandpacks with the help of low concentration of silica (1 wt. %) and Xanthan gum (0.35 wt.%) yielded additional recovery up to ~39%.

Environmentally friendly and relatively inexpensive biodiesel (as a by-product of many industrial applications) is an ideal candidate for enhanced heavy oil recovery. Previously, application of biodiesel in heavy oil recovery came with limitations such that in enhanced heavy oil recovery, it is most effective when added to steam at high temperature and pressure conditions. However, the results from the laboratory scale cold flooding experiments with SBDWE demonstrated that SBDWE can be effectively used as a chemical additive using low concentrations of biodiesel.

Key words: Cold Production of Heavy Oil, biodiesel emulsion, microemulsion flooding, low cost chemical additives.

4.2 Introduction

Steam treated biodiesel (BD)-water emulsion was observed to facilitate the movement of bitumen from solids (Babadagli and Ozum 2012). It is expected that steam carries the vapor form of BD but according to previous observations, BD must be condensed in order to act as a surfactant that can reduce IFT. Previous study also demonstrated that surfactant behavior of biodiesel can lead to enhanced recovery of the residual oil by 13% when 0.3% BD was added on mass of steam. Based on these conclusions, this paper studies thermal processing of biodiesel to generate stable biodiesel in water emulsion by varying variables such as water volume injected into the reactor to generate steam, concentration of biodiesel injected into the steam, soaking time of biodiesel in the reactor under the steam condition, and storage time for the collected biodiesel in water emulsion samples. The addition of silica nanofluid to improve the stabilization of biodiesel-in-water emulsion is considered based on glycerol's affinity to silica and silica's hydrophilic nature. Once optimal conditions for biodiesel in water emulsion generation are established, SBDWE is generated en masse and stored for sandpack flooding to study its capacity to enhance heavy oil recovery and to determine its applicability in a real reservoir setting. For sandpack flooding experiments, polymer (Xanthan gum) was also added at very low concentration (0.35 wt. %) to help stabilize SBDWE in the porous media and therefore improving its interaction with heavy oil. Acronyms such as SBDWE or SBDW are used throughout the paper to refer to Steam Treated Biodiesel in Water Emulsions.

4.3 Materials

Heavy oil. Heavy dead crude oil from an oil field in Western Saskatchewan was used throughout this study. At room temperature of 25°C, density and viscosity of the oil were measured to be 0.9714 g/cm³ at 25°C and 3,437 cP, respectively. The API gravity of the oil is 13.14°.

Biodiesel. Biodiesel is fatty acids methyl ester, which can be produced from fats (fatty acids glycerides). Density of biodiesel in this study is 0.8770 g/cm³ at 15°C and was measured using the ASTM standard D1298. Lipid by-products and lipid derivatives such as BD, which is methyl esters of fatty acids (C_nH_m-COOCH₃; $m < 2n + 1$) and Fatty Acids Mono Glycerides (FAMG, C_nH_m-COOCH₂-CHOH-CH₂OH; $m < 2n + 1$) are surfactants that can affect the recovery of bitumen.

Table 24—Biodiesel property.

Property	Value (% mass)	Test method (ASTM)
Ester	97.3	EN 14103
Methanol	N/A	EN 14110
Monoglycerides	0.285	D6584
Diglycerides	0.000	D6584
Triglycerides	0.000	D6584

Silicon dioxide nanofluid: Ludox CL-X from Sigma-Aldrich with an average particle size of 22 nm was chosen because of its environmentally-friendliness and its low cost. Yoon et al. (2016) determined the surface area of Ludox CL-X to be 130 m²g⁻¹ using Brunauer-Emmet-Teller method.

Polymer: BARAZAN® D PLUS™ Xanthan gum was used in this study. Xanthan gum is a high molecular weight water-soluble polymer which is often employed to reduce the mobility of injected water. Polymers can also improve the efficiency of water and oil contact area and therefore facilitating the displacement of reservoir oil (Sandvik and Maerker 1977). Xanthan gum is also surface active and known to have an impact on the equilibrium droplet size by lowering the oil-water interfacial tension. Studies show that 1wt. % xanthan gum solution alone can decrease the interfacial tension of water at water and air interface (Hennock et al. 1984; Prudhomme and Long 1983).

4.4 Methodology

4.4.1 Steam treatment of the BD-W emulsion samples.

High pressure steam can lead to formation of BD in water emulsion (SBDWE). This was demonstrated through the visual inspection of the condensates (biodiesel in water emulsions) that were obtained from BD bitumen recovery tests (Babadagli and Ozum 2012). Biodiesel is first treated with steam (created with distillate water) at high pressure (180 psi) and high temperature (200°C) conditions in order to generate biodiesel-in-water emulsions. **Figure 28** displays the schematic diagram of the set up.

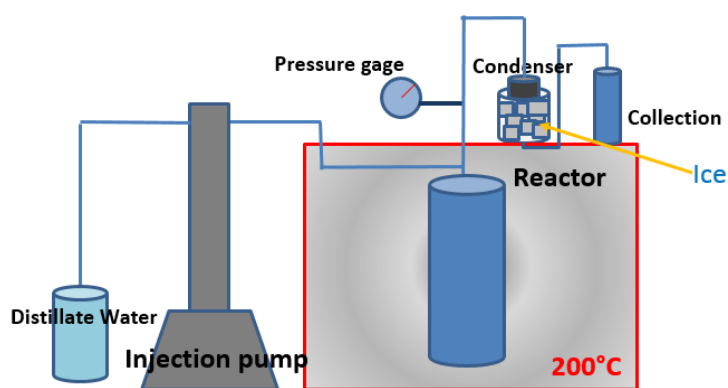


Figure 28—SBDWE treatment set up.

The treatment procedure is as follows:

1. Untreated biodiesel (raw form) is injected in the system/reactor at 1.2 ml per 1L of water (injected biodiesel concentration can be varied);
2. Distillate water is then injected into the system at 10ml/min rate;
3. Steam is created in the oven and the system is kept at 200°C for 4 h. The pressure in the system is maintained at 180 psi during this time.
4. Treated sample is then condensed, collected into vials and kept at ambient conditions for several weeks (can be varied).

The temperatures and pressures applied in this study were selected based on our previous experience on heavy-oil recovery tests using biodiesel (Babadagli and Ozum 2012). Other easily-manipulated variables such as concentration of biodiesel injected into the steam, volume of distillate water injected, soaking time of the biodiesel inside the reactor under the steam condition, and storage time for the collected samples were modified independently in each treatment to determine the impact of these variables on the emulsification capacity of SBDWE

and also to discover the most optimal conditions for SBDWE generation through steam treatment. The steam treatment conducted at optimal conditions is expected to produce SBDWE samples that have similar or equivalent visible texture, thickness, and color of the condensates obtained from the aforementioned BD bitumen recovery tests (**Figure 29**).



Figure 29—Biodiesel condensates (Babadagli and Ozum 2012).

Surfactant behavior of the SBDWE was tested through various methods such as glass tube experiments with heavy oil, microvisualization tests in accordance with heavy oil, and water emulsion generation test procedures employed in previous chemical screening test studies (Lee and Babadagli 2017; Lee and Babadagli 2018). Additional spreading tests were conducted to observe the static interaction between the oil and biodiesel-in-water sample. SBDWE samples generated at their optimal conditions were then collected and injected into the prepared sandpack for sandpack flooding experiments to observe their capacity to improve oil recovery.

4.4.2 Spreading test

One drop of oil (0.1 ml) was smeared on top of a flat and solid glass cell. With water or any liquid that is lipophobic, the polar water molecules would be repelled from the hydrophobic nature of oil and the drop would remain stable and maintain its original shape. A rough equivalent amount of prepared SBDWE samples were dropped next to the oil drop and the spreading behavior of oil was visualized over 2 h. Spreading behavior of oil with one SBDWE sample at its varied condensation times was also recorded over 4 weeks. Roughly a 1:1 ratio between SBDWE and heavy oil was also applied in this case. The purpose of this test is to visualize whether the oil drops spread or collapse due to change in interfacial tension between two fluids.

4.4.3 Glass tube test

Superior quality 33 expansion borosilicate clear (Type 1, Class A) vials, which can hold 20 ml in volume, and their matching caps were used for this glass tube test. Brine solutions/oil mixtures were made up of 1:1 water-oil ratio in each vial (2 g each). Created emulsions or unmixed samples with heavy oil were then observed over 24 h and their quality was studied by naked-eye observation. Winsor type 4 emulsion formation is the characteristic of high quality heavy oil and brine emulsion and obtaining this was the objective of this study. A total of four types of mixtures were tested in the glass tube tests: (1) Heavy oil with soft brine (2.5 wt. % NaCl), (2) heavy oil with hard brine (2.5 wt. % NaCl, 0.1 wt.% CaCl₂,0.01 wt.% MgCl₂), (3) heavy oil, SBDWE with soft brine (1:0.5:0.5), (4) heavy oil with hard brine and SBDWE (1:0.5:0.5). Two types of brines were used in order to determine the resilience of SBDWE to divalent cations that are commonly found in real reservoir settings and can often be responsible for rendering chemicals ineffectual.

4.4.4 Microscopic visualization

SBDWE samples after the treatment were injected into the visualization glass chambers and studied under the Axiostar plus transmitted-light microscope. Their interaction with heavy oil was also visualized to observe their capacity to form emulsions with heavy oil. For some samples, silica nanofluids were injected to determine their potential in possibly improving the stability of SBDWE samples. This is considering silica's behavior as a high capacity adsorbent (Manuale et al. 2014). Previous studies also have demonstrated that glycerol in biodiesel has a strong affinity for the surface of silica (Mazzieri et al. 2008). Using this aforementioned property and considering silica's hydrophilic nature, silica nanofluids were injected to improve the stability of SBDWE and therefore further enhancing its emulsification with heavy oil.

4.4.5 Sandpack flooding

Canada and Venezuela are famously known for having huge resources of unconventional heavy oil and bitumen that are characterized by high porosity and high permeability. Therefore, high porosity, high permeability sandpack method was employed to simulate conditions of a typical heavy oil reservoirs in these countries. High porosity, high permeability reservoirs are typically excellent candidates for chemical flooding (Delamaide et al. 2014). Core flooding apparatus was set up with an injection pump (Teledyne ISCO syringe pump), a core holder, and measuring

cylinder or vials to collect the sample (**Figure 30**). The core holder was tightly packed with sands saturated with heavy oil of 11.74 °API. Porosity of the sandpack was measured to be ~35%. Polymer (Xanthan gum) was injected (0.35 wt. %) to further stabilize the emulsions and increase the oil and SBDWE contact area, thus improving the recovery.

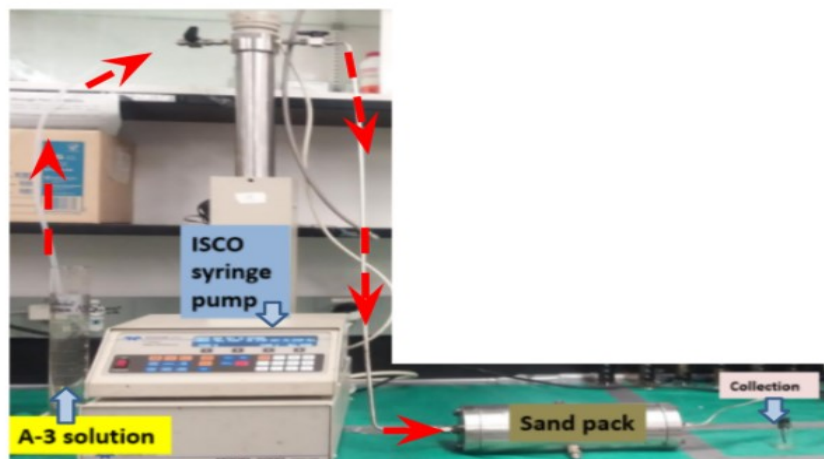


Figure 30—Sandpack flooding set up.

4.5 Results

4.5.1 Steam-treated biodiesel-in-water emulsion sample.

Table 25 displays the results of SBDWE samples generated under various conditions. Condensation or creaming of biodiesel on the surface forming a film or formation of water-in-biodiesel emulsion indicates poor quality SBDWE. Poor quality SBDWE samples were defined by large biodiesel droplets witnessed under the microscope and also by their constant shift in shapes and sizes such as in the case of SBDWE1 with comparatively low injected water volume and SBDWE7 with relatively short soaking time (**Table 25**). However, poor quality SBDWE was not always correlated with poor performance in its interaction with heavy oil (SBDWE7). As long as the microscopic visualization was conducted immediately after the samples were produced, interaction between the poor quality SBDWE and heavy oil seemed to be optimal. However, these poor quality emulsions (SBDWE7) seemed to lose their stability shortly after their production. High quality SBDWE samples such as SBDWE 6 or 8 were characterized by copresence of big oil droplets (~50 μm in diameter on average) and smaller-sized (<1 μm in diameter on average) heavily aggregated droplets. These samples maintained their stability for several days and showed active interaction with heavy oil both at the interface and in bulk phases.

Table 25—SBDWE generation under various conditions.

Name	Injected biodiesel concentration (vol. %)	Injected water (ml)	Pressure (cP)	Soaking time (hrs)	Emulsion samples	
					Visualization <small>500µm</small>	Interaction with heavy oil
SBDWE1	0.12	500	180	4		*
SBDWE2	0.12	600	180	4.5		****
SBDWE3	0.12	700	180	4		**
SBDWE4	0.12	875	180	4		***
SBDWE6	0.12	938	180	4		****
SBDWE7	0.12	938	N/A (40psi)	1		****
SBDWE8	0.12 BD + 1 silica	938	180	4		****
SBDWE9	0.4	938	180	4	NA	NA
SBDWE10	0.8	938	180	4	NA	NA
SBDWE11	1.6	938	180	4	NA	NA

*= poor, **= average, ***= good, ****= excellent.



SBDWE9



SBDWE10



SBDWE11

Figure 31—SBDWE samples with varied injected biodiesel concentrations.

Figure 31 displays results from steam treatment experiments conducted with exaggerated concentrations of injected biodiesel. SBDWE9 samples were generated using 0.4% concentration of biodiesel, which is about 3.3 times higher than the concentration of biodiesel used throughout the study. It was also observed that after producing ~55ml of stable SBDWE samples, in lieu of producing biodiesel-in-water emulsions, high viscosity, gel-like water-in-biodiesel emulsions began to be produced. In the case with SBDWE10 samples, which were generated using 0.8% biodiesel concentration, an even higher amount of water-in-biodiesel emulsions was generated after ~55ml of SBDWE production. SBDWE11 was generated with 1.6% biodiesel concentration and after 20 ml of SBDWE production, water-in-biodiesel emulsion began to be produced in an amount about 3 times higher than that of SBDWE10. From these results it can be concluded that an optimal concentration of biodiesel exists, which can be used for generation of stable SBDWE samples.

4.5.2 Spreading test

Heavy oil with SBDWE6 displayed the most optimal spreading capacity out of all three cases including that of SBDWE1 and SBDWE3 (Table 25). SBDWE6 was the good quality emulsion sample generated with the highest volume of water in the steam treatment experiments during which time all other variables remained constant with the other two cases (SBDWE1, SBDWE3). Two hours after the initial interaction, heavy oil spread over the glass surface due to IFT reduction caused by SBDWE (**Figure 32**). **Table 26** also displays the comparative spreading results of SBDWE at different storage periods. Texture, consistency and stability of SBDWE samples can evolve over time and an optimal storage period exists for SBDWE samples. The spreading results (Table 26), for instance, show that the particular SBDWE used for this test was most stable after 2 week of storage period and, consequently, results in rapid, efficient spreading of heavy oil.

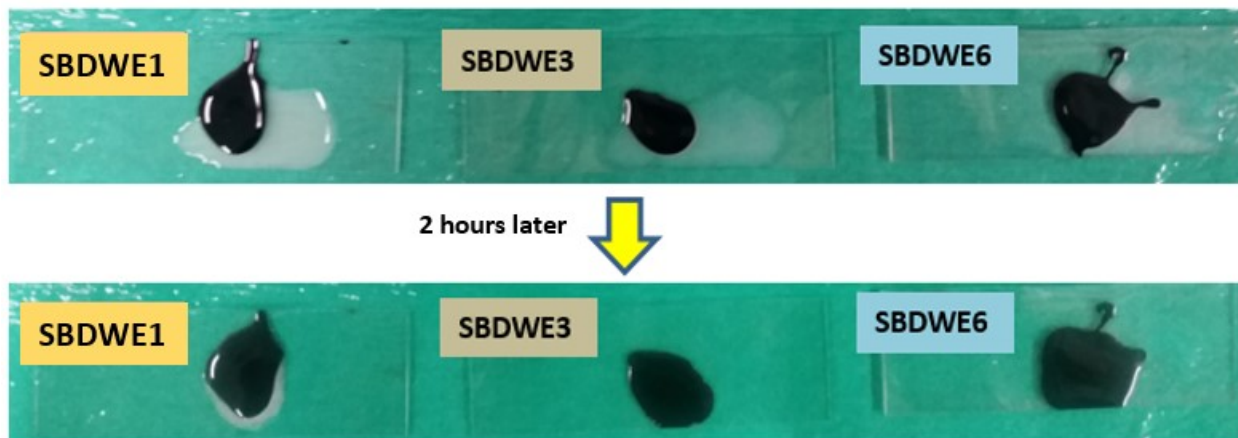


Figure 32—Spreading test.

Table 26—Change in SBDWE stability over time.

<u>400µm</u>	Length of period of the biodiesel emulsion samples kept at ambient conditions	Biodiesel in water Emulsion samples	Spreading
	1 hour		
	2 weeks		
	3 weeks		Loss of emulsion
	4 weeks		

4.5.3 Glass tube tests

Glass tube tests were conducted using both soft brine and hard brine to study the resilience of SBDWE to hard brines, which contain divalent cations that are often found in real reservoir settings (**Figure 33**). The tests showed that while divalent ions can hinder emulsification between SBDWE and heavy oil, it does not lead emulsions to completely lose emulsification capacity. Glass tube tests confirmed the ability of the SBDWE samples to reduce interfacial tension between heavy oil and biodiesel in water emulsion under both soft and hard brine conditions. The SBDWE sample used in these glass tube tests were 3 weeks old with homogeneous texture resembling the condensate shown in Figure 29. The glass tube test results confirmed the robustness of SBDWE in their ability to form stable emulsions under challenging brine conditions. In **figure 33**, SB refers to soft brine ($\text{NaC} = 2.5 \text{ wt.}\%$), HB refers to hard brine ($\text{NaCl} = 2.5 \text{ wt.}\%$, $\text{CaCl}_2 = 0.1 \text{ wt.}\%$, $\text{MgCl}_2 = 0.01 \text{ wt.}\%$) and BD-W refers to (Steam treated) BioDiesel in Water emulsion.

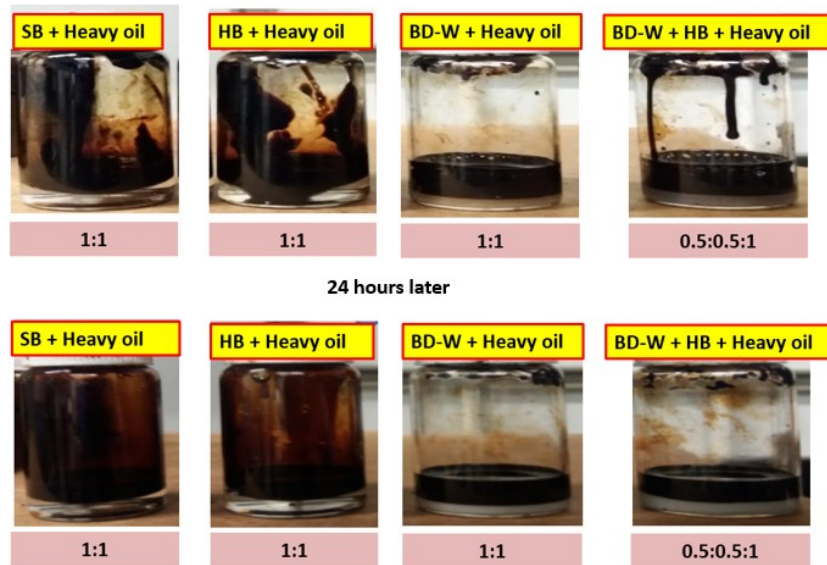


Figure 33—Glasstube test results.

4.5.4 Microscopic visualization

4.5.4.1 Original biodiesel and its interaction with oil.

Figure 34 displays the interaction between untreated biodiesel and oil. A 1:1 ratio of biodiesel and oil was applied for this visualization study. Biodiesel concentration was exaggerated for these tests for the theoretical purpose of making the fluid interaction more discernible and apparent. Light green color is indicative of emulsification between heavy oil and SBDWE. The

dark phase (Figure 34) is oil and the dark streaks demonstrate the spreading of oil into the biodiesel phase. The spreading process was observed to be rapid and continuous while oil the spread into the biodiesel phase, which is characterized by its distinct bright yellow color. **Figure 35** demonstrates two cases of interaction: biodiesel in water emulsion with heavy oil and water in biodiesel emulsion with heavy oil. Water in biodiesel in heavy oil case also displays thin streaks of oil flowing into the biodiesel phase in a similar way that the raw form of original biodiesel interacts with oil.

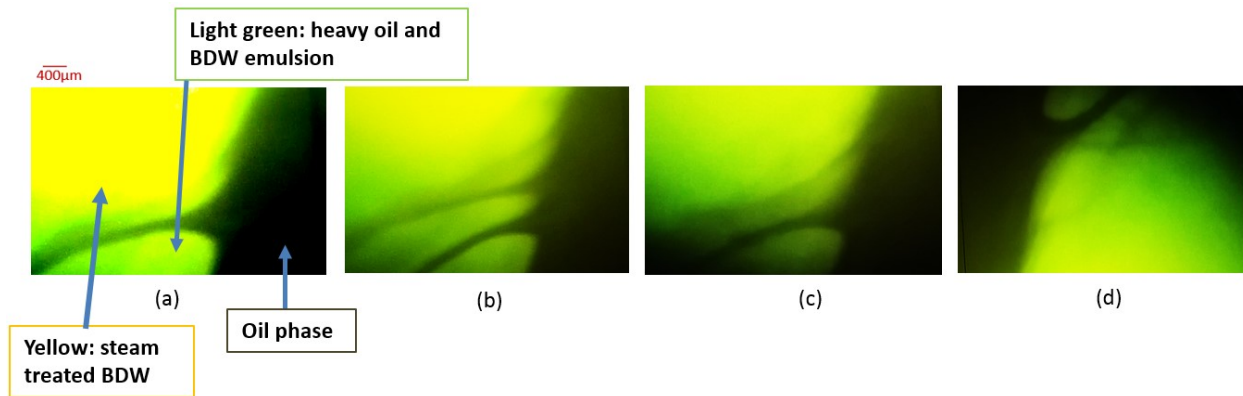


Figure 34—Original biodiesel and its interaction with oil.

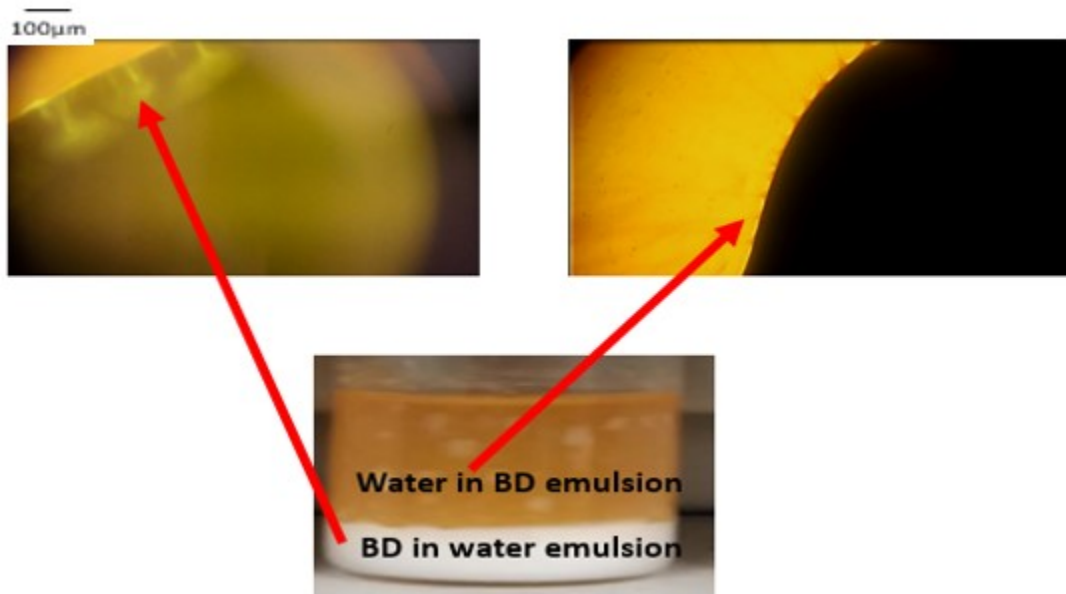


Figure 35—Micrographic analysis of SBDWE (Steam treated BioDiesel in Water Emulsion) and SWBDE (Steam treated Water in BioDiesel Emulsion).

4.5.4.2 SBDWE1.

SBDWE1 is representative of poor quality biodiesel-in-water emulsion. Concentration of biodiesel injected in this emulsion was 0.12%, injected water was 500 ml and the pressure measured in the reactor was 180 psi. Soaking time of biodiesel under steam conditions was 4 h (Table 25). As SBDWE1 displayed poor emulsification capacity, in an effort to increase its stability and improve its interaction with heavy oil, various emulsion stabilization methods were adopted. These efforts included adding silica, and maintaining the emulsion samples in an oven at a temperature of 50°C higher than room temperature.

Figure 36 with SBDWE1 shows that not only the biodiesel droplets of this emulsion cannot attach affectively to the interface and interact with the heavy oil phase, they are also large in size without any small aggregated droplets around them, which is indicative of poor quality emulsion. Some flocculation of these large-sized droplets was observed, which is also indicative of unstable emulsion. Once silica was added (**Figure 37**), oil droplets seemed to deform in shape and smaller particles began to appear with little interaction between SBDWE1 and heavy oil. In an effort to improve stability, the emulsion sample was kept in the oven at 50°C as an increase in temperature can reduce IFT and viscosity of the dispersed phase leading to better emulsification (**Figure 38**). As shown in Figure 38, aggregation of biodiesel droplets at the interface between SBDWE and heavy oil was observed. However, in this interaction, biodiesel droplets still did not penetrate into the oil phase. **Figure 39** displays the interaction between silica added SBDWE1, which was kept at 50°C for 24 h, and heavy oil. A thin streak of faint light green emulsified phase appears, implying that some of the biodiesel droplets penetrated into the oil phase, which is in contrast to Figure 38. Overall, some improvement in interaction between heavy oil and SBDWE was observed with addition of silica and increase in storage temperature.

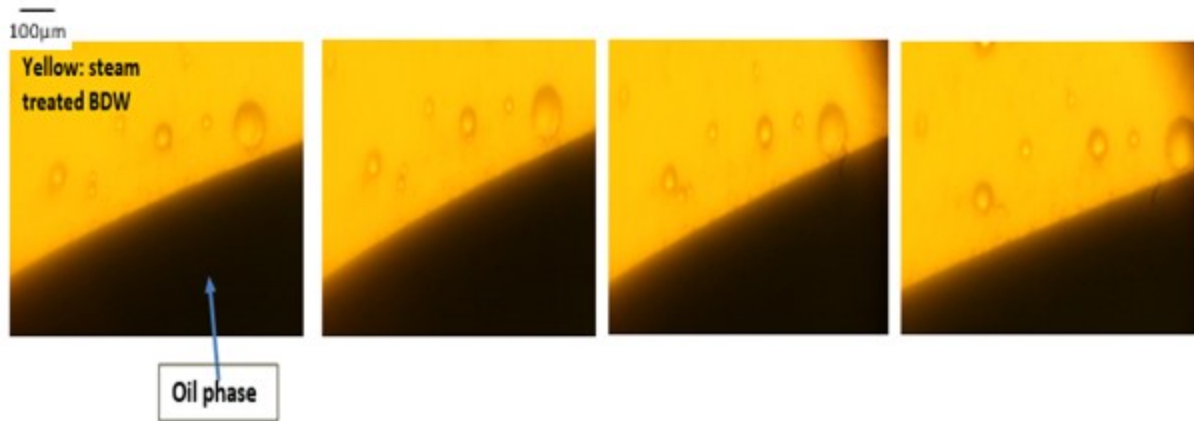


Figure 36—SBDWE1 and heavy oil.

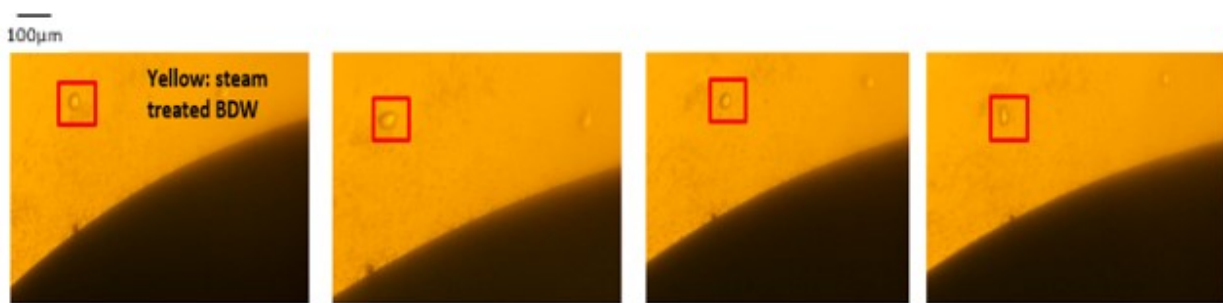


Figure 37—SBDWE1 with heavy oil after addition of silica.

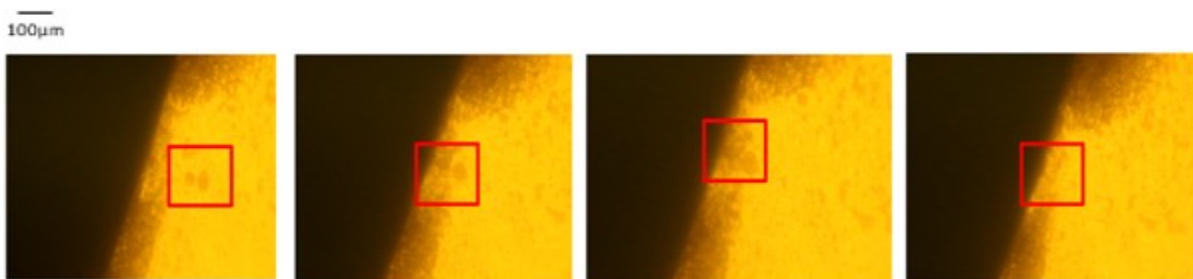


Figure 38—SBDWE1 (24 hr after being maintained in the oven at 50°C).

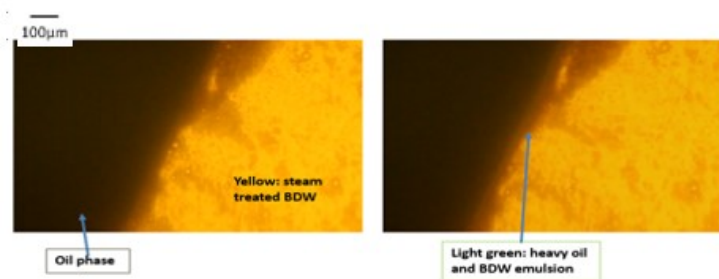


Figure 39—Silica added SBDWE1 case (24 hr after being maintained in the oven at 50°C).

4.5.4.3 SBDWE6.

SBDWE6 is representative of high quality biodiesel-in-water emulsion. Concentration of biodiesel injected in this emulsion was 0.12%, which, in this case, was injected with 938 ml of water and the pressure in the reactor was measured to be 180 psi. Soaking time of biodiesel under steam condition was 4 h (Table 25). In an effort to increase its stability even further than observed in **Figure 40** with formation of emulsified phase, silica was added and their interaction was observed under the microscope.

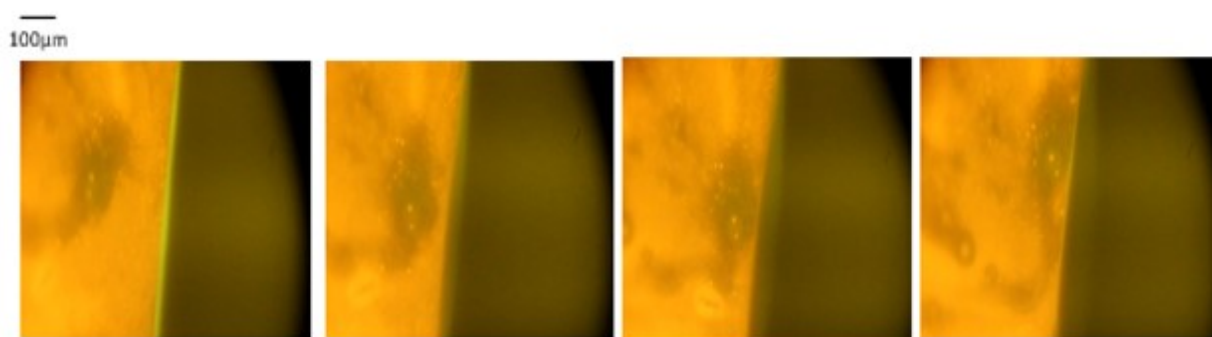


Figure 40—SBDWE6 without addition of silica.

With addition of silica to the SBDWE sample, emulsion phase was observed to spread first into the oil phase. Oil phase then began to expand due to the interaction between small biodiesel droplets with silica and the to the emulsion part of the oil phase. This phenomenon could be explained by glycerol's natural affinity to silica. Hydrophilic silica, which has the potential to adsorb glycerol and therefore is no longer fully hydrophilic, activates the interaction between SBDWE and heavy oil by penetrating into the oil phase with SBDWE, leading to rapid spreading of heavy oil due to IFT reduction (**Figures 41 and 42**). The yellow indicates SBDWE, light green indicates emulsion phase, and dark green is representative of heavy oil.

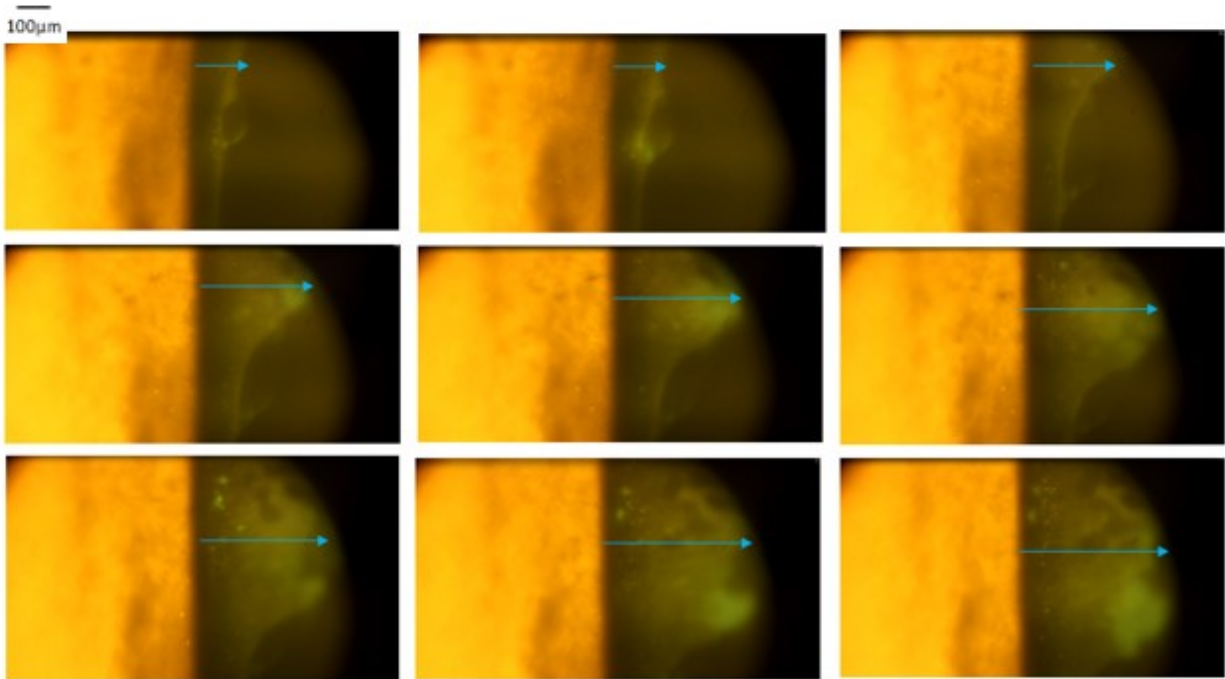


Figure 41—SBDWE6 with silica (initial).

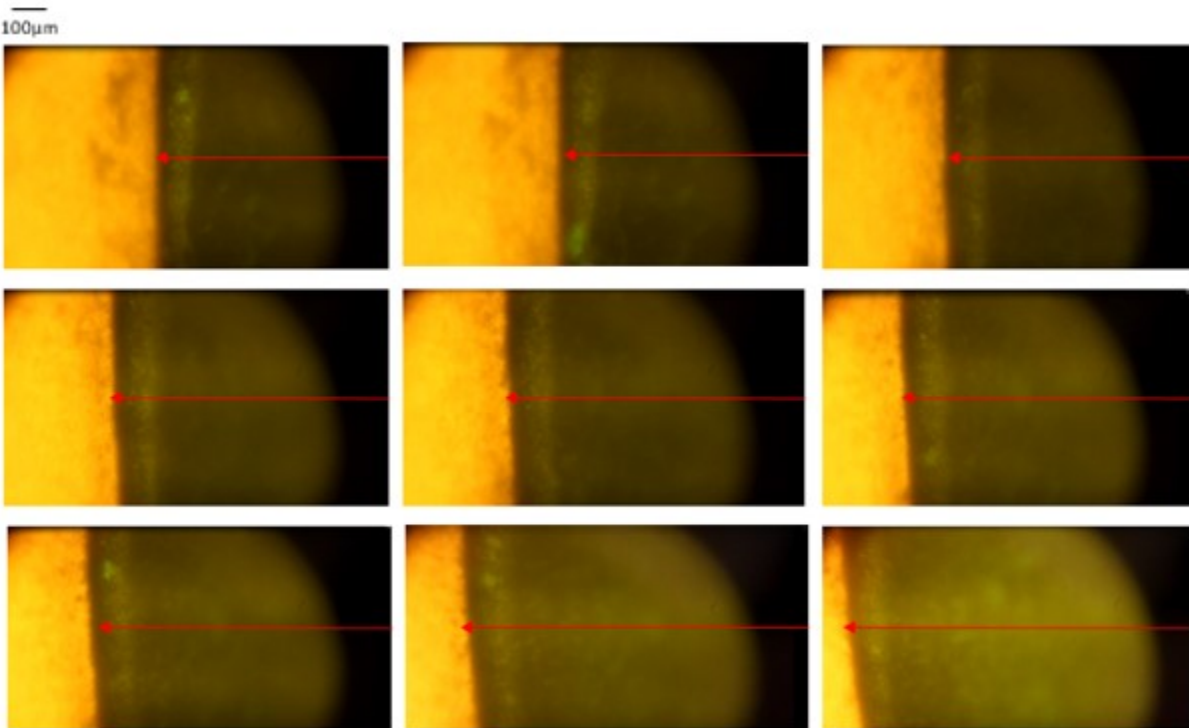


Figure 42—SBDWE6 with silica: expansion of oil phase (final).

4.5.4.4 SBDWE3

SBDWE3 emulsion was initially not very stable and was characterized by its lack of interaction with heavy oil. Concentration of biodiesel injected in this emulsion was 0.12%, injected water was 700 ml and the pressure measured in the reactor was 180 psi. Soaking time of biodiesel under steam condition was 4 h. Due to the lack of stability that is characterized by this emulsion, it was left to be observed over the 3-week period to check any potential change in the consistency, texture, and stability of the emulsion samples. **Figures 43 and 44** display the results of SBDWE2's interaction with heavy oil 3 weeks after the steam treatment. As displayed in Table 26, steam treated SBDWEs' texture and stability can change over time. It was observed that SBDWE3's stability was most optimal after 3 weeks, and after 4 weeks SBDWE3 began to lose its stability with biodiesel creaming at the top. Figure 43 shows that even prior to adding silica, SBDWE3 actively interacts with the oil phase and some emulsion formation can be observed while SBDWE3 penetrates into the oil phase. However, with addition of silica, interaction becomes even more dynamic and animated as the emulsion phase becomes more prominent at the interface (Figure 44).

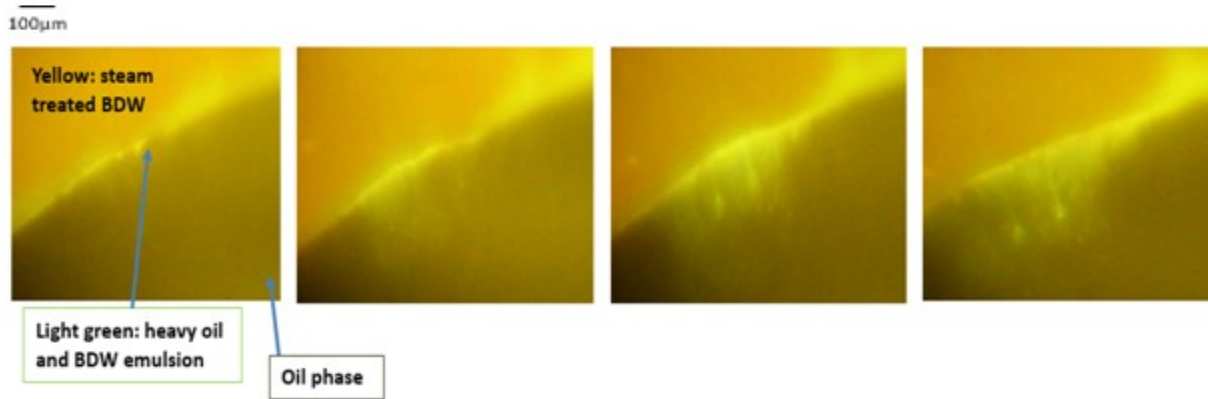


Figure 43—SBDW3 #2 before adding silica (3 week old)

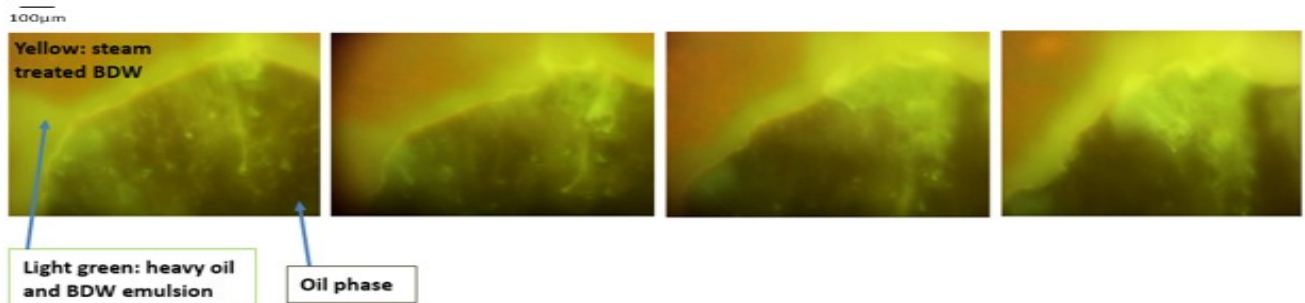


Figure 44—SBDW3 #2 case after adding silica (3 week old).

4.5.4.5 Optimal sample

By micrographic analysis, the most optimal SBDWE samples (**Figure 18**) seem to be characterized by copresence of big oil droplets (about 50 μm in diameter) and smaller aggregated droplets ($<1 \mu\text{m}$ in diameter). These are the samples that were generated using the highest volume of water with the longest soaking time. This can lead to the conclusion that recovery mechanisms for SBDWE generations are significantly enhanced with the increase in the amount of steam used to generate SBDWE.



Figure 45—STDW6 sample.

4.5.5 Sandpack flooding

Sandpack flooding and addition of polymer in sandpack flooding

Polymers are unlikely to perform well in displacing heavy oil of viscosities more than a couple hundred mPa.s (Thomas et al. 1999). However, in this study, not only Xanthan gum flooding could recover oil of 3,437 cP with a very low polymer concentration (0.35%), it was observed that polymer could enhance the capacity of SBDWE to recover oil by providing better surface contact, as well (**Figure 46**). The latter result is due to SBDWE's capacity to decrease IFT between water and oil and polymer's property to improve the efficiency of water contact and also reduce oil-water interfacial tension (Sandvik and Maerker 1977; Hennock et al. 1984; Prudhomme and Long 1983).

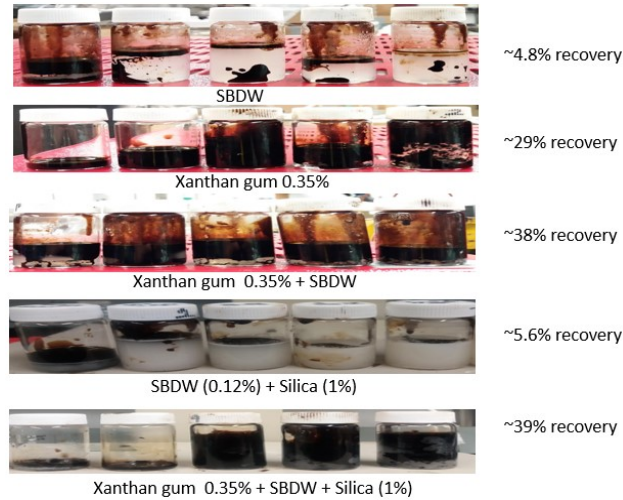


Figure 46—collected samples at every 0.1 PV

Even though there was some improvement in oil recovery when SBDWE was injected, the recovery fell dramatically at around 0.05 PV (**Figure 47**). The cause of this decrease in recovery did not seem to be due to the loss of stability in SBDWE, based on the visualization analysis of collected samples (Figure 46), but rather because SBDWE could not sufficiently interact with oil. This conclusion was drawn based on the observation of produced samples. The aqueous phase was cloudy rather than transparent, which would have been because of an aqueous phase consisting purely of distillate water. Adding Xanthan gum into the SBDWE system led to a dramatic increase in oil recovery (**Figure 48**). Even though the recovery began to decrease at around 0.85 PVI, the recovery was still higher than the recovery attempts made with SBDWE only. These results indicate that the ability of biodiesel to increase in SBDWE-oil contact and IFT reduction in water emulsion and polymer can lead to excellent heavy oil recovery.

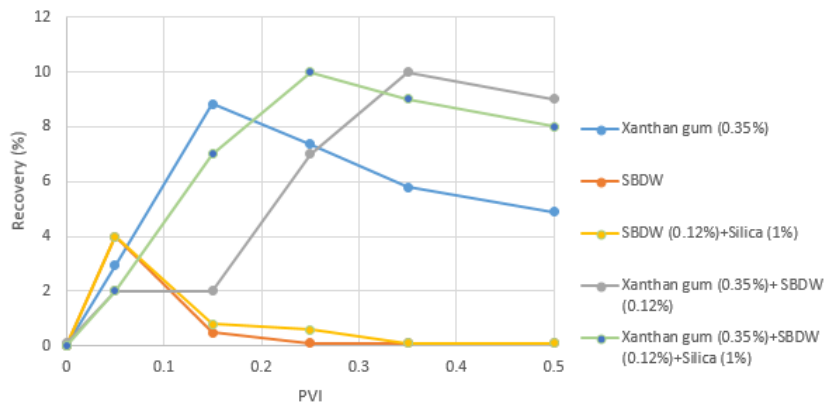


Figure 47—Recovery results from sandpack flooding experiments

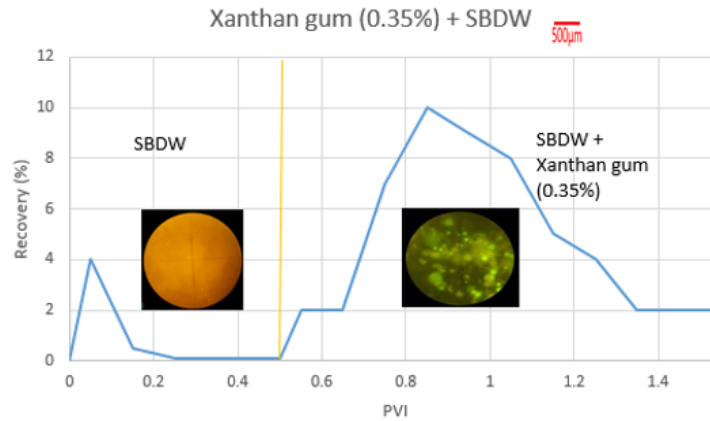


Figure 48—Dramatic improvement in oil recovery with addition of Xanthan gum

Xanthan gum flooding was also conducted to create a base case necessary for comparison analysis with SBDWE with polymer experiment. For the Xanthan gum flooding case, whilst the overall recovery was high compared with the SBDWE or SBDWE with silica case, the recovery began to decrease at around 0.15 PVI. Rapid production and continuous decrease in recovery from its peak was the characteristic of this flooding test. With Xanthan gum and SBDWE flooding, the production began to increase dramatically from 0.15 PVI. In the case with Xanthan gum, SBDWE with addition of silica, the recovery began to increase after 0.05 PV. Final recovery results were pretty similar for the cases with Xanthan gum +SBDWE and Xanthan gum + SBDWE + silica with the latter case with the addition of silica achieving a higher recovery by a margin, roughly about 1% more than the previous case. It shows that silica can initially contribute to oil recovery but the enhancement cannot be maintained. It is possible that silica rapidly loses its stability as an emulsification enhancer and cannot quite contribute to the SBDWE stability for a long period of time. Adding chemicals such as silica or SBDWE can also degrade the quality of polymer mixture based on the chemical reaction between polymer and miscellar fluids (Sandvik and Maerker 1977), which can explain the slower oil recovery found in the case of Xanthan gum mixture with SBDW or SBDW with silica.

In the case with SBDWE sandpack flooding and SBDWE sandpack flooding tests with silica, the role of silica seemed to be even more insignificant. These results because these solutions simply did not have sufficient energy to contact heavy oil and interact accordingly as Xanthan gum was not added. In conclusion, high recovery results could be achieved with a mere 0.5 PVI of Xanthan gum mixture with SBDW (Figure 47). Adding SBDWE to Xanthan gum flooding can improve the recovery by 9%, which is a significant amount in a real reservoir setting. To

achieve ~39% oil production, a mere 0.5 PVI of 0.35 wt. % Xanthan gum and 0.12 wt. % of biodiesel are needed. This result confirms the cost-effective, practical applicability of SBDWE in the heavy oil recovery industry.

4.6 Conclusions

The following conclusion can be made:

1. Aggregation of biodiesel droplets at the interface between SBDWE and heavy oil leads to formation of emulsion.
2. Heterogeneity in biodiesel particle sizes does not play a significant role in SBDWE's interaction with heavy oil; however, coalescence and creaming are indicative of poor emulsification of SBDWE and therefore should be prevented.
3. Injection of high concentration biodiesel can lead to SWBDE (Steam treated Water in Biodiesel Emulsion) as opposed to SBDWE (Steam treated Biodiesel in Water emulsion).
4. Addition of silica can enhance interaction between heavy oil and SBDWE; however, it does not greatly contribute to oil recovery based on the results from the sandpack flooding tests.
5. Low injected water volume (represents volume of steam in the system) is not effective in homogenizing SBDWE; therefore, application of high injected water volume to generate SBDWE is recommended.
6. Soaking time of biodiesel under the steam condition can have a significant impact on its stability; the longer the soaking time, the more stable SBDWE can be generated.
7. Glass tube naked-eye visualization is not sufficient to truly capture the behavior of SBDWE and understand its interaction with heavy oil. Microscopic visualization and sandpack flooding tests are recommended to confirm the capacity of SBDWE to generate emulsions in a porous media.
8. With the addition of low concentration of polymer (0.35%) to SBDWE in sandpack flooding, dramatic increase in oil recovery can be achieved. SBDWE injection with low concentration of polymer is a cost-effective way to enhance heavy oil recovery.

Chapter 5: Impact of hard divalent cations on heavy oil-in-water emulsification

5.1 Preface

Many reservoir formation brines are characterized by high salinity and contain high concentrations of divalent ions such as calcium, magnesium and potassium. These challenging conditions can render the surfactants ineffective during chemical flooding for enhanced heavy oil recovery. In order to solve these issues, glass tube experiments, microscopic visualization and sandpack flooding experiments were conducted in this study at low salinity/hard brine, high salinity/hard brine conditions using commercial chemicals, which are designed for specific reservoir brine conditions. Recovery results show that complex colloidal solution introduced in the previous study with Silica and DTAB along with screened chemicals from glass tube tests in this study can enhance heavy oil recovery significantly with an addition of low concentration polymer (xanthan gum). The results confirmed the robustness of the complex colloidal solution formula to enhance oil recovery with a low concentration of polymer at any reservoir brine conditions. The study also demonstrates the potential of polymer as an emulsion stabilization additive for enhanced heavy oil recovery by in-situ emulsion generation.

5.2 Introduction

Many heavy oil reservoirs around the world are not appropriate for thermal enhanced oil recovery applications. For these fields, it is essential to apply non-thermal recovery methods that are economically feasible such as cost-effective chemical flooding. Previous studies have shown that complex colloidal solution injection with Silica and DTAB and an anionic surfactant can enhance heavy oil recovery at low-salinity soft brine conditions by in-situ emulsification (Lee and Babadagli 2017). Enhanced heavy oil recovery could also be observed with biodiesel-in-water emulsion flooding with low concentration of polymer at soft brine, low salinity conditions due to IFT reduction, increased heavy oil and solution contact, and improved mobility ratio (Lee et al. 2018). However, previous experiments were conducted at soft brine conditions, which limit the aforementioned chemicals' potential to be applied at hard brine reservoir conditions. In real reservoir settings, hard divalent cations such as magnesium, calcium, and potassium exist and can have a great impact on the formation brine properties (Collins 1975; Pollock 2013). These ions can cause problems such as surfactant retention and precipitation. Calcium and sodium ratio, for instance, can also have an impact on the optimal ionic strength, which can affect the phase behaviour and IFT of a surfactant and a crude oil (Tichelkamp et al. 2016). In order to challenge these issues, in this study, two types of brines were synthesized in the lab: high salinity/hard brine and low salinity/hard brine. Chemicals were first screened through glass tube tests in their capacity to generate emulsions at these hard brine conditions. After the preliminary glass tube screening where emulsification capacity of the chemicals were tested, selected chemicals were further tested for sandpack flooding tests, and the produced emulsion samples were visualized under the microscope to observe the phase behaviour and investigate the impact that the hard divalent cations can have on in-situ emulsification.

5.3 Materials

Heavy oil: Heavy dead crude oil in this study is from an oil field in Western Saskatchewan. At room temperature (25°C) and atmospheric pressure, density was measured to be 0.9714 g/cm³ and viscosity was measured to be 3,437 cP. The API gravity of the oil is 13.14°.

Surfactants: In a research study with sodium dodecyl sulfate and sodium dodecyl sulfonate and their interaction with divalent cations Ca²⁺ and Mg²⁺, results showed that sulfonate surfactants performed better than sulfate surfactants in enhancing oil recovery because sulfate surfactants tend to bind the ions more easily than sulfonate surfactants which can lead the ions to affect the hydration structure (Yan et al. 2010). Based on these previous findings, sodium dodecyl sulfate and sodium dodecylbenzene sulfonate were tested along with internal olefin sulfonate surfactants from the Enordet series. Alcohol-based surfactants from the Enordet series were also tested. Hard brine resistant surfactants from the Aspiro series were tested in accordance with the optimal salinity ranges recommended by their manufacturers. Detailed compositions of the chemicals are listed in **Tables 27 and 28** (BASF 2014; Shell 2018). Surfactants from Enordet series were tested and screened in a the previous study with alcohol alkoxy sulfate surfactants resulting in higher quality emulsification than internal olefin sulfonate surfactants at 2.5% NaCl brine condition without any hard divalent ions (Lee and Babadagli 2017).

Table 27—Aspiro surfactants.

	Name	Type	Components	pH	Optimal range of Salinity(pp m)	Temp
A	Aspiro S 2425 X	Co-surfactant	D-Glucopyranose, oligomers, decyl octyl glycosides	11.5-12.5	NA	NA
B	Aspiro S 2410	Surfactant	D-Glucopyranose, oligomeric, C10-16 Alkyl glycosides, D-Glucopyranose, oligomers, decyl octyl glycosides	8.5	NA	NA
C	Aspiro S 2430 X	Co-surfactant	D-Glucopyranose, oligomers, decyl octyl glycosides	Approx. 8	25,000 - 120,000	60
D	Aspiro S 2850 X	Surfactant	Trade secret	5.5-6.5	50,000 -150,000	100
E	Aspiro S 2455 X	Surfactant	N/A	11.5-12.5	N/A	N/A
F	Aspiro S 8310	Surfactant	40~70%: Oxirane, 2-methyl-,polymer with oxirane,	8-9	0-120,000	60

			mono(hydrogen sulfate), C16-18-alkyl ethers, sodium salts, butyl diglycol, alcohols, ethoxylated propoxylated, sodium hydroxide, disodium hydrogen orthophosphate		
G	Aspiro S 2420 X	Surfactant	D-Glucopyranose, oligomeric, C10-16-alkyl glycosides, D-Glucopyranose, oligomers, decyl octyl glycosides	0-120,000	60

Table 28—Enordet surfactants.

Enordet	Surfactant type/Components	Optimal salinity range against octane	Di-valent ion tolerance #	Temperature
O352	Internal Olefin Sulfonate	0.1-1	Limited	90 with 2 wt.% (up to 200)
O332	Internal Olefin Sulfonate	9-13	Limited	90 with 2 wt.% (up to 200)
J11111	Alcohol Alkoxy Sulfate or alkyl Ether Sulfate	0.5-2	Excellent	50
J771	Alcohol Alkoxy Sulfate or alkyl Ether Sulfate	1.5-4	Excellent	50
J13131	Alcohol Alkoxy Sulfate or alkyl Ether Sulfate	0.5-2	Excellent	50

Polymer: BARAZAN® D PLUS™ Xanthan gum was used in this study based on its good performance in stabilizing emulsion and improving oil recovery in previous studies (Lee et al. 2018). Sandvick and Maerker (1977) stated that polymers can also improve water and oil contact which can subsequently displace oil more efficiency and thus, enhancing oil production. Xanthan gum is also known to have an oil-water interfacial lowering property which makes it an ideal

surfactant stabilization agent for this emulsion study (Hennoek et al. 1984) (Prudhomme and Long, 1983).

Brine: Two types of brines were used in this study. **Type 1** brine is a low salinity brine and its composition is detailed in **Table 29**. **Type 2** brine is a high salinity brine as detailed in **Table 30**. High salinity brines used in this study were synthesized in the lab based on the brine composition analysis results conducted with brine samples collected from produced reservoir fluids from the Lloydminster field in West Saskatchewan, Canada. Low salinity brines were synthesized in accordance with low salinity composition suggested by Steve et al. (2016). Two types of brines were studied in this study to match the recommended range for salinity and hardness appropriate for each chemical.

Table 29—Low salinity brine (Type 1).

Components	Concentration (ppm)
NaCl	10,000
CaCl ₂	1000
MgCl ₂	100
KCl	0

Table 30—High salinity case (Type 2).

Components	Concentration (ppm)
NaCl	80,000
CaCl ₂	1000
MgCl ₂	500
KCl	100

5.4 Methodology

5.4.1 Glass tube test

Surfactants were tested for their ability to form emulsion at hard brine conditions. Surfactants from the Enordet series along with Sodium Dodecyl Sulfate and Sodium Dodecyl Benzene Sulfonate were tested with low salinity brine with hard divalent ions (Table 29) and surfactants from Aspiro series were tested with high salinity brine with hard divalent ions (Table 30).

Addition of polymer was considered based on the previous findings regarding polymer's efficiency as an emulsion stabilization agent as introduced in Chapter 4. More detailed glass tube screening process is discussed in Chapter 2.1 wt.% concentration of surfactant was used for all glass tube and sandpack flooding experiments except in complex colloidal solution tests where 0.5% surfactant was used in the mixture with DTAB (0.04%) and Silica (1%) following the results from the previous study findings (Lee and Babadagli 2018).

5.4.2 Sandpack flooding test

Conducting sandpack flooding experiments is an essential task in determining whether the selected chemical from the glass tube screening tests can enhance heavy oil recovery by in-situ emulsification in porous media. Many factors including chemical adsorption (Gogoi 2011; Li et al. 2016) and insufficient contact energy between oil and solution can reduce the potential for enhanced heavy oil recovery. **Table 32** displays inconsistent results found between glass tube experiment emulsion samples and produced samples collected from the sandpack experiment. As seen in Table 32, glass tube experiments using IOS0332 with colloidal solution consisted of Silica and DTAB at high salinity, hard brine conditions, stable emulsions, which transitions from Winsor type 4 emulsion to Winsor type 1 emulsion after 1 hour without phase separation could be observed. However, 1 PVI sandpack flooding with the complex colloidal solution with IOS0332 at hard brine conditions gave poor oil recovery results and produced samples displayed distinct two phase separation (Table 32).

These results contradicted the recovery results from colloidal complex flooding experiments conducted with alcohol propoxy sulfate surfactants at low salinity, soft brine conditions, which displayed high quality produced emulsion samples in glass tube experiments and in various flooding experiments (Lee and Babadagli 2018). This contradiction in emulsion production results indicates that hard divalent ions can have a serious impact on in-situ emulsification in porous media. Therefore, understanding the behaviour of hard divalent ions and their impact on in-situ emulsification in the porous media is an essential task.

For the sandpack flooding setup, high porosity and high permeability sandpacks were used in order to match common reservoir characteristics that exist in heavy oil reservoirs in Canada and

Venezuela, which are two countries known for their huge heavy oil reserves. Teledyne ISCO syringe pump was used to inject the solution into the sandpack. The core holder used in this setup was tightly packed with sands saturated with heavy oil of 3,437 cP viscosity. Flow rate of 0.6 ml/min was applied in the flooding experiments. **Table 31** indicates chemical combinations that were used in the flooding experiments. A surfactant from Aspiro series and SDBS surfactant with addition of Xanthan gum were selected for further sandpack flooding experiments based on their optimal results from the glass tube tests. The phrase “colloidal solution” may be used throughout the study to refer to Silica and DTAB combination. Addition of colloidal solution was considered in this study based on positive in-situ emulsification results from the sandpack flooding experiments observed in Chapter 3.

Table 29—Sandpack flooding.

System	Chemical composition	Brine
#1	Aspiro A + Xanthan gum	Type 2
#2	SDBS + Xanthan gum	Type 1
#3	Aspiro A + Silica + DTAB + Xanthan gum	Type 2
#4	SDBS + Silica + DTAB + Xanthan gum	Type 1

Table 30—Glass tube results and core flooding results from IOS0332 with colloidal solution without addition of polymer.

Glass tube results	Immediately after	1 hour later
		
Core flooding results (1PV injected)		

5.5 Results

5.5.1 Glass tube tests

Tables 33 and 34 display low salinity/hard brine test results with surfactants from the Enordet series and SDS, SDBS. This experiment shows that alcohol-based Enordet surfactants in particular were able to generate Winsor type 4 emulsions initially but the two phase emulsion separation could be observed 10 minutes after the agitation in all cases. However, when 0.35% Xanthan gum was added, all the chemicals listed in Tables 33 and 34 successfully generated stable, high quality Winsor type 4 emulsions except IOS0352 and J11111 whose emulsion stability could not last for more than 10 minutes until they separated into two distinct phases. In particular, SDBS with polymer gave good emulsification results forming microemulsion in the glass tube tests. Therefore, SDBS with polymer additive combination was selected for further sandpack flooding experiments to test their capacity to enhance heavy oil recovery.

Table 31—Low salinity tests with Enordet series and SDS and SDBS.

	SDS	SDS+P	SDBS	SDBS+P	IOS 0352	IOS 0352+ P	IOS 0332 P	IOS 0332+ P
Con. (wt. %)	1%	(Surfactant) 1% + (Polymer) 0.35%	1%	(Surfactant) 1% + (Polymer) 0.35%	1%	(Surfactant) 1% + (Polymer) 0.35%	1%	(Surfactant) 1% + (Polymer) 0.35%
Immediately after								
10 minutes later								

Table 32—Alcohol-based Enordet surfactants.

	J771	J771+P	J11111	J11111+P	J13131	J13131+P
Con. (wt.%)	1%	(Surfactant) 1% + (Polymer) 0.35%	1%	(Surfactant) 1% + (Polymer) 0.35%	1%	(Surfactant) 1% + (Polymer) 0.35%
Immediately after						
10 minutes later						

Glasstube results from Aspiro surfactant series at high salinity and hard brine condition (8% NaCl) showed that Winsor type 4 emulsions could not be formed with surfactants alone (Tables 35, 36). Emulsion samples transitioned from Winsor type 4 to Winsor type 2 within 10 minutes for all surfactants. However, with addition of xanthan gum (0.35%), stability of the emulsion generated with surfactant A (Aspiro S 2425 X) greatly improved. The stability of this emulsion sample generated with A and xanthan gum maintained over 24 hour period.

Table 33—Aspiro surfactant series 1.

	A	A+P	B	B+P	C	C+P	D	D+P
Con. (wt.%)	1%	(Surfactant) 1% + (Polymer) 0.35%						

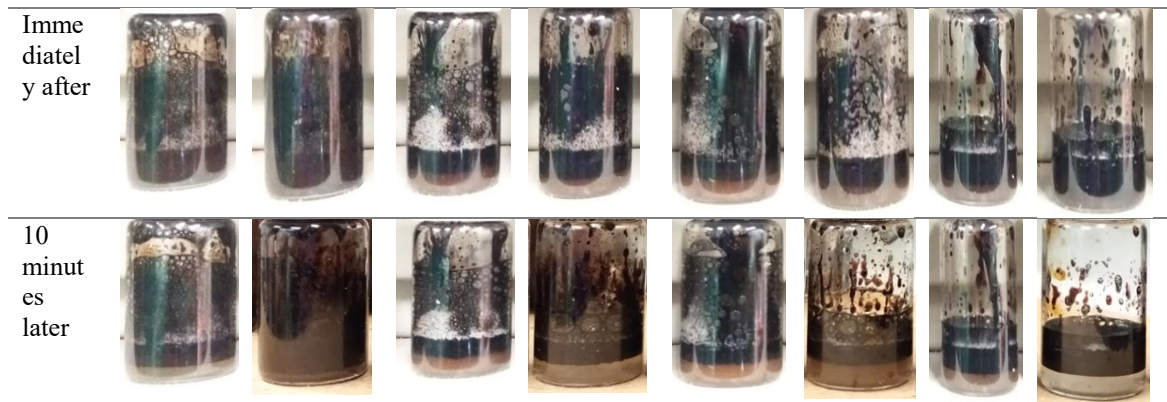


Table 34—Aspiro surfactant series 2.

	E	E+P	F	F+P	G	G+P
Con. (wt.%)	1%	(Surfactant) 1% + (Polymer) 0.35%	1%	(Surfactant) 1% + (Polymer) 0.35%	1%	(Surfactant) 1% + (Polymer) 0.35%
Immediately after						
10 minutes later						

5.5.2 Sandpack flooding

In total of 4 sandpack flooding experiments were conducted (Table 31). Aspiro surfactant sandpack flooding experiments were conducted at high salinity/high divalent ion conditions (System #1, #3) and SDBS sandpack flooding experiments were conducted at low salinity/high divalent conditions (System #2, #4). Sandpack flooding results show (**Figure 49**) that in the case with surfactant flooding with System #1 (Aspiro A + Xanthan gum), production began with

oil/water-in-oil emulsion recovery for the initial 0.1 PVI of solution injection, which was soon followed by oil and water production in a non-emulsified form during 0.4 PVI of solution injection period. Then, Winsor type 3 emulsion production, which is characterized by oil (top)/microemulsion (middle)/water (bottom) could be observed for ~0.5 PVI period followed by fully stable Winsor type 4 emulsion production at ~ 1PVI. In the case with System #2 (SDBS + Xanthan gum), two distinct produced emulsion types could be observed. For 0.9 PVI of solution, oil and water were produced in an unmixed, separated form. Then, fully emulsified Winsor-type-4 emulsion production followed. System #3 (Aspiro A + Silica + DTAB + Xanthan gum) was characterized by oil/water-in-oil emulsion production followed by Winsor type 1 emulsion, then Winsor type 4 emulsion generation could be observed at around ~ 0.9 PVI. System #4 (SDBS + Silica +DTAB+ Xanthan gum) was characterized by oil and water-in-oil emulsion production for 0.5 PVI of solution followed by Winsor type 4 emulsion production.

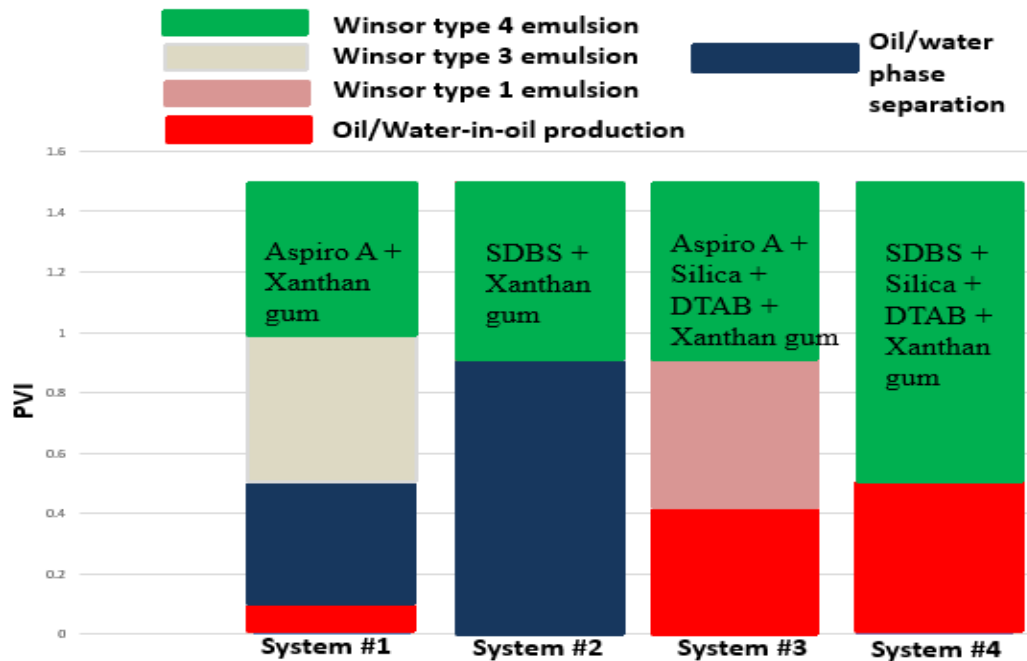


Figure 49—produced emulsion types with PVI.

It was observed that in the case with System #1, #2, #3, after approximately 1 PV injection of chemical solution, some emulsion generation began to be observed until fully developed Winsor type 4 oil-in-water emulsions began to be produced. Formation of Winsor type 4 oil-in-water emulsions at ~ 1 PVI could be potentially due to gradual viscosification of polymer. Polymer viscosification of the aqueous phase is an important component in stable emulsion generation.

Viscosity measurement of the brine with Xanthan gum with Brookfield viscometer showed that in the high salinity case (type 2 brine), initial viscosity was measured to be 2 cP and it increased to 54 cP after 40 minutes of being stored at ambient conditions. 40 minute interval between the two measurements was selected based on the duration of time required for ~1 PVI injection into the sandpack system at 0.6 ml/min. In the case with low salinity brine, initial viscosity was measured to be 2 cP and the viscosity increased to 91 cP 40 minutes after the first measurement.

More rapid viscosity increase was observed in the case with low salinity brine in comparison with the high salinity brine. These results suggest that xanthan gum viscosification may be affected by salts and ions in the brine and viscosity of the solutions can increase drastically within 40 minute period which is time equivalent to ~ 1 PVI. For system #4 however, viscosification effect was not displayed in an apparent manner as other systems in the sandpack flooding recovery results with emulsion type transitioning from oil/water-in-oil emulsion to Winsor type 4 emulsion at 0.5 PV injected. This is possibly due to optimal compatibility between the chemicals and the polymer, which accelerated the polymer viscosification.

In general, emulsification was shown to gradually improve in all cases (Table 37, Figure 49). When complex colloidal solution is added (System #3, #4), it could be observed that from the initial injection period, high oil recovery could be obtained. In the case with SDBS with colloidal solution and polymer (System #4), oil recovery could be observed until 0.5 PVI and then Winsor type 4 oil-in-water emulsion began to be generated. And after 1 PVI injection, increase in the size and number of oil droplets in the emulsion phase could be observed which indicates increase oil production.

Table 35—Glass tube experiment results and micrographic visualization.

	0.5 PVI	1 PVI	1.5 PVI
 Silica (1%) + DTAB (0.04%)+ Aspiro (0.5%) +Xanthan Gum (0.35%)			

Oil production

Winsor type 1 emulsion

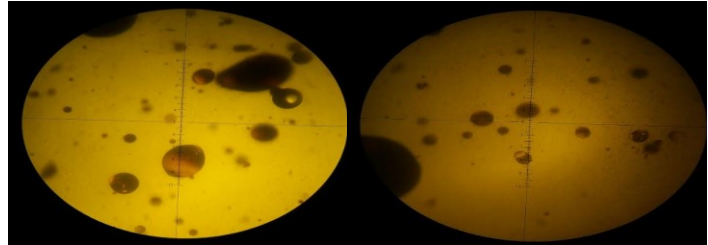
Winsor type 4 emulsion

* Micrographs only

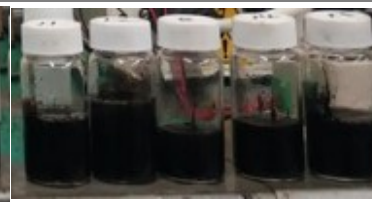
*Micrographs only

display large visible oil droplets

display large visible oil droplets



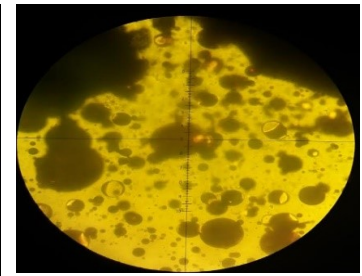
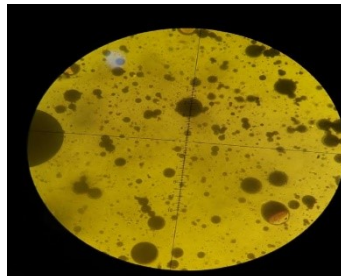
Aspiro (1%) +
Xanthan Gum
(0.35%)



Oil production/two
phase separation

Winsor type 3 emulsion

Winsor type 4 emulsion



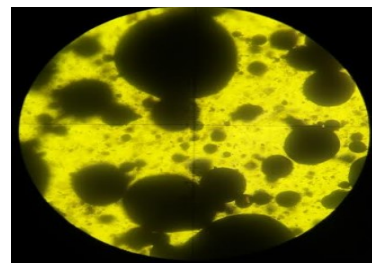
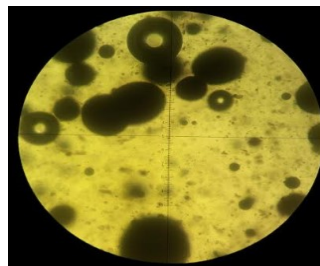
Silica (1%)
+ DTAB
(0.04%)+
SDBS
(0.5%)
Xanthan
Gum
(0.35%)

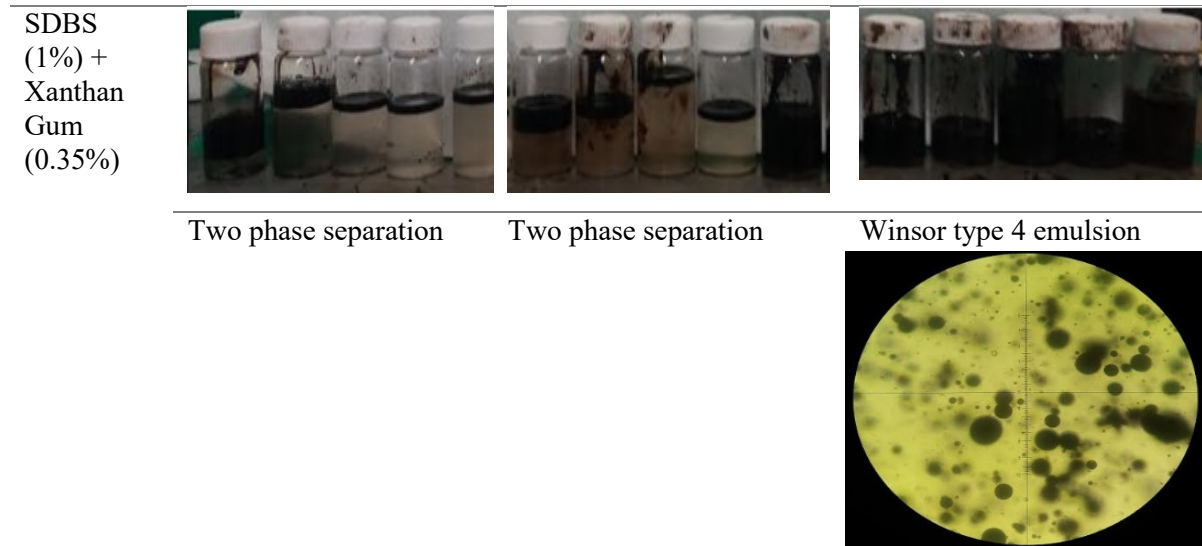


Oil production

Winsor type 4 emulsion

Winsor type 4 emulsion





It could be seen from **Figure 50** that high cumulative oil recovery is characterized by high oil and water-in-oil emulsion recovery which in the case of System #3 is 38% and for system #4 is 32% and for system #1 is 20%. For system #2, however, there was not a production period where only oil or water-in-oil was produced. Instead, oil was produced together with water not in an emulsion form which consisted 18% of the total recovery. Oil/water separate phase production was also observed with system #1 which contributed ~4% recovery and the results demonstrated that this type of oil/water separate phase production is exclusive to sandpack flooding experiments conducted with surfactant and polymer without the colloidal solution.

System #1 and system #3 showed production of various emulsion types. For System #1, Winsor type 3 emulsions which are characterized by oil (top)/microemulsion (middle)/water (bottom) contributed to the total recovery of about 7% and it came after a short period of production of oil/water phase separation. After Winsor type 3 emulsion production, Winsor type 4 emulsion production followed. Emulsion generation at the later stage of the production period (~After 0.5 PV) could be explained by gradual polymer viscosification which led to stable emulsion generation. For system #3, 37% of the recovery was contributed by oil and water-in-oil emulsion generation followed by 15% of the recovery through Winsor type 1 emulsion generation which is characterized by 2 phases: oil (top)/microemulsion (bottom). Winsor type 1 emulsion soon transitioned into Winsor type 4 emulsions at 0.8PVI. For all system cases, Winsor type 4 emulsions began to be generated towards the end of the production period.

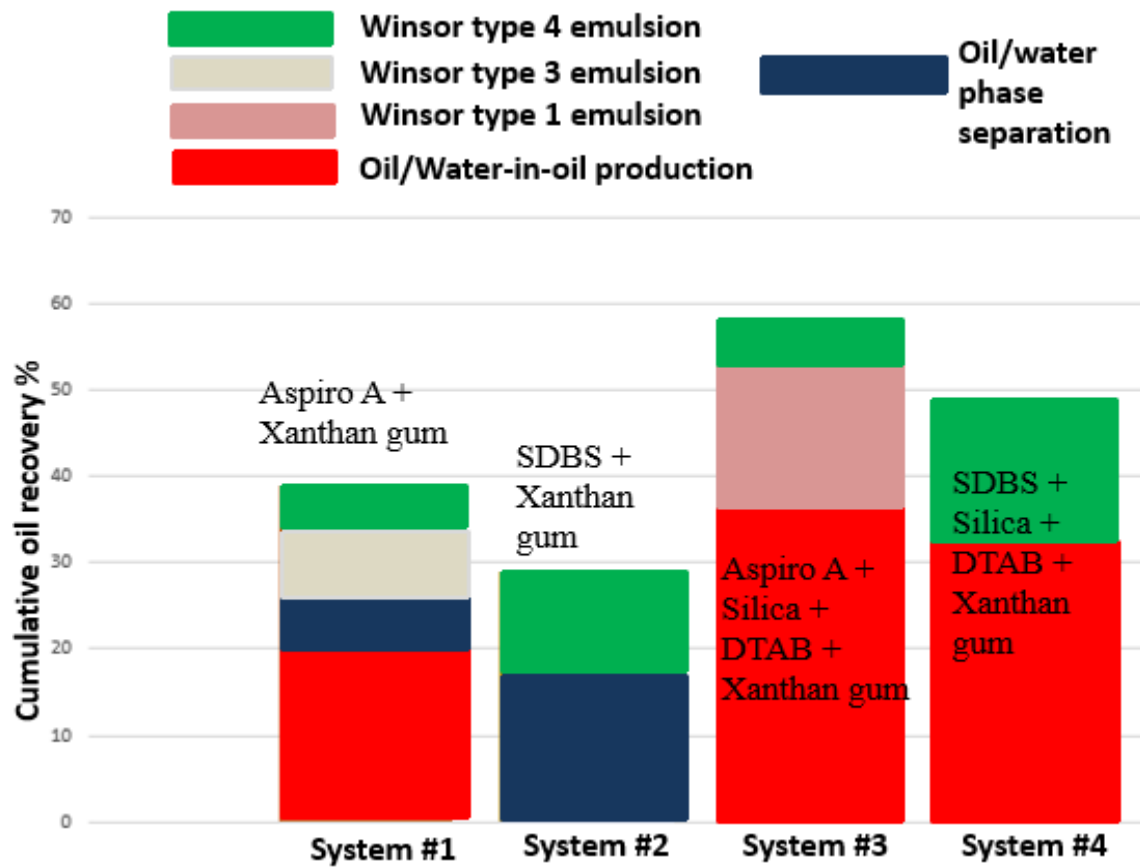


Figure 50—produced emulsion types with cumulative oil recovery.

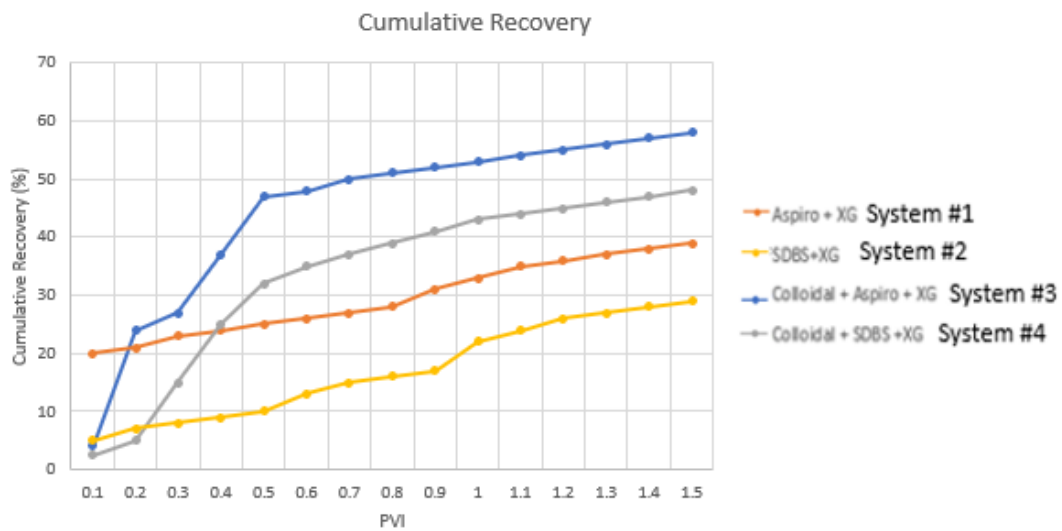


Figure 51—Sandpack flooding results (Cum. recovery vs PVI).

Figure 51 displays cumulative sandpack flooding recovery results. Approximate recovery values were used in this analysis due to the difficulty in estimating the recovery in many samples as they have remained in the emulsified form (Winsor type 4 or Winsor type 3) after weeks of being stored for natural separation by gravity. Microscopic visualization of the emulsified samples (Table 37) was used to estimate the values more effectively. At 1.5 PV injection of chemical solutions, 58% final recovery could be obtained in the case with Aspiro flooded with colloidal solution and Xanthan gum (System #1) followed by 48 % recovery with SDBS surfactant flooded with colloidal solution and Xanthan gum (System #4); 39% recovery with Aspiro A surfactant with Xanthan gum (System #1) and 29% recovery for SDBS with Xanthan gum (System #2). Increase in recovery at 0.9 PVI for sandpack flooding with SDBS and Xanthan gum (System #2) and at 0.8 PVI for sandpack flooding with Aspiro A surfactant with Xanthan gum flooding (System #1) could be observed as well. For colloidal solution flooding cases with Aspiro A surfactant and SDBS (System #3), initially steep increase in recovery is observed due to high oil production. However, after 0.5 PVI for both Aspiro and SDBS with colloidal solution case (System #3, 4) oil recovery remained constant without any apparent increase.

Chemical injections with colloidal solution and polymer (System #3, #4) gave higher recovery results than chemical injections with polymer only (System #1, #2). In the case with colloidal solution flooding, Aspiro surfactant A (System #3), ~19% increase in recovery was observed and in the case with colloidal solution flooding with SDBS (System #4), ~19% increment could be observed after 1.5 PV injection of the solution. The results from this study demonstrate the significance of polymer additive in chemical flooding by emulsification at hard brine conditions. Hard divalent cations, which are common in reservoirs, can be detrimental to heavy-oil-in water emulsification with surfactants and adding an appropriate polymer as an emulsion stabilization additive can improve the stability of emulsions significantly. Polymer application in emulsion stabilization for heavy oil recovery has great potential and it deserves attention.

5.6 Conclusions

1. Addition of a small concentration of polymer can help with oil-in-water emulsification by increasing contact energy between the solution and oil.

2. For low salinity cases with hard divalent ions, alcohol-based surfactants along with sulfonate surfactants performed well and gave high oil recovery results by emulsification with addition of low concentration polymer.
3. For high salinity cases with hard divalent ions, an Aspiro surfactant with high pH performed well and gave and good heavy oil recovery results by in-situ emulsification in sandpack flooding tests with addition of low concentration polymer.
4. Salinity and hardness can have a great impact on the stability of emulsions and it is important to select an appropriate surfactant which is compatible with all reservoir brine types.
5. Glass tube experiments are often considered to be fundamental screening tests to determine emulsification capacity of chemicals but they cannot be a guaranteed source for understanding how the chemicals will behave in a real reservoir environment and therefore, it is important to test the chemicals' capacity to generate emulsions in a porous media.
6. Complex colloidal solution composed of Silica + DTAB and surfactant can increase heavy oil recovery significantly at any brine conditions with addition of polymer.

Chapter 6: Conclusion and Future Work

6.1 Conclusions and Contributions

Unconventional and conventional, commercial chemicals, which include anionic surfactants, cationic surfactants, polymers, carbonate powders, ionic liquids, nanofluids, and SBDWE (Steam-treated-BioDiesel-in-Water-Emulsion), were screened for their capacity to generate emulsions. It was concluded that using a conventional commercial surfactant alone is not sufficient to generate Winsor type 4 heavy oil-in-water emulsions that can survive in a porous media. In an effort to find robust chemical combinations that can generate stable emulsions at low concentrations, synthesis of complex colloidal solutions fortified and stabilized by nanofluids was studied along with biodiesel-in-water emulsion that can function as a surfactant additive using a very low concentration of biodiesel after the steam treatment.

The results show that anionic surfactants of alcohol propoxy sulfate components can generate Winsor type 4 heavy oil in water emulsions with addition of Silica and DTAB at an optimal flow rate leading to roughly 27% recovery. An optimal flow rate can differ based on the characteristics of the porous media as the rate can have an impact on the stability of the injected solutions. Lab synthesized Biodiesel-in-water emulsions (also referred to as SBDWE or SBDW throughout this study) were also studied as their potential function as a stable surfactant additive. It was shown that when SBDWE is injected into the sandpack of 35% porosity with 0.35% of Xanthan gum, high heavy oil recovery could be observed at ~39% recovery. High salinity/hard brine environments require hardness-resistant chemicals designed for and compatible with these environments and show that with addition of 0.35% Xanthan gum to a surfactant composed of D-glucopyranose, oligomers, decyl octyl glycosides with the aforementioned colloidal solution in a chemical flooding at high salinity/hard brine conditions in a porous media, high oil recovery by in-situ emulsification could be observed at 1.5 PV injection. These results indicate that for heavy oil recovery by in-situ emulsification, surfactant additive, and polymer can work as high performance heavy oil recovery agents. It should also be noted that glass tube experiments and IFT analyses do not provide sufficient data to determine the real applicability of chemical solutions. Therefore, experiments involving a porous media such as sandpack flooding and core flooding experiments are recommended to confirm the applicability of the chemical solutions in real reservoir settings. Viscosification of solutions is also essential in enhanced heavy oil recovery by in-situ emulsification for better oil surface and solution contact and mobility.

6.2 Limitations and Future Work

Core and sandpack flooding experiments with chemicals selected in the study have displayed the general tendency of decrease in stable emulsion generation after 1 PVI ~ 1.5 PV of chemical injection without addition of polymer. Nanofluids in particular seemed to aggregate easily and lose stability in the porous media, which is detrimental for maintaining high quality Pickering emulsions even though this aggregation property could be helpful in separation of oil and brine after the production of heavy oil-in-water emulsions. Research results demonstrate that nanofluids must be stabilized for their effective application in a real reservoir setting. Various thermal conditions can also exist throughout the reservoir and the temperature difference found in various parts of a real reservoir could also contribute to the stability loss of solutions in the porous media and thus attention regarding this matter is required. Improving conformance and sweep efficiency, heavy oil, and solution contact energy are fundamental bases for heavy oil recovery by high quality emulsification of heavy oil and brine. Therefore, understanding the impact that viscosifying agents can have on emulsification should be researched, such as investigating polymer types and their optimal concentrations for various brine types for cost-effective heavy oil recovery. In addition, to improve the flooding experiment design, differential pressure throughout the core flooding experiments should be monitored and recorded to have better control over the differential pressure across the core or sandpack samples. The impact of variation in pressure gradients on emulsification should be investigated.

References

Chapter 1

- Arab, D., Kantzas, A., Bryant, S. et al. 2018. Nanoparticle-Fortified Emulsification of Heavy oil. SPE EOR Conference at Oil and Gas West Asia, Muscat, Oman, 26-28 March. DOI: 10.2118/190377-MS.
- Barnes, J.R., Dirkzwager, H., Smit, J.R. et al. 2010. Application of Internal Olefin Sulfonates and Other Surfactants to EOR. Part 1: Structure – Performance Relationships for Selection at Different Reservoir Conditions. SPE Improved Oil Recovery Symposium, Tulsa, Oklahoma, USA, 24-28 April. DOI: 10.2118/129766-MS.
- Chopra, S., Lines, R.L., Schmitt, R, D. et al. 2010. Heavy Oils: Reservoir Characterization and Production Monitoring. DOI: 10.1190/1.9781560802235.
- Farouq S.1976. Non-Thermal Heavy Oil Recovery Methods. SPE Rocky Mountain Regional Meeting, Casper, Wyoming.11-12 May. DOI: 10.2118/5893-MS.
- Gu, H., Cheng, L., Huang, S., et al. 2015. Steam Injection for Heavy Oil Recovery: Modelling of Wellbore Heat Efficiency and Analysis of Steam Injection performance. Energy Conversion and Management 97: 166-177. DOI:10.1016/j.enconman.2015.03.057.
- Glover, C., Puerto M., Maerker, J., et al. 1979. Surfactant Phase Behavior and Retention in Porous Media, SPEJ 183-193.
- Kamal, M., Adewunmi, A., Sultan A., et al. 2017. Recent Advances in Nanoparticles Enhanced Oil Recovery: Rheology, Interfacial Tension, Oil Recovery, and Wettability Alteration. Journal of Nanomaterials. DOI: 10.1155/2017/2473175.
- Kazemzadeh, Y., Sourani, S., Doryani, H. et al. 2014. Recovery of Asphaltenic Oil During Nano Fluid Injection. Petroleum Science and technology 33(2): 139-146 DOI: 10.1080/10916466.2014.956898.
- Mohsenzadeh, A., Al-Wahaibi, Y., Jibril, A. et al. 2015. The Novel use of Deep Eutectic Solvents for Enhancing Heavy Oil Recovery. J. Pet. Sci. Eng. 130: 6-15. DOI: 10.1016/j.petrol.2015.03.018.
- Ogolo, N.A., Olafuyi, O.A., and Onyekonwu, M.O. et al. 2012. Enhanced oil recovery using nanoparticles. SPE Saudi Arabia Section Technical Symposium and Exhibition, Al-Khobar, Saudi Arabia, April 8–11.

- Sheng, J. 2001. *Modern Chemical Enhanced Oil Recovery: Theory and Practice*. Gulf Professional Publishing.
- Raffa, P., Broekhuis, A., Picchioni, F. 2016. Polymeric Surfactants for Enhanced Oil Recovery: A Review. *J.Petro.Eng.* **145** (723-733). DOI: 10.1016/j.petro.2016.07.007.
- Wu, Y., Mahmoudkhani, A., Watson, P. et al. 2012. A Non-Thermal Surfactant-Polymer Based Technology for Enhanced Heavy Oil Recovery in Oil Sand and Ultra Shallow Reservoirs. SPE Heavy Oil Conference Canada, Calgary, AB, Canada, 12–14 June.
- Yang, H., Britton, C., Liyanage, P., et al. 2010. Low-Cost-High-Performance Chemicals for Enhanced Oil Recovery. SPE Improved Oil Recovery Symposium, 24-28 April. SPE-129978-MS DOI:/10.2118/129978-MS.
- Zhang, R., and Somasundaran, P. 2006. Advances in adsorption of surfactants and their mixture at solid/solution interfaces. *Adv. Colloidal Interface Sci.*, **123-126** (213-9).

Chapter 2

- Alvarado, V., Wang, X., Moradi, M., 2011. Stability proxies for water-in-oil emulsions and implications in aqueous-based enhanced oil recovery. *Energies* 4, 1058–1086. <https://doi.org/10.3390/en4071058>.
- Ashrafizadeh, S., Motae, E., Hoshyargar, V., 2012. Emulsification of heavy crude oil in water by natural surfactants. *J. Petrol.* 86–87, 137–143. <https://doi.org/10.1016/j.petro.2012.03.026>.
- Bancroft, W.D., 1913. Theory of emulsification. *J. Phys. Chem.* 17, 501–519.
- Barboriak, D., Padua, A.O., York, G.E., et al., 2005. Creation of DICOM-aware applications using ImageJ. *J. Digit. Imag.* 18, 91–99.
- Barnes, J.R., Dirkzwager, H., Smit, J.R., et al., 2010. Application of internal olefin sulfonates and other surfactants to EOR. Part 1: structure – performance relationships for selection at different reservoir conditions. In: SPE Improved Oil Recovery Symposium, Tulsa, Oklahoma, USA, 24–28 April. <https://doi.org/10.2118/129766-MS>.
- Barnes, J.R., Smit, J.R., Smit, J.P., et al., 2008. Development of surfactants for chemical flooding at difficult reservoir conditions. In: SPE/DOE Improved Oil Recovery Symposium, Tulsa, Oklahoma, USA, 19–23 April. <https://doi.org/10.2118/113313-MS>.
- Binks, B.P., Yin, D., 2016. Pickering emulsions stabilized by hydrophilic nanoparticles: in situ surface modification by oil. *Soft Matter* 12, 6858. <https://doi.org/10.1039/c6sm01214k>.

- Böker, A., He, J., Emrick, T., et al., 2007. Self-assembly nanoparticles at interfaces. *Soft Matter* 3, 1231–1248. <https://doi.org/10.1039/b706609k>.
- Chavalier, Y., Bolzinger, M.A., 2013. Emulsions stabilized with solid nanoparticles. *Colloids Surf* 439, 23–34. <https://doi.org/10.1016/j.colsurfa.2013.02.054>.
- Chopra, S., Lines, R.L., Schmitt, R.D., et al., 2010. Heavy Oils: Reservoir Characterization and Production Monitoring. <https://doi.org/10.1190/1.9781560802235>.
- Dahbag, M.S.B., Hossain, M.E., AlQuaraishi, A.A., et al., 2016. Efficiency of ionic liquids as an enhanced oil recovery chemical: simulation approach. *Energy Fuels* 30, 9260–9265. <https://doi.org/10.1021/acs.energyfuels.6b01712>.
- Daniel-David, D., Le Follotec, A., Pezron, I., et al., 2008. Destabilization of water-in-crude oil emulsions by silicone copolymer demulsifiers. *Oil Gas Sci. Technol.* 63, 165–173. <https://doi.org/10.2516/ogst:2008002>.
- Girish, V., Vijayalakshmi, A., 2004. Affordable image analysis using NIH image/imagej. *Indian J. Canc.* 41, 47.
- Gould, J., Garcia, G.G., Wolf, B., 2016. Pickering particles prepared from food waste. *Materials* 9, 791. <https://doi.org/10.3390/ma9090791>.
- Gupta, S., 2016. Effects of Chemical Structure of Anionic Surfactants on the Wettability of a Carbonate System. Master's Thesis Louisiana State University and Agricultural Mechanical College.
- Hamedi-Shokrlu, Y., Babadagli, T., 2014. Stabilization of nanometal catalysts and their interaction with oleic phase in porous media during enhanced oil recovery. *Ind. Eng. Chem. Res.* 53, 8464–8475. <https://doi.org/10.1021/ie4042033>.
- Johnson Jr., C.E., 1976. Status of caustic and emulsion methods. *J. Petrol. Technol.* 85–92. <https://doi.org/10.2118/5561-PA>.
- Jones, T.J., Neustadter, E.L., Wittingham, K.P., 1978. Water-in crude oil emulsion stability and emulsion destabilization by chemical demulsifiers. *J. Can. Pet. Technol.* 17, <https://doi.org/10.2118/78-02-08>, PETSOC-78-02-08.
- Liu, Q., Dong, M., Ma, S., 2006. Alkaline/surfactant flood potential in western Canadian heavy oil reservoirs. In: SPE/DOE Symposium on Improved Oil Recovery, Tulsa, OK. USA, 22–26 April.

- Liu, Q., Dong, M., Ma, S., et al., 2007. Surfactant enhanced alkaline flooding for western Canadian heavy oil recovery. *Colloid. Surface. Physicochem. Eng. Aspect.* 293, 63–71.
- Mele, A., Tran, C., Lacerda, S., 2003. The structure of a room-temperature ionic liquid with and without trace amounts of water: the role of C[BOND]H...O and C[BOND]H...F interactions in 1-n-Butyl-3-Methylimidazolium tetrafluoroborate. *Angew. Chem.* 115, 4500–4502. <https://doi.org/10.1002/ange.200351783>.
- Mohsenzadeh, A., Al-Wahaibi, Y., Jibril, A., et al., 2015. The novel use of deep eutectic solvents for enhancing heavy oil recovery. *J. Petrol. Sci. Eng.* 130, 6–15. <https://doi.org/10.1016/j.petrol.2015.03.018>.
- Pal, M., Rai, R., Yadav, A., et al., 2014. Self- aggregation of sodium dodecyl sulfate within (choline chloride + urea) deep eutectic solvent. *Langmuir* 30, 13191–13198. <https://doi.org/10.1021/la5035678>.
- Poteau, S., Argillier, J.F., Langevin, D., et al., 2005. Influence of pH on stability and dynamic properties of asphaltenes and other amphiphilic molecules at the oil-water interface. *Energy Fuels* 19, 1337–1341. <https://doi.org/10.1021/ef0497560>.
- Risch, S.J., Reineccius, G.A., 1988. Effect of emulsion size on flavor retention and shelf stability. *ACS (Am. Chem. Soc.) Symp. Ser.* 370, 67–77.
- Saha, D., 2010. Hydrocolloids as thickening and gelling agents in food: a critical review. *J. Food Sci. Technol.* 47, 587–597. <https://doi.org/10.1007/s13197-010-0162-6>.
- Sheng, J., 2001. In: Sheng, J. (Ed.), *Modern Chemical Enhanced Oil Recovery: Theory and Practice*. Gulf Professional Publishing <https://doi.org/10.1016/B978-1-85617-745-0.00009-7>.
- Sjöblom, J., 2001. Demulsifiers in the oil industry. In: *Encyclopaedic Handbook of Emulsion Technology*. CRC Press, New York, Mar 16, 2001.
- Stamkulov, N.S., Mussabekov, K.B., Aidarova, S.B., et al., 2008. Stabilization of emulsions by using a combination of oil soluble ionic surfactant and water soluble polyelectrolytes. *J. Colloids and Surf.* 335, 1–3. <https://doi.org/10.1016/j.colsurfa.2008.10.051>.
- Wang, Q., Hu, C., Zoghbi, A., et al., 2017. Oil-in-Oil-in-Water pre-double emulsions stabilized by nonionic surfactants and silica particles: a new approach for topical application of rutin. *J. Colloids and Surf.* 522, 399–407. <https://doi.org/10.1016/j.colsurfa.2017.02.067>.

Wu, Y., Mahmoudkhani, A., Watson, P., et al., 2012. A non-thermal surfactant-polymer based technology for enhanced heavy oil recovery in oil sand and ultra shallow reservoirs. In: SPE Heavy Oil Conference Canada, Calgary, AB, Canada, 12–14 June.

Yoon, K., Son, H., Choi, S., et al., 2016. Core flooding of complex nanoscale colloidal dispersions for enhanced oil recovery by in situ formation of stable oil-in-water pickering emulsions. *Energy Fuels* 30, 2628–2635. <https://doi.org/10.1021/acs.energyfuels.5b02806>.

Zhang, T., Davidson, D., Bryant, S.L., et al., 2010. Nanoparticle-stabilized emulsions for applications in enhanced oil recovery. In: SPE Improved Oil Recovery

Chapter 3

Al-Anssari, S., Arif, M., Wang, S. et al. 2017. Stabilizing Nanofluids in Saline Environments. *J. Colloid Interface Sci.* **508** (2017): 222-229. DOI: 10.1016/j.jcis.2017.08.043 0021–9797.

Arla, D., Siquin, A., Palermo, T. et al. 2007. Influence of pH and Water Content on the Type and Stability of Acidic Crude Oil Emulsions. *Energy & Fuels* **21** (3):1337–1342. DOI: 10.1021/ef060376j.

Arguelles, F. 2015. Pore Scale Investigations on the Dynamics of SAGD Process and Residual Oil Saturation Development. Ph.D thesis, Department of Civil and Environmental Engineering, University of Alberta.

Binks, B., Murakami, R., Armes, S., et al. 2006. Effects of pH and Salt Concentration on Oil-in-Water Emulsions Stabilized Solely by Nanocomposite Microgel Particles. *Langmuir* **22** (5): 2050–2057. DOI: 10.1021/la053017.

Binks, B. and Rodriguez, J. 2007. Enhanced Stabilization of Emulsions Due to Surfactant-Induced Nanoparticle Flocculation. *Langmuir* **23**: 7436–7439.

Chavalier, Y. and Bolzinger, M.A. 2013. Emulsions Stabilized with Solid Nanoparticles. *Colloids Surf.* **439**: 23–34. DOI: 10.1016/j.colsurfa.2013.02.054.

Chen, X., Song, X., Huang, J. et al. 2017. Phase Behavior of Pickering Emulsions Stabilized by Graphene Oxide Sheets and Resins. *Energy Fuels* **31** (12): 13439–13447. DOI: 10.1021/acs.energyfuels.7b02672.

Delamaide, E., Bazin, B., Rousseau, D. et al. 2014. Chemical EOR for Heavy Oil: the Canadian Experience. SPE EOR Conference at Oil and Gas West Asia, Muscat, Oman, 31 March – 2 April. DOI: 10.2118/169715-MS

- Gandomkar, A. and Rahimpour, M. et al. 2015. Investigation of Low-Salinity Waterflooding in Secondary and Tertiary Enhanced Oil Recovery in Limestone Reservoirs. *Energy Fuels* **29** (12): 7781–7792. DOI: 10.1021/acs.energyfuels.5b01236.
- Goloub, T. and Koopal, L. et al. 1997. Adsorption of Cationic Surfactants on Silica. Comparison of Experiment and Theory. *Langmuir* **13** (4): 673–681. DOI: 10.1021/la960690d.
- Graham, B. May, E., and Trengove, R. 2008 Emulsion Inhibiting Components in Crude Oils. *Energy Fuels* **22** (12): 1093–1099. DOI: 10.1021/ef700529m.
- Hankins, N. and Harwell, J. 1997. Case Studies for the Feasibility of Sweep Improvement in surfactant-Assisted Waterflooding. *J. Pet. Sci. Eng.* **17** (1): 41–62. DOI: 10.1016/S0920-4105(96)00055-1.
- Kumar, S. Aswal, V., and Kohlbrecher, J. 2012. Size-Dependent Interaction of Silica Nanoparticles with Different Surfactants in Aqueous Solution. *Langmuir* **28** (25): 9288–9297. DOI: 10.1021/la3019056.
- Lee, J. and Babadagli, T. 2017. Screening of Chemicals for Low Cost Heavy Oil Recovery through Microemulsion Stability Tests. SPE/IATMI Asia Pacific Oil & Gas Conference and Exhibition, Jakarta, Indonesia. 17–19 October, DOI: 10.2118/186344-MS.
- Li, Y. Zhang, W. Kong, B. et al. 2016. Mixtures of Anionic/Cationic Surfactants: A New Approach for Enhanced Oil Recovery in Low-Salinity, High-Temperature Sandstone Reservoir. *SPE J.* <https://doi.org/10.2118/169051-MS>.
- Ma, S. Dong, M. Li, Z. et al. 2006. Evaluation of the Effectiveness of Chemical Flooding using Heterogeneous Sandpack Flood Test. *J. Pet. Sci. Eng.* **55** (3): 294–300. DOI:10.1016/j.petrol.2006.05.002.
- Paria, S. and Khilar, K.C. 2004. A Review on Experimental Studies of Surfactant Adsorption at the Hydrophilic Solid-Water Interface. *Adv Colloid Interface Sci.* **110** (3): 75–95. <https://doi.org/10.1016/j.cis.2004.03.001>.
- Sheng, J. 2015. Investigation of Alkaline-Crude Oil Reaction. *Petroleum* **1** (1): 31–39. DOI: 10.1016/j.petlm.2015.04.004.
- Upadhyaya, A., Acosta, E., Scamehorn, J. et al., 2007. Adsorption of Anionic-Cationic Surfactant Mixtures on Metal Oxide Surfaces. *J. Surfact Deterg.* **10** (4): 269–277. DOI: 10.1007/s11743-007-1045-3.

- Yoon, K., Son, H., Choi, S. et al. 2016. Core Flooding of Complex Nanoscale Colloidal Dispersions for Enhanced Oil Recovery by in Situ Formation of Stable Oil-in-Water Pickering Emulsions. *Energy & Fuels* **30** (4): 2628–2635. DOI: 10.1021/acs.energyfuels.5b02806.
- Zhu, Y. Fu, T. Liu, K. et al. 2017. Thermoresponsive Pickering Emulsions Stabilized by Silica Nanoparticles in Combination with Alkyl Polyoxyethylene Ether Nonionic Surfactant. *Langmuir* **33**: 5724–5733. DOI: 10.1021/acs.langmuir.7b00273.

Chapter 4

- Babadagli, T. and Ozum B. 2012. BioDiesel as Additive in High Pressure and Temperature Steam Recovery of Heavy Oil and Bitumen. *Oil & Gas Science and Technology – Rev. IFP Energies Nouvelles* **67** (3): 413–421. DOI: 10.2516/ogst/2011164.
- [Hennock, M., Rahalkar, R., and Richmond, P. 1984. Effect of Xanthan Gum upon the Rheology and Stability of Oil-Water emulsions. *J. Food Science* **49** \(September\). DOI: 10.1111/j.1365-2621.1984.tb14968.x](#)
- Lee, J. and Babadagli, T. 2017. Screening of Chemicals for Low Cost Heavy Oil Recovery through Microemulsion Stability Tests. SPE/IATMI Asia Pacific Oil & Gas Conference and Exhibition, Jakarta, Indonesia, 17–19 October. DOI: 10.2118/186344-MS.
- Lee, J. and Babadagli, T. 2018. Improvement of Microemulsion Generation and Stability Using New Generation Chemicals and Nano Materials During Waterflooding as a Cost-Efficient Heavy-Oil Recovery Method. SPE Trinidad and Tobago Section Energy Resources Conference, Port of Spain, Trinidad and Tobago, 25–26 June. DOI: 10.2118/191171-MS.
- Manuale, D., Greco, E., Clementz, A. et al. 2014. Biodiesel Purification in One Single Stage Using Silica as Adsorbent. *J.Cej* **256**: 372–379. DOI: 10.1016/j.cej.2014.07.022.
- Mazzieri, V., Vera, C., and Yori, J. 2008. Adsorptive Properties of Silica Gel for Biodiesel Refining. *Energy Fuels* **22** (6): 4281–4284. DOI: 10.1021/ef800479z.
- Prudhomme, R. and Long, R. 1983. Surface Tensions of Concentrated Xanthan and Polyacrylamide Solutions with Added Surfactants. *J. Colloid Interface* **1** (93): 274. DOI: 10.1016/0021-9797(83)90406-X.
- Sandvik, E. and Maerker, J. 1977. Application of Xanthan Gum for Enhanced Oil Recovery. *Extracellular Microbial Polysaccharides* **45**: 242–264. DOI: 10.1021/bk-1977-0045.ch019.

Yoon, K., Son, H., Choi, S. et al. 2016. Core Flooding of Complex Nanoscale Colloidal Dispersions for Enhanced Oil Recovery by In Situ Formation of Stable Oil-in-Water Pickering Emulsions. *Energy & Fuels* **30** (4): 2628–2635. DOI: 10.1021/acs.energyfuels.5b02806.

Chapter 5

BASF. 2014. Aspiro™ EOR Polymers and Surfactants. www.oilfield-solutions.basf.com/.../Aspiro_-_EOR_Polymers_and_Surfactants.pdf.

Glover, C., Puerto M., Maerker, J., et al. 1979. Surfactant Phase Behavior and Retention in Porous Media, SPEJ 183-193.

Gogoi, S. 2011. Adsorption-Desorption of Surfactant for Enhanced Oil Recovery, Transport in Porous Media **90** (2):589-604. DOI: 10.1007/s11242-011-9805-y.

Hennock, M., Rahalkar, R., Richmond, P. Effect of Xanthan Gum upon the Rheology and Stability of Oil-Water emulsions. *J. Food Science*, **49**. DOI: 10.1111/j.1365-2621.1984.tb14968.x.

Lee, J. and Babadagli, T. 2017. Screening of Chemicals for Low Cost Heavy Oil Recovery through Microemulsion Stability Tests. SPE/IATMI Asia Pacific Oil & Gas Conference and Exhibition, Jakarta, Indonesia. DOI: 10.2118/186344-MS.

Lee, J and Babadagli, T. 2018. Improvement of Microemulsion Generation and Stability Using New Generation Chemicals and Nano Materials during Waterflooding as a Cost-Efficient Heavy-Oil Recovery Method. SPE Trinidad and Tobago Section Energy Resources Conference, Port of Spain, Trinidad and Tobago. DOI: 10.2118/191171-MS.

Lee, J, Babadagli, T, Ozum, B. 2018. Microemulsion flooding of heavy oil using biodiesel under cold conditions. SPE International Heavy Oil Conference & Exhibition, Kuwait City, Kuwait. (To be presented) SPE-193642-MS.

Pollock, T. 2013. Surfactant/Polymer Flood Design for a Hard Brine Limestone Reservoir MSc Thesis, the University of Texas at Austin.

Prudhomme, R. and Long, R. 1983. Surface tensions of concentrated xanthan and polyacrylamide solutions with added surfactants. *J. Colloid Interface* **1** (93): 274 DOI: 10.1016/0021-9797(83)90406-X.

- Rojas, G., Ali, F. 1986. Scaled Model Studies of Carbon Dioxide/Brine Injection Strategies for Heavy Oil Recovery from Thin Formations. *JCPT* **1**(25) DOI: 10.2118/86-01-07.
- Yan, H., Yuan Shi, Xu Gui, et al. 2010. Effect of Ca²⁺ and Mg²⁺ Ions on Surfactant Solutions Investigated by Molecular Dynamics Simulation. *Langmuir* **26**(13): 10448-10459 DOI: 10.1021/la100310w.
- Sandvik, E., Maerker, J. 1977. Application of Xanthan Gum for Enhanced Oil Recovery. *Extracellular Microbial Polysaccharides* **45**: 242-264 DOI: 10.1021/bk-1977-0045.ch019.
- Shell Chemicals. 2018. Enordet: Detergents for Enhanced Oil Recovery https://www.shell.com/business-customers/chemicals/our-products/higher-olefins-and-derivatives/enordetsurfactants/_jcr_content/par/tabbedcontent/tab/textimage.stream/1526660841427/d23dc571f05cc98f0cdb9d7dc91cd8f3cb6b7a6c315ce51d7150c99af8a29cf2/enordet-brochure-en.pdf.
- Sim, S., Wassmuth, f. and Bai, J. 2016. Application of Low Salinity Micellar Emulsion in Chemical EOR of Heavy Oil. SPE Canada Heavy Oil Technical Conference, Calgary, Alberta 7-9 June 2016. SPE-180744-MS.
- L, K., Jing, X., He, S et al. 2016. Static Adsorption and Retention of Viscoelastic Surfactant in Porous Media: EOR Implication. **30** (11): 9089-9096 DOI: 10.1021/acs.energyfuels.6b01732.
- Tichelkamp, T., Khanamiri, H., Nourani, M., et al. 2016. EOR Potential of Mixed Alkylbenzenesulfonate Surfactant at Low Salinity and the Effect of Calcium on “Optimal Ionic Strength,” **30** (4) 2919-2924 DOI: 10.1021/acs.energyfuels.6b00282.